Modelling the Economic, Time and Workability Advantages of the Slipjoint through Discrete-Event Simulation

MSc Transport, Infrastructure and Logistics Thesis

Cian Rippen

Delft University of Technology

TU Delft

DOT

Modelling the Economic, Time and Workability Advantages of the Slipjoint through Discrete-Event Simulation

by

Cian Rippen

to obtain the degree of Master of Science

at the Delft University of Technology,

to be defended publicly on Friday 29th of August at 10:45.

Student number:	5054141	
Report number:	2025.TIL.9090	
Project duration:	February 17, 2025 – August 29, 2025	
Thesis committee:	Prof. dr. ir. E. B. H. J. van Hassel,	TU Delft, chair
	Prof. dr. ir. M. van Koningsveld,	TU Delft
	dr. ir. J. van der Tempel,	DOT
	ir. David Tiemens	DOT

Cover:	Cover: Single Lift Offshore Wind Turbine Installation Using a Slipjoint (DOB Academy)
Style:	TU Delft Report Style, with modifications by Daan Zwaneveld and Cian Rippen

An electronic version of this thesis is available at http://repository.tudelft.nl/.

TU Delft

DOT

Preface

After finishing my Bachelor of Science in Mechanical Engineering, I wanted to continue my studies in a slightly different direction, as I found that I was ready for something new. Because of my interest in rail and air transport networks and logistics, I chose the MSc Transport, Infrastructure and Logistics (TIL). Another aspect that attracted me to TIL, was the high degree of customisation of the curriculum which was possible. I was able to choose my subjects so that they still contained elements of Mechanical Engineering, which I was (and am) still fond of. During my time at TIL, I attended a course called Shipping Management, given by Edwin van Hassel. This was one of my favourite courses, sparking an interest in Maritime Technology. It was through this course that I discovered an interest in the field of Offshore Engineering, fuelled by the enormous scale of the equipment and projects. When it came time to start the preparations for my thesis, I wanted to see if I could combine this new interest with a TIL thesis. Through a random encounter with David Tiemens in the supermarket, I got in touch with Delft Offshore Turbine (DOT). Their CEO, Jan van der Tempel, had a research proposal for me: modelling the impact of the Slipjoint on offshore installation logistics. This assignment combined TIL and Offshore Engineering perfectly, marking the start of my thesis project. Now, eight months later, the finished product lies before you.

I would like to thank my supervisors Edwin van Hassel and Mark van Koningsveld for their support and feedback during the project. You helped me to delve deep into the subject matter, but also to take a step back sometimes to look at the bigger picture. I would also like to thank DOT for providing me with the opportunity to carry out this project. I would specifically like to thank Jan van der Tempel and David Tiemens for their help during the project. You helped me to connect theoretical research to practical applications, and our discussions helped me include aspects of the problem I hadn't yet considered. Also a big thanks to all the other DOT employees who were kind enough to help me with any questions I had about the world of offshore wind energy.

Last but not least, I want to thank my friends, parents, my little brother Luka, and my girlfriend Ineke for their love and support throughout not just my thesis project, but my whole time as a student at the TU Delft. I look forward to what the future brings with all of you.

I hope you enjoy reading my thesis.

Cian Rippen
Delft, August 2025

Summary

In recent years, costs in the offshore wind energy sector have risen significantly. Rising interest rates, shortage of skilled labour and a supply chain which is under pressure due to the ever increasing size of offshore wind turbines all cause costs to increase. At the same time, the pressure to realise sustainable energy continues to grow. The installation phase is one of the most expensive and resource-intensive parts of offshore wind projects. Reducing the installation duration could aid in significantly reducing the installation costs, and make offshore wind farms more economically feasible.

The Slipjoint is a novel connection method developed by Delft Offshore Turbine (DOT), that aims to reduce offshore installation time, and therefore installation cost, by removing the need for bolting or grouting connections between wind turbine parts. When coupled with a complete pre-assembly strategy, it enables installation of offshore wind turbines with a single lift.

This paper presents a Discrete-Event Simulation (DES) model that compares traditional and Slipjoint-based wind turbine installation methods in terms of time, cost, and weather sensitivity. The model gives insight into how weather, vessel characteristics, and campaign timing influence installation performance of both the standard and Slipjoint-based installation methods. A multi-year simulation is run over a range of weather datasets, to give insight into installation performance as a function of start date. The multi-year model is applied to two case studies: the Ecowende wind farm in the North Sea, and the Star of the South wind farm off the coast of mainland Australia, near Tasmania. The standard installation method is compared to the Slipjoint method. The Slipjoint method is run with two values for the capacity to investigate the impact of the capacity on performance. Results show that the Slipjoint can reduce installation duration by 30 to 60%. Increased vessel dayrate and mobilisation costs, caused by the need for Heavy-Lift Vessels for the Slipjoint method, partially offset the economic gain from the reduction in installation time. Still, a cost reduction of 0 to 30% can be achieved, depending on the vessel capacities which can be achieved. Furthermore, the Slipjoint methods are shown to have a higher weather workability, meaning they are less affected by bad weather conditions than the standard installation method. This enables them to have a wider envelope in which the installation campaigns can start. These results show the potential of the Slipjoint to change the way offshore wind farms are installed, in order to make offshore wind energy more economically feasible.

Contents

Nomenclature

Abbreviations

Abbreviation	Definition
AIS	Automatic InformationSystem
DES	Discrete-Event Simulation
DNV	Det Norske Veritas
DOT	Delft Offshore Turbine
DST	Decision-Support Tool
HLV	Heavy-Lift Vessel
HMC	Heerema Marine Contractors
MILP	Mixed-Integer Linear Programming
OWF	Offshore Wind Farm
OWT	Offshore Wind Turbine
RNA	Rotor-Nacelle Assembly
SJOR	Slipjoint Offshore Research
SJOQ	Slipjoint Offshore Qualification
TRL	Technology Readiness Level
WTIV	Wind Turbine Installation Vessel

1

Introduction

As the demand for renewable energy continues to grow, so does the demand for wind energy. Offshore wind energy, specifically, is expected to grow significantly in the near future. In the Netherlands, the amount of electrical power generated by offshore wind farms is expected to grow from 4.7 gigawatt in 2024 to 21.5 gigawatt in 2032 (Noorzeeloket, 2025). Achieving this goal by 2032 will be a tremendous challenge, and every way to accelerate this process will increase the chances of success and aid the energy transition.

Recently, the offshore wind sector has had to face a significant increase in costs. Vattenfall estimates that the costs of building offshore wind farms have increased by as much as 40% (Johnny Wood, 2023). This increase is due to increased cost of capital, higher prices for resources, inflation, geopolitical tensions and shortages of experienced personnel (Fuchs et al., 2025). On top of the increasing costs comes an increase in complexity of offshore wind. The continuous search for cost reductions by increasing turbine size has caused the installation supply chain to lag behind. Investments in installation vessels carry risk, as these vessels might quickly become redundant as newer, larger turbines become the norm and outgrow their installation vessels. The rapid growth of the turbines and the economic challenges have caused a shortage of experienced and capable personnel. This adds more challenges to the already tough environment of the offshore wind sector.

1.1. Offshore Wind Turbine Installation

When looking at the installation process of offshore wind turbines, it can be seen that the traditional method of installing wind turbines at sea comes with challenges. Wind turbines are assembled completely at sea, meaning a lot of operations have to be carried out at sea. This includes assembling the tower, nacelle and blades at sea (see Figure 1.1), as well as bolting the turbine to the foundation and connecting the cables within the turbine. This process is costly, as the use of specialised installation vessels is expensive and assembling at sea is time-intensive.

Furthermore, the installation process is sensitive to changes in the weather, as the installation process cannot be carried out in rough weather conditions (Oelker et al., 2021). This means that if the weather conditions get outside acceptable levels, the installation has to be interrupted and postponed, resulting in cost overshoot. The weather windows in which installation can be carried out are limited, so decreasing installation time decreases the risk of overrunning this window.

Reducing the number of steps required for installing an offshore wind turbine can significantly

reduce the installation time, making the process less sensitive to weather changes and therefore decreasing operational and delay costs. This could make offshore wind more economically attractive again, and thereby aid in the energy transition.

Figure 1.1: Traditional installation method: assembly at sea (source: (OffshoreWIND.biz, 2025))

1.2. The Slipjoint

The Slipjoint connection aims to achieve this reduction in installation complexity. Developed by Delft Offshore Turbine (DOT), it is an innovative connector for wind turbines. It can be used to quickly connect the tower to the foundation, or to connect the nacelle to the tower, or both. It works by connecting two conical tubes to each other, which are held in place by their geometry, gravity, and a combination of friction and hoop stresses (DOT, 2025). A schematic view of a Slipjoint can be seen in Figure 1.2. The friction connection ensures that the installation time of a wind turbine is reduced significantly, as the two pieces no longer need to be bolted or grouted together to ensure a good connection. Once the tower is lowered onto the foundation, it settles because of gravity, and no extra installation steps are necessary to ensure a good connection between tower and foundation.

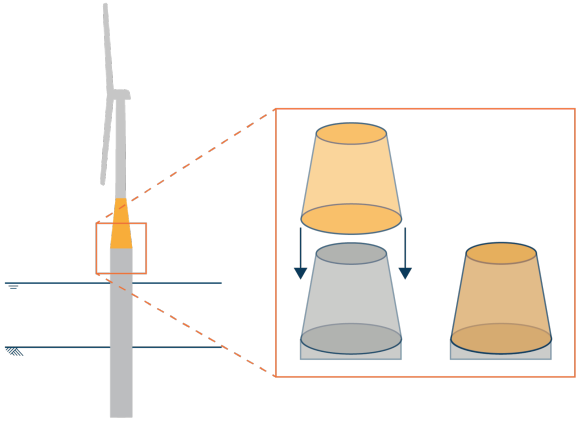

Figure 1.2: The Slipjoint mechanism. (DOT, 2025)

1.3. Problem Statement

The rising costs in the offshore wind sector are becoming increasingly problematic, and will have to be addressed soon if the goals for future growth are to be met. One way to reduce costs is by reducing installation times, as time spent offshore is very costly, especially with specialised vessels such as the ones used for wind turbine installation. The Slipjoint aims to achieve a reduction in installation time by reducing the number of offshore operations. Reducing the number of offshore lifts per turbine by even one can produce large time savings, saving

money. However, currently there does not exist a quantitative framework to evaluate the possible time and cost savings of the Slipjoint when compared to traditional installation methods. This makes it difficult for stakeholders to assess whether the Slipjoint has an advantage over traditional methods for the installation of a new Offshore Wind Farm (OWF). A structured, quantitative comparison framework is needed to aid decision-making when considering the use of Slipjoint for the realisation of OWFs.

1.4. Research Objective and Questions

The objective of this thesis is to develop and apply a simulation-based Decision-Support Tool (DST) to quantitatively compare the performance of traditional installation methods and the Slipjoint installation method. The focus of the DST will be on assessing differences in installation duration, costs and weather workability. These performance parameters will be evaluated using Discrete-Event Simulation (DES), a simulation method which will be discussed in Chapter 2.

This leads to the following main research question, which is addressed in this thesis:

> *"How can the installation processes of offshore wind farms using the Slipjoint and traditional methods be quantitatively compared to create a decision support tool for offshore wind farm development?"*

To support the main research question, the following sub-questions are formulated:

1. In what ways does the Slipjoint change the offshore installation process compared to the traditional method?
2. How can discrete event simulation be used to accurately model these installation processes?
3. How can the two methods be compared in terms of time, cost and weather workability?
4. How does the Slipjoint installation compare to traditional installation for the Ecowende and Tasmania wind farms?

The first subquestion is answered in Chapter 2. The second and third subquestions are answered in Chapter 3. The fourth subquestion is answered in Chapter 5. Finally, the main research question is answered in Chapter 7

1.5. Scope

The focus of this study lies on the installation phase of the realisation of offshore wind farms. This phase is shown in Figure 1.3 within the high-level process of the realisation of an OWF. This graph shows the processes as being completely serial, while often the processes are executed partially in parallel. For example, foundation installation can be executed in parallel to superstructure installation. In this study, it is assumed that there are always turbine foundations available for superstructure installation. In other words, it is assumed that the foundation installation process does not suffer delays which could impact the installation of the wind turbines. This study focuses purely on the logistical aspect of the loading, transport, and installation of the wind turbine superstructures. Other affairs such as structural integrity, energy generation performance, or maintenance are not considered.

1.6. Reading Guide

In this chapter, the current climate of the offshore wind sector is explained, the Slipjoint is introduced, and the aim and scope of the research are given. In Chapter 2, an overview of the

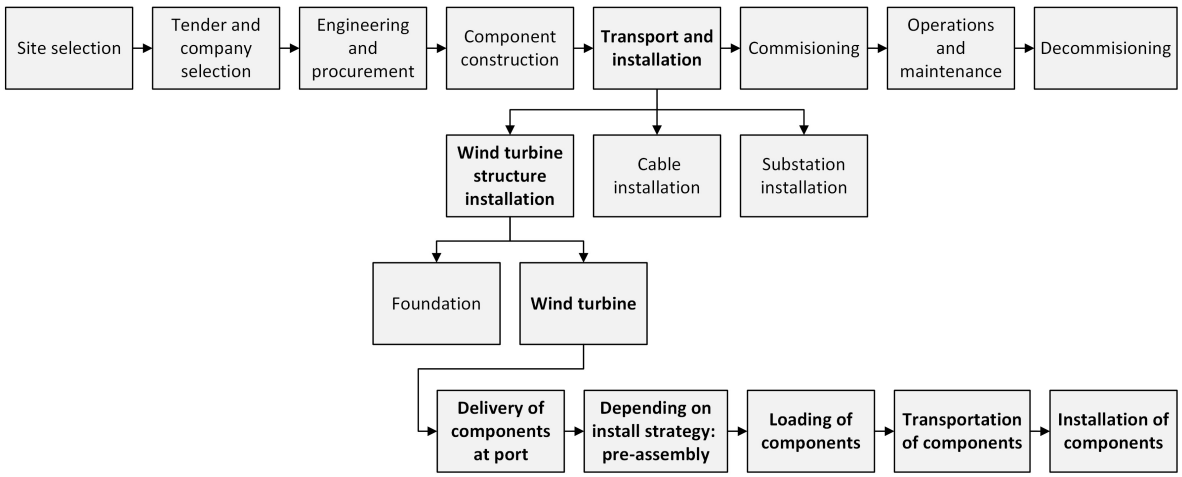

Figure 1.3: The life-cycle phases of an OWF, and the location of this study within this framework. Adapted from (Tjaberings et al., 2022)

current common practices in offshore wind turbine installation is given, literature regarding the modelling of offshore logistics is given, and a research gap is identified. Chapter 3 gives an overview of the methodology which is used to construct the DST: model structure, assumptions, data gathering and model validation are presented. The two case studies are discussed in Chapter 4. In Chapter 5, the DST is applied to the case studies and the results are laid out and investigated. In Chapter 6 the results are interpreted and discussed. The entire thesis is concluded in Chapter 7, and recommendations for future research are given.

2

Literature Review

In this chapter, a literature review regarding offshore wind farms and slip joints is presented. It aims to provide a structured overview of the current state of knowledge in offshore wind farm installation, modelling of offshore logistics and the use of slip joints. A focus is laid on literature regarding possible ways to reduce the installation time and costs. The literature review is structured as follows. The current common practices regarding the installation process of offshore wind farms is discussed in Section 2.1. The use of slip joints for (offshore) wind turbines is discussed in Section 2.2. In Section 2.3, the existing literature regarding modelling and simulation of offshore logistics is discussed. Lastly, a knowledge gap is identified in Section 2.4.

2.1. Common Practices in Offshore Wind Turbine Installation

In Figure 1.3, a high-level process chart of the procurement of an OWF is shown. The installation phase of the offshore wind turbines (OWT) and its subphases are highlighted. Earlier in the process, during the engineering and procurement phase, decisions and plans are made regarding the manner in which the installation will be carried out. The decisions taken here greatly influence the course of the installation. There are a wide variety of possible transportation and installation strategies, which are laid out below.

The wind turbine installation phase consists of three subphases: loading, transportation and installation. To execute these phases, multiple different strategies can be employed. Different pre-assembly and loading strategies are discussed in Section 2.1.1. Possible transportation strategies are shown in Section 2.1.2. Lastly, installation strategies are discussed in Section 2.1.3. Regardless of which strategies are chosen for the loading, transport and installation phases, the process always starts with the OWT components being delivered to the base port. Once all components are present and the transportation equipment is ready, the installation campaign can begin.

2.1.1. Pre-assembly and loading strategies

OWTs are usually broken down into the following components: the tower, nacelle, rotor and the three blades, see Figure 2.1. These components are then loaded onto the transportation vessel. This can be done by either the crane of a Heavy Lift Vessel (HLV), if the HLV serves as the transport vessel, or by a crane at the dock if it is a barge. Whether the transport vessel is a HLV or a barge depends on the transportation strategy, which will be discussed in Section 2.1.2. Furthermore, a choice can be made to (partially) pre-assemble the OWTs prior to loading onto

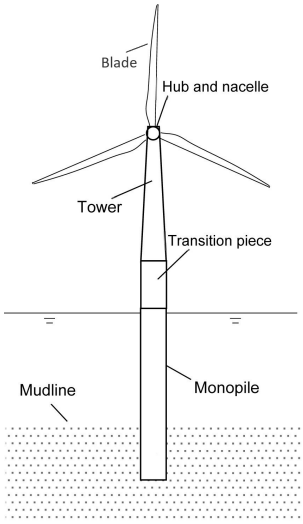

Figure 2.1: The parts of an OWT. Adapted from (Jiang, 2021)

the transportation vessel. This pre-assembly is carried out on the quayside and can reduce loading time and installation time, which will be discussed further in Section 2.1.3. Different degrees of pre-assembly are possible. For example, the rotor and nacelle are often already pre-assembled prior to loading. Further pre-assembly can be done by already attaching two of the three blades to the rotor-nacelle assembly. This strategy is called the 'bunny ears' strategy, as the pre-assembly is transported vertically and the two blades sticking up resemble two bunny ears, see Figure 2.2a. It is also possible to attach all three blades before loading. This is called a 'rotor star' strategy. The entire rotor assembly with the three blades attached is transported horizontally, see Figure 2.2b. In this strategy, the rotor is not attached to the nacelle before transport. Lastly, it is possible to completely pre-assemble the OWT on the quayside. The complete pre-assembly is then lifted onto the transportation vessel in one go, and transported to the offshore site.

(a) Bunny ears transport strategy **(b)** Rotor star transport strategy

Figure 2.2: The bunny ears and rotor star strategies. (source: OffshoreWIND.biz)

2.1.2. Transportation strategies

To transport the OWT components to the installation site, a transportation vessel is needed. This can be either a HLV, which then also performs the installation, or it can be a dedicated transport ship such as a barge. This barge acts as a feeder, transporting the OWT to the offshore installation site, where a HLV then transfers the OWT and performs the installation. This is called a feeder strategy. Employing feeders to transport the OWTs ensures that the HLV, which is often the most expensive vessel to operate, is used almost solely for installation

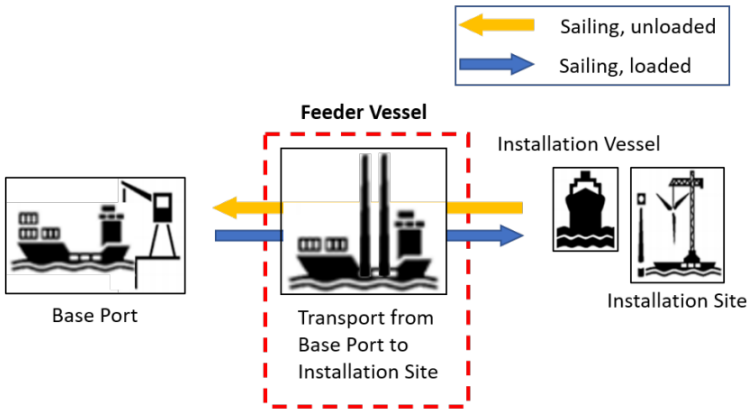

Figure 2.3: Diagram of the feeder strategy, adapted from (Smorenberg, n.d.)

of OWTs. However, using feeders comes with additional cost for the operation of the feeders and increases the number of lifting operations, and therefore the complexity of the installation. This trade-off is analysed in (Oelker et al., 2021), (Scholz-Reiter et al., 2011), and (Barlow et al., 2015).

2.1.3. Installation strategies

The installation strategy of the OWTs is dependent on the chosen pre-assembly and transportation strategies. In the most common installation strategy, a Wind Turbine Installation Vessel (WTIV) is used to both transport and install the OWTs. No pre-assembly is done in this strategy, apart from assembling the rotor and the nacelle. Often, this WTIV will be a jack-up vessel. This is a vessel which can extend four or more legs underneath itself onto the seabed, and lift itself out of the water. This way, the ship does not sway in the waves of the ocean and stability is increased, making the precise installation of the components possible. An example of a jack-up vessel designed for offshore wind installations is given in Figure 2.4. These jack-up vessels install OWTs one component at a time: first the tower, then the nacelle and lastly the three blades are installed one-by-one. Transporting all the components without any pre-assembly enables the WTIV to be loaded in a space-efficient manner, but it does mean many lifting operations have to be carried out during the installation, which is a time-intensive process.

Figure 2.4: A jackup vessel. This vessel has been raised higher than necessary for demonstration purposes. Source: (OffshoreWIND.biz, 2025)

A reduction in installation time can be achieved by using parallel assembly and installation. Heerema Marine Contractors (HMC) developed a technique called the Rotor-Nacelle Assembly (RNA) method. This method was first tested in 2022 aboard the Thialf during the installation of a Vestas V174 – 9.5MW turbine (Heerema, 2022). Two different cranes on the Thialf were used to simultaneously assemble components while installing others. While one crane was installing the tower, the other was assembling the RNA on top of a support tower on board the Thialf. When the RNA was completed, it was lifted onto the tower in its entirety. This RNA method was later also used during the DOT6000 FOX project, where both the tower and RNA were installed using a Slipjoint connection (DOT, 2019).

If a pre-assembly strategy is chosen, fewer lifting operations are needed. The bunny ears pre-assembly, as can be seen in Figure 2.2a, pre-assembles the nacelle and two blades. This strategy brings the number of required lifts down from five to three: the tower, nacelle with rotor and two blades, and the last blade. The rotor star strategy fully pre-assembles the nacelle and blades, and loads them in one lift, as can be seen in Figure 2.2b. This strategy also requires three lifts: the tower, nacelle and rotor-blade assembly. Lastly, a full pre-assembly is possible. The fully pre-assembled strategy only has one lift: the OWT is lifted from the quayside to the vessel in one go. This reduces the loading and installation time significantly, but also raises lifting capacity constraints. The loading and installation process can be seen in Figure 4.5.

2.2. Slip-joints as a Connector for Wind Turbines

The first time a slip joint was used for a wind turbine was in the 1990s. A company called Windmaster used a slip joint for the installation of their onshore wind turbines. When Windmaster was taken over by another company in 1998, the use of the slip joint was stopped (Segeren, 2018) (Kamphuis, 2016). That is, until interest picked up again. In 2003, Van der Tempel and Schipholt published a paper about the possible use of a slip joint for offshore purposes (Tempel & Schipholt, 2003). In this paper, the authors inspect an onshore Windmaster turbine in Scheveningen, which used a slip joint connection. They investigated a possible offshore application by performing measurements on the turbine. They concluded that a slip joint connection was feasible for offshore wind turbines, with the possible benefit of reduced installation time, but further research into the mechanical behaviour of the connection was needed.
In the years that followed, further research into the Slipjoint was done. At the TU Delft, several master thesis and PhD studies were dedicated to the Slipjoint. Kamphuis (2016) investigated the mechanical behaviour of the Slipjoint connection of an onshore 500kW onshore wind turbine, for the DOT500 project. This turbine was installed by DOT at the Maasvlakte in Rotterdam, and used a Slipjoint connection between the tower and its foundation. The turbine tower was not specifically designed or manufactured to accommodate a Slipjoint, causing the contact area between the tower and foundation to be suboptimal. Despite this, it was found that the stresses within the material were well within the yield limit (Kamphuis, 2016). In a PhD study, (Segeren, 2018) researched vibration-induced settlement of slip joint connections for offshore wind turbines. He proposed to design the lower conical section to have a higher angle than the upper conical section. During installation, this would cause the lower section to elastically deform, ensuring good contact between the two sections. To enable the parts to fit well together, a vibrational installation technique was investigated. It was concluded that, using the correct frequencies, good settlement could be achieved.
After its onshore test, the 500kW turbine was used in an offshore test called Slipjoint Offshore Research (SJOR) project. This project consisted of the offshore installation of a monopile with a slipjoint connection, the offshore installation of a 500kW wind turbine with a Slipjoint connection, and subsequent testing of the Slipjoint connection. The turbine from the DOT500 project was outfitted with a new Slipjoint connector, and installed in a single lift onto a monopile. The

installation took less than one hour, showcasing the potential for Slipjoints to provide time savings in OWT installation (DOT, 2016). Further testing was performed in the Slipjoint Offshore Qualification (SJOQ) project, with the goal of increasing the Technology Readiness Level (TRL) of the Slipjoint technology to TRL 8-9, meaning that the technology has been tested and used in an operational setting. This goal was reached during the project, with an A-level certification by Det Norske Veritas (DNV) being achieved, which is comparable to TRL 8-9 (DOT, 2018). In the FOX6000 project, several other features of the Slipjoint were tested. One of these was the Slipjoint sea-fastening: using a Slipjoint lower section to fasten the tower onto the deck of the transportation vessel. Furthermore, a Slipjoint connection between the nacelle and the tower was tested. For this project, a larger 3MW turbine was used. During this project, the RNA installation technique mentioned in Section 2.1.3 was tested. The monopile-tower and tower-nacelle Slipjoint connections were attached and detached several times, repeatedly showcasing the ability of the Slipjoint to enable quick installation and removal of turbine parts (DOT, 2019). In 2020, two 9,5MW OWTs were installed at the Borselle V offshore wind farm using DNV-GL certified underwater Slipjoints. This was the first commercial use of Slipjoint technology (Van Oord, 2020).

It can be seen that the existing literature regarding slip joints focuses mainly on the technical design aspects of the slip joint itself, and the tests performed were on a small scale. So far, to the best of the authors knowledge, no research has been done regarding the costs and time savings when installing offshore wind turbines with a slip joint. The search queries used in the literature review are shown in Table 2.1. The citations in relevant papers were also used to find more relevant papers.

Search engine	Search query	Results
Scopus	slipjoint	0
Scopus	slip AND joint AND wind AND offshore	15
Scopus	slip-joint AND wind AND offshore	12
Google Scholar	slip AND joint AND wind AND offshore	>25.000

Table 2.1: Slip joint literature search queries

2.3. Offshore Logistics Modelling

While there may not be any literature regarding the logistics of offshore installation using the Slipjoint, there exists extensive literature regarding the simulation of offshore installation logistics via traditional installation methods. An overview of the current state of knowledge is given below.

(Paterson et al., 2018) develop a probabilistic simulation tool to investigate the performance of installation vessels and the associated installation risk in the construction of the UKs first and second round of OWF realisations. The authors generate several scenarios which are simulated using a Monte Carlo simulation along with weather data to predict the performance of installation vessels. This is done retrospectively, and the deviations of the actual installation times from the predicted installation times are used to assess the installation risk of the vessels.

(Scholz-Reiter et al., 2011) analyse the supply chain of offshore installations to identify the basic conditions and disturbances. Based on this, the authors develop a planning and control concept, and develop a Mixed-Integer Linear Programming (MILP) model to minimize the install time of offshore wind turbines under different weather conditions.

(Irawan et al., 2017) also use linear programming to optimize scheduling for the installation

of OWTs. The authors solve the model using both exact methods and metaheuristics. Their model uses a bi-objective function to minimise both costs and install time. The trade-off between these objectives is investigated.

(Amorosi et al., 2024) use MILP programming to calculate upper and lower bounds for installation costs. The authors simulate installation of foundations, superstructures and cables, with a focus on the latter. A light-robust MILP is used to incorporate weather uncertainty.

(Barlow et al., 2015) uses DES to model the installation time and costs for wind farms of different sizes, starting times and installation strategies under varying weather conditions. the authors identify which operations are critical for overall delays, and what relationships exist between vessel operational limits and installation duration. The same authors expanded their research into vessel characteristics in (Barlow et al., 2014). Here, the authors investigate the impact of certain vessel characteristics (capacity, speed, and significant wave height limits for sailing and jacking). It is concluded that vessel speed has an inverse linear relation with installation time, whereas vessel capacity and significant wave height limits for sailing and jacking have an inverse non-linear relation with installation time.

(Devoy McAuliffe et al., 2024) also employ DES to develop a tool in which both the capital and installation costs of fixed and floating wind farms can be calculated. Several options are given, such as assembly strategy, seabed preparation, cable laying strategy and options for the substructure. The authors validate their simulation results against the installation of the Hywind Scotland OWF.

(Tjaberings et al., 2022) investigate different installation strategies for substructures for offshore wind farms. the authors use DES and find that using multiple installation vessels reduces costs, and using the installation vessels as transport vessels is more cost-efficient than using dedicated transport vessels.

(Vis & Ursavas, 2016) develop a decision-support tool to compare different installation strategies (seperate parts, bunny ears, rotor star, see also Figure 2.2) under different conditions (distance to shore, vessel capacity). The different installation strategies are simulated using DES. The authors conclude that the bunny-ears strategy has a reduced installation time compared to the seperate parts strategy, due the reduced number of lifts. Furthermore, the bunny-ears strategy enables a higher vessel capacity than the rotor-star strategy, making it the most time- and cost-efficient strategy.

(Ait Alla et al., 2017) investigate the possible advantages of a base port feeder strategy in which feeder vessels transport components from the manufacturer to a base port, where they transfer the components to an installation vessel in order to reduce overall installation time. The authors compare conventional strategy with the base port feeder strategy for different OWF locations, sizes, and with and without weather influences. the authors find that the feeder concept only provides a time and cost reduction when the OWF is located close to shore, consists of a limited number of OWTs, and weather conditions are favourable. In (Oelker et al., 2018), the same authors expand on (Ait Alla et al., 2017) to investigate the possible benefits of an offshore feeder concept. In this concept, feeder vessels transport components from the manufacturer to the installation vessel at the windfarm, where the components are transshipped. The authors reach a similar conclusion, namely that the offshore feeder concept works best for smaller OWFs which lie closer to shore, during favourable weather conditions. the authors also find that using two feeder vessels outperforms one vessel, as the installion vessel has a reduced waiting time.

In (Oelker et al., 2021), the same authors investigated the possible benefits of using a tuned

mass damper during blade installation to increase wave limitations. The increased wave limitations were used in a DES to investigate the time and cost savings. The authors found that a 13.1% reduction in vessel cost could be achieved if the wave limit was increased from 1 to 1.3 meters by using tuned mass dampers.

(Muhabie et al., 2018) also uses DES to simulate the transport, assembly and installation of an offshore wind farm. The authors use both a deterministic and probabilistic method to incorporate weather effects into the model. the authors compare the two methods and show a good agreement between the methods, showing that probabilistic methods are a feasible method to incorporate weather effects into DES models. The probabilistic method, however, does need a large number of iterations to reach convergence of simulation outputs.

(O'Sullivan et al., 2011) use a stochastic event-sequencing model similar to DES to simulate different installation strategies. the authors compare a feeder strategy with one installation vessel to a more traditional installation strategy using either one or two jackup vessels. A Markov model is used to create weather simulations. The simulation is run multiple times so that the weather simulations converge to the initial Metocean data statistics.

A trend which can be seen in the mentioned papers is that most use DES, and incorporate weather in either a stochastic or deterministic manner. Some consider pre-assembly, but hardly any discuss full pre-assembly in depth.

For the literature review regarding simulation of installation of offshore wind farms, the search queries which were used can be seen in Table 2.2. Here, relevant papers were also found by looking at the citations of relevant papers.

Search engine	Search query	Results
Scopus	offshore AND wind AND farm AND installation AND simulation	247
Scopus	offshore AND wind AND farm AND installation AND discrete AND event AND simulation	15
Google Scholar	offshore AND wind AND farm AND installation AND simulation	> 18.000

Table 2.2: Search queries for offshore wind farm installation simulation.

2.4. Knowledge Gap

Figure 2.5 provides an overview of the current research on installation strategies for offshore windfarms. It includes which types of structure is investigated (foundation, turbine or cables), how the influence of weather was modelled (stochastic or deterministically), whether a pre-assembly strategy was considered, and whether the use of a Slipjoint is considered.

As can be seen in the table, most studies employ DES. This is because the installation of offshore structures, especially OWTs, is a process with many sequential steps, which all have certain conditions under which they can be executed. Furthermore, the installation of an OWF has a cyclic nature: the installation vessel(s) install the OWTs in multiple batches or cycles. DES operates in a sequenced and cyclic manner, making it very suitable to model the installation of OWFs, see also Section 3.1. For this reason, this research will also employ DES to simulate the installation of OWTs. Furthermore, it can be seen that the researches are almost evenly divided between stochastically and deterministically integrating weather influences into the simulations. In this research, a deterministic method is chosen. This approach ensures that the simulation uses realistic historical weather patterns, therefore ensuring the model pro-

duces realistic weather windows. By avoiding probabilistic weather scenarios, the comparison between the standard and Slipjoint method can be fairly made, and results can be more easily verified and replicated.

From Figure 2.5 it can be seen that none of the papers in the literature have considered the possible impact of the use of a Slipjoint on the installation performance. Therefore, there exists a gap in the knowledge which this research aims to fill. In this research, the impact of the use of a Slipjoint on installation performance such as installation time, cost, and weather workability will be analysed using DES. In the next chapter, the application of the DES model will be outlined.

Study	Structure	Model type	Weather	Pre-assembly	Slipjoint
Ait Alla et al. (2017)	T	DES	D	✗	✗
Amarosi et al. (2024)	F&T&C	MILP	D	✗	✗
Barlow et al. (2014)	F&T	DES	S	✓	✗
Barlow et al. (2015)	F&T	DES	S	✓	✗
Devoy McAuliffe et al. (2024)	F&T	DES	S	✓	✗
Irawan et al. (2017)	F&T	MILP	S	✗	✗
Muhabie et al. (2018)	F&T	DES	D&S	✓	✗
Oelker et al. (2018)	T	DES	D	✗	✗
Oelker et al. 2021	T	DES	D	✗	✗
O'Sullivan et al. (2011)	F&T	DES	S	✓	✗
Paterson et al. (2018)	F&T	MCS	S	✓	✗
Scholz-Reiter et al. (2011)	F&T	MILP	S	✗	✗
Tjaberings et al. (2022)	F	DES	D	✗	✗
Vis and Ursavas (2016)	T	DES	S	✓	✗
This study	**T**	**DES**	**D**	✓	✓

Abbreviations

T	Turbine	DES	Discrete-Event Simulation
F	Foundation	MILP	Mixed Integer Linear Programming
C	Cable	MCS	Monte Carlo Simulation
D	Deterministic	S	Stochastic

Figure 2.5: An overview of the reviewed literature showing structure type, weather simulation method, pre-assembly, and the use of Slipjoints in the installation process.

3

Methodology

3.1. Discrete-Event Simulation

From Chapter 2, it has become clear that Discrete-Event Simulation is the most suitable method of modelling the construction of offshore wind farms. To compare the installation of OWFs using traditional installation methods and the Slipjoint installation method, a DES model is constructed. DES is a modelling technique to simulate systems in which the states of the objects within the system are changed at discrete points in time. The changes in state are triggered by certain events beginning or ending. For example, the activity 'sailing to OWT' can be triggered by the activity 'loading OWT parts' ending. The state of an object does not change if it is not involved in an event. The progression of time in the simulation is modelled through the occurrence of events, it is not continuous. Events can be manually sequenced in serial or parallel to each other, or programming logic (if, while, for, etc.) can be used to trigger and stop certain events based on other events occurring. Using a combination of sequencing and logic, complex systems with many different activities and entities can be modelled. DES uses object-oriented programming concepts to model the entities in the model. Classes are used to define what types of objects there are in the model, and what properties they have. Objects can then be instantiated from the class, and their properties are specified to define their behaviour. These entities are then used in events to run the simulation. Weather effects can be incorporated into the simulation by postponing events when weather conditions exceed the set limits. These factors make DES well-suited for sequential, weather-dependent, and time-sensitive processes such as the installation of OWTs.

3.2. Simulation Software

There are many different simulation software environments in which DES can be used. There exist roughly two types of tools to construct DES models in: GUI-based tools and programming based tools. Each approach offers different advantages and trade-offs, depending on the complexity of the system being modelled and the desired flexibility when constructing the model. GUI-based tools such as FlexSim, Arena, and Simio use drag-and-drop interfaces and preset modules to construct simulation models visually. These tools are useful for quick and efficient programming of systems, and can provide good presentations of the model. However, GUI-based tools can be limiting when a high degree of customization is required, as the scripting language is often less advanced than conventional programming languages like Python.
Programming-based tools such as SimPy (Python), DESMO-J (Java) or OMNeT++ (C++) offer greater flexibility and customisation over the model structure and logic. These tools are

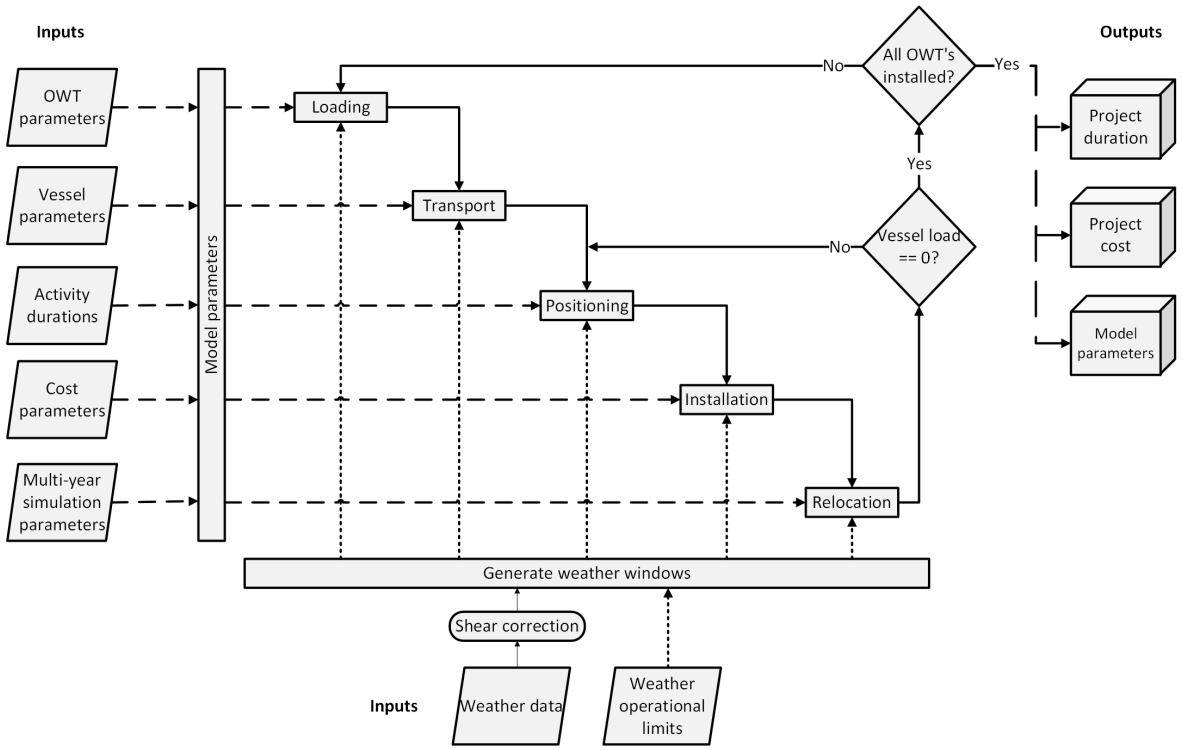

Figure 3.1: An overview of the DES model structure, inspired by (Tjaberings et al., 2022).

favoured in academia, where reproducibility and integration with other analytical libraries are important. Programming-based tools enable fully customised simulation models and data analysis. There is, however, a steeper learning curve associated with the use of a programming-based tool.

For this study, a fully customisable model, advanced data processing and the possibility to integrate with other models was needed. Therefore, a programming-based tool was selected. After consultation with the thesis supervisors, OpenCLSim was recommended as simulation tool. After some research into the program and alternatives such as Salabim, Simulus and CIW, OpenCLSim was selected due to it being well-suited for simulation of offshore logistics. OpenCLSim is a Simpy-based Python package designed for cyclic, rule-driven activities (OpenCLSim, 2023). It was developed by the Ports and Waterways department of the Civil Engineering facility at the TU Delft, along with Van Oord, Deltares and Witteveen+Bos. It can be used to compare the performance of different operational strategies. OpenCLSim also features a Weather plugin, allowing the user to simulate the influence of weather conditions on the process being simulated. The plugin uses Metocean datasets, many of which are publicly available. OpenCLSim was developed specifically for simulating offshore logistics, making it ideal for this research. Furthermore, because the software is Python-based and open-source, full customisation of the simulation is possible, and the simulations can be reproduced.

3.3. Model Structure

A diagram of the simulation model structure is given in Figure 3.1. The model takes parameters to create installation site, vessel and port objects. See Section 3.7 for more information about the models input parameters and their quantification. The created objects are then used in activities. Loading, transport, positioning (including jackup/down or (de)submerging), installation and relocation activities are sequenced and cycled through. Conditional logic controls

ensure the new cycle begins at the right activity. The model uses weather windows to incorporate weather influences in the simulation. Using the shear-corrected weather data (see Section 3.8 and the operational weather limits, the model generates workable weather windows. These are timeframes in which the weather states do not exceed the operational limits of the vessel or activity being simulated. Before each activity can take place, the model checks if there is a sufficiently large weather window available in the weather dataset to execute the activity. If this is not the case, the model will enter a waiting state, until a weather window of sufficient length becomes available. The necessary length of the weather window depends on the activity duration and on the weather operational limits set by the user. When the simulation has been completed, i.e. all OWTs are installed, the model will generate the results. The total durations, costs, and the parameters used in the simulation are saved to a .json file for postprocessing.

Figure 3.2 shows the logic flow of the model when it is simulating a standard installation. It can be seen that, if a weather window of sufficient length is not available, a waiting activity is started, which ends when a suitable weather window becomes available. The dotted lines indicate cycle logic flow. The model returns to an earlier part of the logic flow to repeat certain activities. In this way, cyclic activities such as loading the parts and installing OWTs are incorporated into the model. The Slipjoint installation methods' logic flow differs from the standard installation method in several aspects, mainly in the loading and installation cycles. The logic-flow diagram of the Slipjoint installation method is given in Figure 3.3. It can be seen that the loading and installation cycles consist of fewer steps, due to the OWTs being loaded and transported completely pre-assembled.

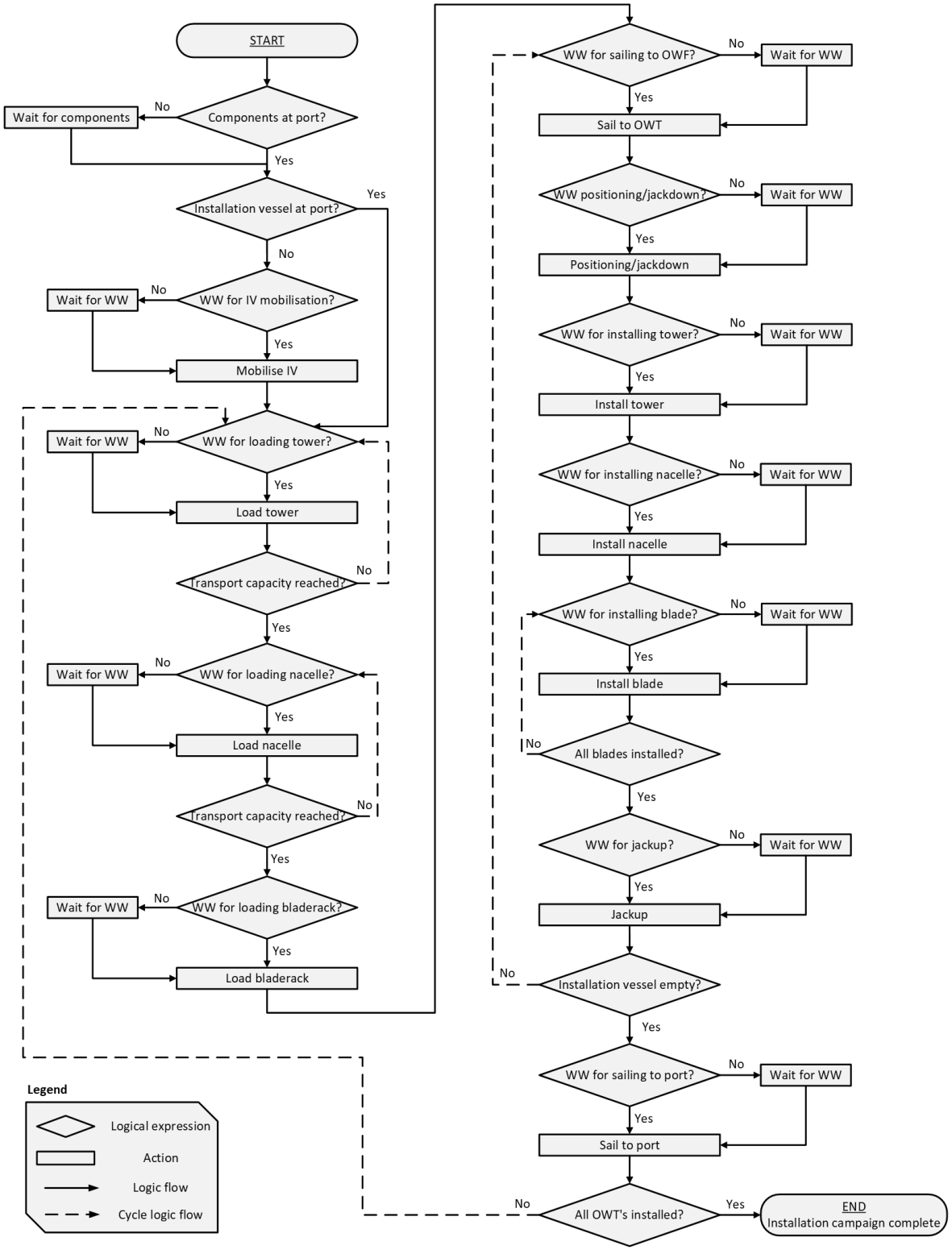

Figure 3.2: Logic-flow diagram of the standard installation model, inspired by (Tjaberings et al., 2022).

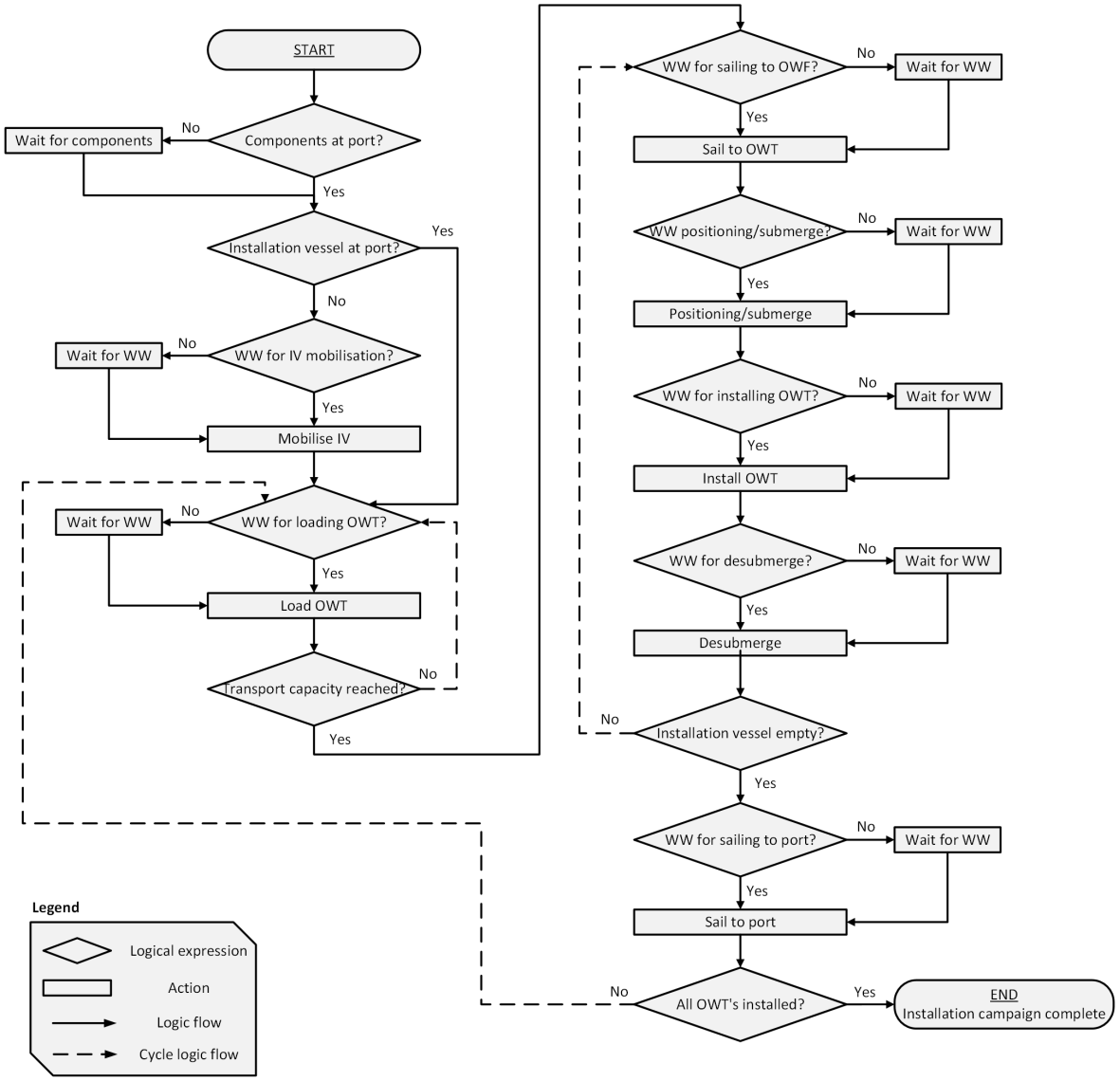

Figure 3.3: Logic-flow diagram of the Slipjoint installation model, inspired by (Tjaberings et al., 2022).

3.4. Modelling Assumptions

To make sure the DES model remains manageable in size and complexity, a set of assumptions have to be made. It is important that the model remains representative of the real-world situation when these assumptions are applied. An overview of the assumptions is given below.

1. **Foundations already in place**
   It is assumed that the monopile foundations for the turbines are always available for installation when the installation of the superstructures begins. In other words, the installation of the superstructures will never be delayed because of delays in the previous foundation installation phase.
2. **Availability of crew and vessels**
   It is assumed that the crew and vessels are available for the entire duration of the simulation. Crew fatigue, vessel maintenance or port restrictions are not taken into account.
3. **No equipment failures**
   It is assumed that all equipment, such as vessels and cranes, do not have any failures which hinder their operations. It is also assumed any necessary maintenance which is carried out does not hinder the installation campaign, and therefore does not influence the durations or cost of the campaign.
4. **Weather forecast**
   The loading and installation activities are affected by the weather. If the weather state is outside the limits, the activity cannot be started. The model works by checking if, for the duration of the upcoming activity, the weather state falls within the limits. It is assumed that the crew always has accurate weather forecasts at their disposal for the duration of the weather windows, ensuring that no activity will be started which lasts longer than the available weather window, and that no activity is interrupted by adverse weather conditions.
5. **Limiting weather state**
   There are three main activity types in the model: loading, transporting and installing. For the loading activities, it is assumed that the wind speed will be the weather factor which is the most limiting, as the installation vessel is situated in the port, where the waves are likely to be less significant than the wind. During transport, the significant wave height is assumed to be the limiting weather factor, as the waves will cause the vessel to heave and roll, affecting the load more than wind. For the installing activity, wind speed is again assumed to be the limiting weather factor, as the installation vessel is jacked up and therefore unaffected by waves (in the case of standard installation using a jackup vessel), or semi-submerged in the case of installation using a semi-submersible. Furthermore, the OWTs are installed using cranes, where the wind will cause them to sway.

3.5. Learning Effects

During an installation campaign, it can be observed that the time it takes to complete certain activities gradually decreases (McDonald & Schrattenholzer, 2001). This is explained by learning effects: as crews gain experience with the tasks they are carrying out and learn the most efficient ways of working, they are able to increase their working speed. In 1936, T. P. Wright first quantified this relation (Wright, 2012). He found that there was a relationship between the doubling of the amount of units produced, and the reduction in production time per unit. The percentage reduction in production time per doubling of working instances is called the learning rate. Since then, learning rates have been shown to be present in many different industries,

albeit with different rates to the airplane manufacturing Wright investigated. The offshore wind sector is no exception: it features learning rates of 8-18% (McDonald & Schrattenholzer, 2001). Accounting for the learning effect in the simulation could increase its accuracy and help to better represent the real world scenario. To incorporate the learning effect into the model, the durations of loading and installing activities are decreased as the number of installed OWTs increases. The following formula is used in the model to account for learning effects:

$$T_n = T_1 \cdot n^{\frac{\log(1-r)}{\log(2)}} \tag{3.1}$$

Where:

- T_n is the installation time for the n^{th} batch,
- T_1 is the base installation time,
- n is the batch number,
- r is the learning rate.

In this formula, a learning rate of 10% means that after each doubling of installation cycles, the installation time is 90% of the original installation time. In other words, the installation time is reduced by 10% for every doubling of the number of installation batches. In this study, a learning rate of 10% is chosen for installation activities, as these are activities where there is room for improvement through learning. This value is in line with learning rates for European wind projects (McDonald & Schrattenholzer, 2001). For loading activities, a learning rate of 5% is chosen, as this is a type of activity where improving efficiency is still possible, but the activities are more routine and therefore the potential improvements are slightly less than installation activities.

3.6. Model Inputs

The model uses a set of user-defined input parameters to run the simulation. These include OWT properties, installation vessel parameters, durations of loading and installing activities, maximum weather states, mobilisation costs and day rates, and parameters defining the multi-year simulation. An overview of the model inputs is given in Table 3.1. Furthermore, the model takes two Metocean datasets as inputs: one dataset of the wind speed and one for the wave height weather parameters. These datasets are loaded into the model, where they are filtered and processed so the model is able to work with them.

3.7. Data Gathering

In order for the model to run, the parameters must be quantified. To ensure a good validity of the model, the values of the parameters must be substantiated and resemble the real situation as closely as possible. For some of the parameters it was possible to get the actual value from reports or documentation. Other parameters were obtained from interviews with experts at Van Oord, Tasports and DOT. In the following subsections, an overview is given on how each parameter was quantified. The gathering of the number of OWTs and their coordinates is given in Chapter 4.

3.7.1. Weather datasets

The weather datasets were obtained from metocean-on-demand.com, a data portal by DHI group (DHI, 2025). For each case study, three datasets are used: one wind dataset at the port site, one wave dataset on the route from the port to the installation site, and one wind

OWT parameters (see Chapter 4)		
number_turbines	The number of turbines to be installed	[-]
OWT_coordinates	A list of Point coordinates of the OWT locations	[-]
Installation vessel parameters		
jackup_capacity	The number of OWTs the installation vessel can transport	[-]
jackup_speed_emtpy	The cruising speed of the installation vessel when empty	[kn]
jackup_speed_full	The cruising speed of the installation vessel when fully loaded	[kn]
mob_cost_jackup	The (de)mobilisation cost of the installation vessel	[$]
day_rate_jackup	The dayrate of the installation vessel	[$]
Weather parameters		
max_wave_sailing	The maximum allowed wave height for the activity 'sailing'	[m]
max_wave_jackupdown	The maximum allowed wave height for the activity 'jacking up/down'	[m]
max_wind_loading	The maximum allowed wind for the activity 'loading'	[m/s]
max_wind_installing	The maximum allowed wind for the activity 'installing'	[m/s]
Activity durations		
tower_load_duration	The time it takes to load one tower onto the installation vessel	[s]
nacelle_load_duration	The time it takes to load one nacelle onto the installation vessel	[s]
bladerack_load_duration	The time it takes to load the bladerack onto the installation vessel	[s]
jack_up_down_duration	The time it takes the installation vessel to perform the jackup/down manoeuvre	[s]
tower_install_duration	The time it takes to install one tower onto the installation site	[s]
nacelle_install_duration	The time it takes to install one nacelle onto the installation site	[s]
blade_install_duration	The time it takes to install one blade onto the installation site	[s]
Multi-year simulation parameters		
num_years	The number of years for which the multi-year simulation is run	[-]
datapoints_per_year	The number of simulation start dates per year	[-]
start_year	The first year to be simulated in the multi-year simulation	[-]

Table 3.1: All model input parameters.

dataset at the installation site. For the Ecowende wind datasets, the COSMO Reanalysis 6km (CREA6) datasets are used. These are high-resolution atmospheric datasets from an atmospheric prediction model. It covers a part of Europe including the North Sea ("BARRA-R2 Dataset Details", 2025). For the Ecowende wave dataset, DHIs Dutch Wind Farm 23 (DWF23) dataset is used. This dataset was specifically developed for offshore wind farm construction ("SW_DWF23 Dataset Details", n.d.). For the Tasmanian wind data, the Bureaus Atmospheric high-resolution Regional Reanalysis for Australia (BARRA-R2) dataset was used. This is an Australian regional atmospheric dataset, used for offshore projects ("BARRA-R2 Dataset Details", 2025). The global high-accuracy Fifth ECMWF ReAnalysis (ERA5) dataset was used for the wave data in the Tasmanian casestudy ("ERA5 Dataset Details", n.d.).

3.7.2. Installation vessel performance and cost parameters

To simulate the installation vessel, several parameters have to be quantified. Different installation vessels are used for the standard installation method and the Slipjoint installation method.

Boreas

For the standard installation method in the Ecowende case study, Van Oords Boreas jackup installation vessel (see Figure 3.4a) will be used (TenneT, 2025). The parameters that have to be quantified are its capacity, sailing speed when full, sailing speed when empty, mobilisation costs and day rate. The capacity of the Boreas to carry 15MW wind turbines is not public knowledge. However, its capacity can be derived from other sister vessels made by the same manufacturer. The Boreas is an Atlas C-Class wind turbine installation vessel produced by Knud E. Hansen. The manufacturer specifies that it can carry parts for six 15MW OWTs at a time, its capacity therefore being 6 (Knud E. Hansen, n.d.). its sailing speed is 12-13 knots (Van Oord, 2021). It is unclear if this concerns the empty or full sailing speed. An interview with Van Oord employees did not provide any clarity, as they could not disclose competitively sensitive information. However, as will become clear in Section 3.9.1, the difference in speed between full and empty vessels is quite small, less than one knot. Therefore, the sailing speed when full is set to be 13 knots, and the sailing speed when empty is set to 12 knots. Because of it being competitively sensitive information, mobilisation costs and day rates of the Boreas could also not be disclosed. Therefore, literature and DOT employees were consulted. The mobilisation costs were estimated to be $1.500.000 for the Ecowende case, when mobilising out of the Rotterdam port (Kaiser & Snyder, 2010). The day rate of the Boreas is estimated at $500.000, which is typical for advanced jackup installation vessels such as the Boreas.

It is not yet known what vessel will be used for the installation of the Star of the South OWF. However, an interview was conducted with the Manager Development Projects of Tasports, in which it became clear that an installation vessel similar to the Boreas would likely be used for the installation of the OWTs. The Boreas itself was even one of the possible installation vessels. Therefore, the same vessel parameters are used for the Star of the South installation vessel as for the Ecowende installation vessel (Boreas). The mobilisation costs, however, do differ from the Ecowende case. For the Star of the South OWF, the mobilisation costs will be higher, as it is likely that the installation vessel will have to be mobilised from a location further away, as there are currently no OWT installation vessels stationed in Australia (Melissa Keane et al., 2023). It is assumed that the vessel has to be mobilised from China, as it is one of the largest offshore wind markets near Australia. The distance to Tasmania is still around 5000 nautical miles, therefore the mobilisation costs are estimated to be $4.500.000 (Kaiser & Snyder, 2010). The dayrate of the installation vessel is assumed to be the same.

(a) (b)

Figure 3.4: Van Oordss newest offshore wind turbine installation vessel Boreas (left, source: (Van Oord, 2021)) and Heeremas Sleipnir (right, source: (OffshoreWIND.biz, 2025))

Heavy-Lift Vessel

For the Slipjoint installation method, using a complete pre-assembly strategy, a Heavy-Lift vessel is needed, see also Section 4.2.2. There are many types of HLVs, each with their own characteristics, to choose from. Table 3.2 shows a list of HLVs and their characteristics, increasing in size and lifting capability.

Vessel	Length [m]	Beam [m]	Lifting Capacity [tn]	Main Crane Type	Owner
Bokalift 1	224	36	3,000	Revolving Crane	Boskalis
Bokalift 2	255	44	4,000	Revolving Crane	Boskalis
Oleg Strashnov	183	47	5,000	Revolving Crane	Seaway 7
Orion	216	49	5,000	Slewing Crane	DEME
Saipem 7000	198	87	2 × 7,000	Revolving Cranes	Saipem
Sleipnir	220	102	2 × 10,000	Dual Slewing Cranes	Heerema

Table 3.2: Overview of Heavy-Lift Vessels and their characteristics.

The most important reason an HLV is necessary for the Slipjoint installation, is the fact that the OWTs are transported upright, and therefore have a very high centre of mass. This high centre of mass can cause stability issues. A ship is stable if there is a righting moment when the ship starts to roll. This righting moment depends on the righting lever, which in turn depends on the horizontal distance between the shifted centre of buoyancy (B1) and the centre of gravity (G). The point where the vertical line from B1 intersects the keel line, on which G generally lies, is called the metacentric height M. As can be seen in Figure 3.5, the vessel remains stable as long as G does not cross M on this line. Raising the centre of gravity (G), for example by transporting wind turbines upright, reduces the distance between B1 and G. If this distance reaches zero or negative values (where G shifts beyond B1), G crosses M, causing the ship to become unstable and risk capsizing. It is therefore critical that the centre of gravity never extends out over the centre of buoyancy. Because the OWTs have such a high centre of gravity, around 100 metres from the deck, the centre of gravity of the vessel including load is raised, raising the risk of the vessel becoming unstable.

To ensure there is no risk of the installation vessel capsizing, the most stable vessel is chosen for this study. Vessel roll stability is determined, among other factors, by its beam. From Table 3.2, it is clear that the Sleipnir has the largest beam. Furthermore, the Sleipnir is a semi-

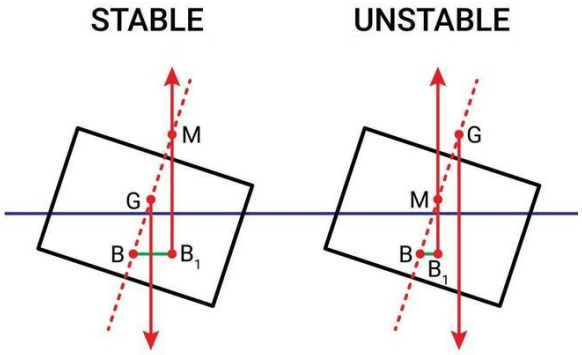

Figure 3.5: Schematical representation of a stable and unstable vessel configuration.

submersible, with large ballast tanks which can be used for extra stability. For this reason, Heeremas Sleipnir (see Figure 3.4b) is chosen. It should be noted that, due to its large beam, the Sleipnir does not physically fit into the Eemshaven and Bell Bay base ports. Choosing the Sleipnir as HLV was done primarily to ensure the chosen HLV was stable while transporting complete OWTs. The maximum dimensions for vessels entering the Eemshaven are 300 by 50 metres, with a maximum depth of 12 metres ("Toelatingsbeleid Eemshaven", n.d.). The vessels Bokalift 1 and 2, Oleg Strashnov and Orion from Table 3.2 all adhere to these dimensions, and would therefore fit into the Eemshaven, but may be more unstable than the Sleipnir when transporting complete OWTs. More research should be done into the minimum requirements for the HLV, so that a vessel with suitable dimensions for the base ports can be selected. However, this is outside the scope of this study.

The Sleipnir is equipped with two cranes, each with a lifting capacity of 10.000 tonnes (Heerema Marine Contractors, 2020). This lifting capacity is needed to load and install complete OWTs, as harbour cranes aren't capable of lifting such masses. For the Sleipnir, the same parameters as the Boreas have to be quantified: capacity, sailing speed when full, sailing speed when empty, mobilisation costs and day rate. In the Sleipnirs technical specifications (Heerema Marine Contractors, 2020), the "minimum service speed" is defined as 10 knots. It is therefore assumed that its sailing speed when full and sailing speed when empty are both 10 knots. The Sleipnirs capacity for transporting OWTs is not known, as it has never been used for installation of large batches of turbines. Furthermore, the OWTs that it will transport are transported completely pre-assembled and upright, something which has also never been done with turbines of this size. To solve this, the Sleipnirs capacity can be treated as a variable, to see what impact different capacities have on its installation performance. To evaluate the impact of the capacity on performance, a capacity of 2 and 4 are simulated. For the Sleipnirs mobilisation cost, experts at DOT were consulted, as well as literature regarding the use of HLVs such as the Sleipnir. A day rate of $800.000 was estimated, with a cost of $3.000.000 for mobilisation to the Eemshaven from Rotterdam, and $9.000.000 for mobilisation to Tasmania from China.

An overview of the installation vessel parameters of the Boreas and the Sleipnir is given below.

3.7.3. Weather parameters

In the simulation model, the weather parameters dictate what the maximum allowed weather states are during operations. In this study, these concern either significant wave height or wind speed. For every activity, a maximum allowed wind speed or wave height is set. As explained in Section 3.4, the wind speed is considered the critical weather factor for loading and installation activities, while the significant wave height is considered the critical weather

		Boreas	Sleipnir
Capacity	[-]	6	2 & 4
Sailing speed when empty	[kn]	13	10
Sailing speed when full	[kn]	12	10
Day rate	[$]	500.000	800.000
Mobilisation cost Ecowende	[$]	1.500.000	4.500.000
Mobilisation cost Tasmania	[$]	3.000.000	9.000.000

Table 3.3: The installation vessel parameters used in the model for the Boreas and the Sleipnir.

factor for the sailing activities. The quantified weather parameters are shown in Table 3.4. These parameters are based on interviews with industry experts, both from DOT and Van Oord, and on existing literature (Oelker et al., 2021; Barlow et al., 2015; Barlow et al., 2014; Muhabie et al., 2018; Rippel et al., 2019; Muhabie et al., 2015).
For Sailing activities, the maximum significant wave height is 2.5 metres. Larger swells could cause the fastenings of the turbine towers, which have a high centre of gravity and are only secured at the bottom, to exceed their stress limits. For transport of complete turbines, this effect is even greater due to their higher mass and centre of gravity. However, the Slipjoint seafastening has greater stress limits than traditional sea fastenings, due to its greater contact area. Furthermore, the Sleipnir is a larger, more stable vessel than the Boreas, compensating for the higher CoG of the complete turbines. For the jackup activities, a stricter maximum significant wave height of 1.8 metres is applied. This is due to the sensitive nature of the jacking up process: the lowering of the four legs has to be done precisely and carefully in order to ensure the vessel can be lifted up safely, without a chance of it suddenly sinking further during installation. Large waves can interfere with the jacking up process. For the loading activities of the towers, nacelles and the bladerack, the wind limit is 12 m/s. Wind speeds that exceed this threshold could hinder loading operations by causing unwanted swaying of the parts being loaded. The same limit applies to the installation of the towers and nacelles. The installation of the blades has a stricter wind limit. This is due to wind turbine blades being designed to be lightweight and to catch the wind. They are therefore more affected by wind gusts than towers or nacelles, necessitating stricter limits. The loading and installation of complete OWTs have stricter wind limits for the same reason.

Standard installation (Boreas)		
max_wave_sailing	[m]	2.5
max_wave_jackupdown	[m]	1.8
max_wind_loading	[m/s]	12
max_wind_installing	[m/s]	12
max_wind_installing_blades	[m/s]	10
Slipjoint installation (Sleipnir)		
max_wave_sailing	[m]	2.5
max_wave_submerging	[m]	3
max_wind_loading	[m/s]	10
max_wind_installing	[m/s]	10

Table 3.4: Maximum weather values for all activities

3.7.4. Activity durations

As explained in Section 3.1, each activity in the simulation model has a duration. The durations of activities like sailing and waiting for weather are calculated by the model. For sailing activities, the duration is calculated by dividing the distance between the start and end point by the installation vessels speed. The distance between two lat-lon coordinates is calculated using the Pyproj Python package. In this package, the Earth is assumed to be an ellipsoid, in order to improve the accuracy of distance calculations over methods in which the Earth is assumed to be a sphere. The package uses the Karney method, a highly accurate and robust algorithm, to calculate the distances between two coordinates (Karney, 2013). The following formula is then used to calculate the durations of the sailing activities:

$$d_{sailing}^{s,e} = \frac{S_{s,e}}{V_{inst.vessel}} \tag{3.2}$$

Where:

- $d_{sailing}^{s,e}$ is the duration of a sailing activity from starting point s to end point e,
- $S_{s,e}$ is the distance between the start point (s) and end point (e),
- $V_{inst.vessel}$ is the speed of the installation vessel.

Before any activity can begin, a weather window of sufficient length is needed, see also Section 3.3. If there is no window of sufficient length available, the vessel enters a waiting state. This is realised through a waiting activity: an activity in which the vessel waits for better weather conditions. If a suitable weather window is immediately available for the next activity, the waiting duration is zero. The duration of waiting activities is calculated as follows:

$$d_{waiting}^{a,b} = t_{b,WW} - t_{a,end} \tag{3.3}$$

Where:

- $d_{waiting}^{a,b}$ is the duration of the waiting activity between activities a and b,
- $t_{b,WW}$ is the time at which a weather window of sufficient length opens up for the next activity,
- $t_{a,end}$ is the time at which the previous activity ended.

For the other activities (loading, positioning, jacking up/down, submerging and installation activities), the model cannot calculate the durations. This is because these activities don't have a set speed at which they are carried out, such as sailing activities, or are dependent on weather windows, such as waiting activities. Therefore, the durations have to be manually specified. To quantify the durations of these activities, interviews with industry experts at DOT and Van Oord were conducted, and literature sources were used (Oelker et al., 2021; Scholz-Reiter et al., 2011; DOT, 2019; Ait Alla et al., 2017; Muhabie et al., 2018; Rippel et al., 2019; Muhabie et al., 2015). The quantified durations are shown in Table 3.5. These values are used in the model to specify how long certain activities take, and to specify the length of the necessary weather windows for each activity.

3.7.5. Total duration of installation campaign

Using the activity durations shown in Section 3.7.4, the total duration of the simulation can be calculated as follows:

$$D_{total} = D_{mobilisation} + D_{sailing} + D_{loading} + D_{installing} + D_{waiting} \tag{3.4}$$

Standard installation (Boreas)		
tower_load_duration	[h]	6
nacelle_load_duration	[h]	4
bladerack_load_duration	[h]	6
jack_up_down_duration	[h]	4
tower_install_duration	[h]	6
nacelle_install_duration	[h]	6
single_blade_install_duration	[h]	4
Slipjoint installation (Sleipnir)		
OWT_load_duration	[h]	3
submerging_duration	[h]	2
OWT_install_duration	[h]	3

Table 3.5: Durations for loading, positioning and jackup/down and installation activities.

Where:

- D_{total} is the total duration of the installation campaign,
- $D_{mobilisation}$ is the total duration of the mobilisation activity,
- $D_{sailing}$ is the total duration of all sailing activities,
- $D_{loading}$ is the total duration of all loading activities,
- $D_{installing}$ is the total duration of all installing activities,
- $D_{waiting}$ is the total duration of all waiting activities.

The total durations per activity are defined below.

$$D_{mobilisation} = d_{mobilisation} \tag{3.5}$$

Where:

- $d_{mobilisation}$ is the duration of the mobilisation activity.

$$D_{sailing} = \Sigma_{p,t \in E}(d^{pt}_{sailing} + d^{tt}_{sailing} + d^{tp}_{sailing}) \tag{3.6}$$

Where:

- E is the set of edges that the installation vessel travels,
- $d^{pt}_{sailing}$ is the duration of sailing activities from port (p) to turbine (t)
- $d^{tt}_{sailing}$ is the duration of sailing activities from turbine to turbine
- $d^{tp}_{sailing}$ is the duration of sailing activities from turbine to port

$$D_{loading} = T(d_{load,tower} + d_{load,nacelle} + d_{load,bladerack}) \tag{3.7}$$

Where:

- T is the number of turbines to be installed in the campaign,
- $d_{load,tower}$ is the loading duration of one tower,

- $d_{load,nacelle}$ is the loading duration of one nacelle,
- $d_{load,bladerack}$ is the loading duration of the bladerack.

$$D_{installing} = T(d_{inst,tower} + d_{inst,nacelle} + 3 * d_{inst,blade}) \tag{3.8}$$

Where:

- T is the number of turbines to be installed in the campaign,
- $d_{inst,tower}$ is the installation duration of one tower,
- $d_{inst,nacelle}$ is the installation duration of one nacelle,
- $d_{inst,blade}$ is the installation duration of one blade.

$$D_{waiting} = \Sigma_{w,a \in A}(d_{wait}^{w,a}) \tag{3.9}$$

Where:

- A is the set of all activities in the simulation,
- $d_{wait}^{w,a}$ is the duration of the waiting activity w before commencing activity a.

Using equations Equation (3.4) to Equation (3.9), the total duration of the installation campaign can be calculated.

For Slipjoint installation, the loading and installation process differs from the standard process (see also Section 4.2.2). Therefore, Equation (3.7) and Equation (3.8) need to be adapted. For Slipjoint installation, they are as follows:

$$D_{loading,slipjoint} = T(d_{load,OWT}) \tag{3.10}$$

Where:

- T is the number of turbines to be installed in the campaign,
- $d_{load,OWT}$ is the loading duration of one OWT

$$D_{installing,slipjoint} = T(d_{inst,OWT}) \tag{3.11}$$

Where:

- T is the number of turbines to be installed in the campaign,
- $d_{inst,OWT}$ is the installation duration of one OWT.

3.7.6. Multi-year simulation parameters

The simulation is run over many years of weather data, to get good estimations of average performance and standard deviations. The parameters which specify the behaviour of the simulation which is run over multiple years are called the multi-year simulation parameters. These parameters are specified by the user. The parameter num_years defines for how many years the simulation will run. The more years are simulated, the more accurate the simulation results will be. The parameter is bounded by the weather datasets, as the simulation needs datapoints of all datasets for every time-point in the simulation. The maximum value

for num_years is therefore determined by subtracting the latest start-date of all datasets from the earliest end-date of all datasets. This ensures that all three types of weather data are available for the complete duration of the simulation. For Ecowende and Tasmania, the latest start date is 01-01-1995 and the earliest end date is 01-09-2019. This makes the maximum number of years which can be simulated 24. The datapoints per year parameter specifies how many start dates are generated per year. This influences the resolution of the results, a higher number of datapoints per year gives a more detailed insight into the installation performance per start date. For the multi-year simulations, 24 start dates per year are used.

3.8. Wind Shear Correction

The wind speed values of both the CREA6 and BARRA-R2 datasets are expressed at a height of 10 metres (“COSMO-REA6 Dataset details”, 2025)(“BARRA-R2 Dataset Details”, 2025). However, the loading and installation activities of offshore wind turbines are carried out at much greater heights. The turbine towers are lifted vertically, with the lifting point at the top of the tower. When loading and installing towers or complete turbines, the lifting point is located at the hub height. For the Vestas V236 OWTs, the hub height is around 150 metres, as indicated in a life-cycle assessment report by Vestas (Vestas, 2024). To ensure that the model remains accurate in its simulation, this discrepancy between measurement height and lifting height must be corrected. This is especially important for the simulation of loading and installing complete turbines, such as during the Slipjoint installation campaigns, as the centre of gravity is located much higher when lifting a complete OWT than it is when lifting just a tower. The wind data values must therefore be expressed at the hub height. To correct the measurements at 10 metres to the hub height of 150 metres, a wind shear correction is applied. The relation between wind speed and height above ground can be given with a power law, as explained in the TU Delft course Offshore Wind Farm Design (van Bussel & Bierbooms, 2004):

$$\frac{U(Z)}{U(Z_r)} = \left(\frac{Z}{Z_r}\right)^{\alpha} \tag{3.12}$$

Where

- Z is the height above ground for which to calculate the horizontal wind speed
- Z_r is the reference height
- $U(Z)$ is the horizontal wind speed at height Z
- $U(Z_r)$ is the known wind speed at reference height Z_r
- α is the wind shear correction factor

This equation ”gives reasonable results for the correct value of α” (van Bussel & Bierbooms, 2004). It can be adapted to calculate the corrected wind speed at the hub height from the wind speed at measurement height:

$$U(Z_h) = U(Z_m)\left(\frac{Z_h}{Z_m}\right)^{\alpha} \tag{3.13}$$

Where

- Z_h is the hub height above ground
- Z_m is the measurement height above ground

- $U(Z_h)$ is the horizontal wind speed at the hub height
- $U(Z_m)$ is the horizontal wind speed at the measurement height
- α is the wind shear correction factor

This formula is used in the model to correct the wind speed dataset from 10 metres above ground to 150 metres. Typical wind shear correction factors range from 0.11 to 0.14 (van Bussel & Bierbooms, 2004). According to (Hsu et al., 1994), a correction factor of 0.11 is accurate for open sea conditions with calm weather. A report by Det Norske Veritas (DNV) on Standards and Recommended Practices (Det Norske Veritas, 2010) states that $\alpha = 0.12$ for open sea conditions with waves. Taking the average of the two and using $\alpha = 0.115$, $Z_h = 150$ and $U(Z_m) = 10$, the wind speed values in the dataset at 10 metres are multiplied by:

$$U(150) = U(10)\left(\frac{150}{10}\right)^{0.115} = 1.365 * U(10) \tag{3.14}$$

3.9. Model Validation

To verify that the model is accurate, a validation is needed. This is usually done by running a simulation of the model on a certain case for which actual results are available, and comparing the output of the model to the real measurements. As the Ecowende and Star of the South wind farms have both not yet begun with construction, a different source must be found for validation. In the interview with Van Oord employees, they recommended that the Wind Peak and the Voltaire installation vessels are both similar vessels to the Boreas, and are already in use. They can therefore be used to validate the model by comparing the model to these vessels.

3.9.1. Wind Peak

The Wind Peak, see Figure 3.6a, is a jackup vessel owned by Cadeler, which is specialised in installation of OWTs. It is a P-Class Wind Turbine Installation Vessel built by COSCO, and has recently gone into operation. In April 2025, it started with the installation of 100 OWTs at the Sofia offshore wind park, located off the coast of England. Data regarding the installation and cycle times is not publicly available. However, the vessels can be tracked using public Automatic Information System (AIS) data. Using the Lautec WindGIS online application(LAUTEC, 2015), the current location, heading and velocity of the vessel can be tracked. More importantly, also the past location, heading and velocity can be tracked. Using the application, data can be collected about the vessels activities. The time the vessel spends at the port, when it leaves port, when it arrives at the OWF, how long it spends installing each OWT, and when it returns to port can all be tracked. This can give a good indication of loading times, installation times and cycle times. The first four batches of six OWTs were analysed, and the results can be seen in Table 3.6. For the complete analysis, see Table A.1. The time spent at port and the time spent offshore are shown, along with a calculation of offshore time per turbine.

3.9.2. Voltaire

The Voltaire, see Figure 3.6b, is an Atlas C-Class Wind Turbine Installation Vessel, made by Knud E. Hansen. The Boreas is the same class vessel, made by the same manufacturer. It is currently installing 277 OWTs at the Dogger Bank wind farm, around 200 kilometre off the coast of Yorkshire. In Dogger Bank phase A, which is under construction at the time of writing, the Voltaire is installing GE Haliade-X 13MW turbines. With a rotor diameter of 220 metres,

Port calls		Port Stay	Offshore Time	Offshore time per turbine
30-06-2025 21:05				
			19,15	3,19
7-6-2025 14:21	11-6-2025 17:24	4,13		
			20,29	3,38
8-5-2025 14:56	18-5-2025 07:22	9,68		
			16,66	2,78
17-4-2025 07:46	21-4-2025 23:07	4,64		
			27,99	4,67
12-3-2025 16:43	20-3-2025 07:58	7,64		
			Average offshore time per turbine:	3,50

Table 3.6: Wind Peak port calls, loading times, offshore times and offshore times per turbine.

(a) (b)

Figure 3.6: Cadelers newest offshore wind turbine installation vessel Wind Peak (left, source: (Van Oord, 2021)) and Jan de Nuls Voltaire (right, source: (OffshoreWIND.biz, 2025))

these are slightly smaller than the Vestas V236 15MW wind turbines that will be installed at Ecowende, which have a rotor diameter of 236 metres. This could make the installation time per turbine slightly shorter than for the larger 15MW turbine, but it should still provide some valuable insight. The Voltaire is again analysed using the Lautec WindGIS software to determine its port calls and offshore times. A calculation can then be made determining the average loading and offshore time per turbine.

3.9.3. Model validation

To validate the model using a comparison to the two vessels mentioned before, the model is run on their respective installation campaigns. The duration outputs are compared with durations of vessels currently in operation. Only the model duration performance could be validated, as no data regarding the installation costs is publicly available.

For the Wind Peak, the model is set to install wind turbines at the Sofia Wind Farm out of Hull Port, starting on March 15th. These parameters replicate the actual installation of the Sofia wind farm, which began in March 2025. To fairly compare the model and the actual installation times of the Wind Peak, the model is set to install 24 turbines, as that is how many the Wind Peak has currently installed. The model was run over the full range of 24 years, and the results are shown in Table 3.8. It can be seen that both the actual times at port and actual offshore times are highly variable. The model underestimates both port times and offshore times for

Port calls		Port Stay	Offshore Time	Offshore time per turbine
28-6-2025 04:13				
			12,45	2,49
9-6-2025 00:30	15-6-2025 17:32	6,71		
			5,14	-
2-6-2025 06:21	3-6-2025 21:14	1,62		
			12,91	2,58
9-5-2025 12:37	20-5-2025 08:28	10,83		
			15,53	3,11
20-4-2025 18:20	23-4-2025 23:52	3,23		
			14,91	2,98
2-4-2025 04:42	5-4-2025 20:30	3,66		
			Average offshore time per turbine:	2,79

Table 3.7: Voltaire port calls, loading times, offshore times and offshore times per turbine.

the Wind Peak. This could be due to the Wind Peak having just being put into service, leading to activities taking longer than planned. Furthermore, the fact that the vessel has just been put into service likely generated extra tasks which had to be carried out, increasing the port and offshore time. However, the model does come within 5% of actual port and offshore times for batch 2, and for port time for batch 4.

	Port Stay			Offshore Time		
	Real	Model	Difference	Real	Model	Difference
Batch 1	7,64	4,74	-38%	27,99	20,76	-26%
Batch 2	4,64	4,42	-5%	16,66	16,04	-4%
Batch 3	9,68	4,15	-57%	20,29	15,93	-21%
Batch 4	4,13	3,97	-4%	19,15	13,05	-32%

Table 3.8: Wind Peak validation

For the Voltaire comparison, the model is set to install turbines at the Dogger Bank A wind farm from the port of Able Seaton. The available port data for the Voltaire starts from the 2nd of April 2025, therefore that is chosen as the starting date in the simulation. Since then, it has completed four trips of installing five OWTs, (see Table 3.7), therefore the number of turbines to be installed is set to 20. The simulation was run over 24 years, and the results are shown in Table 3.9. Firstly, it can be seen that the durations of the port stays vary significantly. This could be due to mechanical breakdown or maintenance of equipment being performed. The model does not account for this, which is reflected in the large differences in actual time spent at the port and the modelled time spent at port for batches two and three. However, the model achieves accuracies within 2% when loading is not hindered. The real offshore times are more consistent, between twelve and a half and fifteen days. It can be seen that the model slightly underestimates offshore time, with an average difference of -9% of modelled offshore time versus actual offshore time per batch. The model performs significantly better here, with a vessel which has been in service for a longer time, than for the Wind Peak comparison.

Overall, it can be seen that the actual offshore and port times are highly variable, causing some discrepancies between the model and reality. The model tends to give more consistent offshore and port times, which reduce throughout the progress of the project due to the

	Port Stay			Offshore Time		
	Real	Model	Difference	Real	Model	Difference
Batch 1	3,66	3,47	-5%	14,91	15,14	2%
Batch 2	3,23	3,15	-2%	15,53	13,45	-13%
Batch 3	10,83	3,16	-71%	12,91	11,98	-7%
Batch 4	6,71	3,04	-55%	12,45	10,18	-18%

Table 3.9: Voltaire validation

weather becoming more favourable. It is hard to say what causes the variability in the actual offshore and port times, as the only available information about the vessels is their location, not what their current activities are. Nevertheless, the model is able to accurately model the port and offshore times to within 5% (Wind Peak) and 7% (Voltaire) of the actual offshore and port times, when there are no other factors delaying these times. This is consistent with the assumptions made in the model, namely to exclude mechanical breakdowns, maintenance and crew availability which could cause delays. In other words, the model is accurate in estimating lower bounds for the installation times. Furthermore, it should be noted that this validation is performed while the project is only just underway. The Wind Peak has installed 24% of its turbines, while the Voltaire has installed just 7% of its total turbines. Re-evaluating the validation of the model when the wind farms are finished would likely yield results closer to reality, as the installation times per turbine reduce.

In this chapter, the model was outlined in detail. The inputs were defined, and the data gathering process for the inputs was explained. The structure of the model was laid out to explain its workings. A validation was performed on the model, and it was found that it was accurate in the estimations of the lower bound durations. In the next chapter, the two case studies which will be used for this study are shown, as well as the installation processes which will be modelled.

4

Case Studies

To quantify the possible benefits of the use of a Slipjoint, two case studies are used. The model is applied to the installation campaign of two yet to be built OWFs. The first is Ecowende, an OWF off the west coast of the Netherlands. The second is the Star of the South OWF, off the south east coast of Australia, near Tasmania. In this chapter, the characteristics of the two installation sites are discussed, and the installation methods which will be compared are explained.

4.1. Installation Sites

In this section, the two installation sites which will be used in the case studies are shown, and their characteristics are discussed.

4.1.1. Ecowende

The first case study is performed on the Karel VI installation site, also known as Ecowende. This site was chosen as a case study for several reasons. Firstly, the installation of the site is carried out with a new, state-of-the-art installation vessel called the Boreas. It is employed by Van Oord, and the installation of the Ecowende windfarm will be its first task. Performing the case study on an OWF that is going to be installed in the near future ensures the technologies that will be used are as modern as possible, making the comparison with the Slipjoint installation as realistic as possible. Furthermore, because there is not yet much experimental data on the installation of windfarms using the Slipjoint, some of the parameters of the model will have to be estimated. For Ecowende, this is also the case, making the comparison more fair.

The Ecowende installation site lies around 50 kilometres off of the west coast of the Netherlands. The base port for the installation of the turbines, however, is the Eemshaven in Groningen, in the north. The sailing distance from the Eemshaven to Ecowende is around 230 kilometres. The installation site has an area of just 90 km^2, and will house 52 turbines. The turbines which will be installed are Vestas V236 15MW offshore wind turbines, bringing the total capacity of the OWF 760MW (TenneT, 2025). Ecowende, as is the case for many windfarms in the North Sea, uses monopiles as the foundations for the turbines. This is done because of they are cost-effective (both for manufacturing and installation), relatively easy to install and have been proven to work well in the conditions of the North Sea.

The coordinates of the turbines at the Ecowende wind park are listed in Appendix B. They were obtained from a government report on the Ecowende permit (Ministeries van Economische

Zaken en Klimaat et al., 2016). This report contained the coordinates of 47 turbines, which was originally the number of turbines to be installed. From (TenneT, 2025) it is clear that the renewed plan is to install 52 turbines. Therefore, five extra coordinates had to be generated and placed added into the set. This was done by interpolating five points between turbine number 22 and 40 in Python. Figure 4.1a shows where the five coordinates were interpolated. The location of the interpolated coordinates were chosen such that they best fit into the existing structure, fitting into the areas shown in the license report. (Ministeries van Economische Zaken en Klimaat et al., 2016).

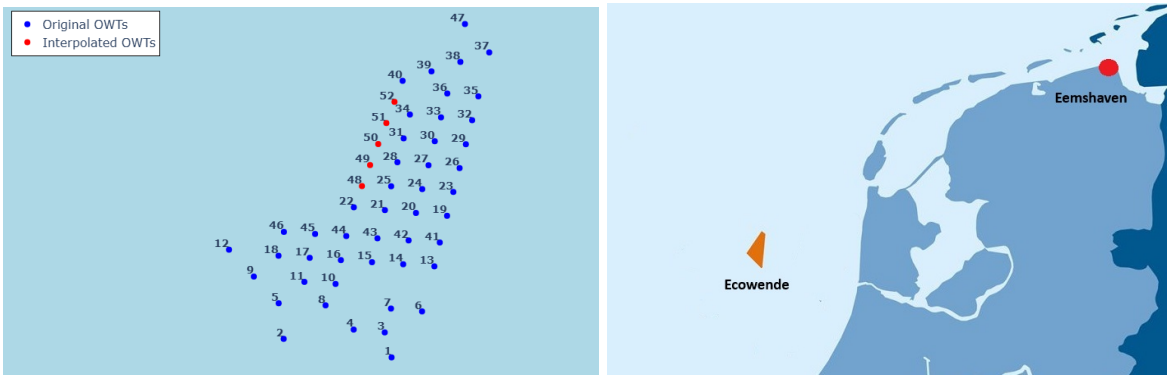

(a) The location of the original and interpolated Ecowende coordinates.

(b) The locations of the Ecowende license area and the Eemshaven. (RVO, 2025)

Figure 4.1: The Ecowende coordinates and license area.

		Ecowende	Star of the South
Area	[km^2]	90	586
# Turbines	[-]	52	150
Turbine power	[MW]	15	15
Total capacity	[GW]	0.76	2.2
Foundation type	[-]	Monopile	Monopile
Distance from base port	[km]	230-245	260-280

Table 4.1: Overview of the main characteristics of the two case study wind farms

4.1.2. Star of the South

For the second case study, an OWF near the south east coast of Australia is chosen. This wind park was chosen because it is different to Ecowende in several aspects, making it possible to analyse in which circumstances the Slipjoint can offer the most benefits. The OWF which will be used in the case study is the Star of the South wind farm, shown in Figure 4.2b. This site is one of several development sites in the Bass Strait, the body of water between mainland Australia and Tasmania. For the same reasons as mentioned in Section 4.1.1, the Star of the South installation site will also employ monopile foundations (Star of the South, 2020). The license site sits just 15 kilometres off the coast of mainland Australia, and has an area of 586 km^2. It is planned to house 150 turbines. The turbines will be of a similar size to the turbines installed at Ecowende, 15MW, producing a total 2.2GW of power (Star of the South, 2020). However, as this project is at an earlier stage of development than the Ecowende wind park, these numbers are preliminary.

An overview of the most important differences between Ecowende and Star of the South is given in Table 4.1. The base port for the case study will be Bell Bay. This port is located on the north end of Tasmania, at a sailing distance of around 260 kilometres from the site, and

is currently expanding its staging areas in preparation for the installation of the foundations and superstructures for the different wind farms in the Bass Strait. For most of these projects, the workload will be divided between Bell Bay in Tasmania and Geelong Port in Victoria. For example, the foundations could be installed out of Geelong Port and the superstructures out of Bell Bay. The installation of the OWTs as it currently planned follows the process shown in Figure 4.3. The alternative Slipjoint installation method would also follow the Slipjoint installation process shown in Figure 4.5.

Because the Star of the South project is in an earlier stage of development, no coordinates of the turbines are yet available. The license area is of a rectangular shape (see Figure 4.2b), so it is probable that the turbines will also be placed in a rectangular grid. Because the number of turbines in the park will be 150, a logical configuration would be a grid of 10 by 15 turbines. The coordinates for the grid were generated in Python and can be seen in Figure 4.2a. The coordinates lie within the defined license area.

(a) The location of the Star of the South generated OWT coordinates.

(b) The locations of Star of the South license area and Bell Bay. (Star of the South, 2020)

Figure 4.2: The Star of the South coordinates and license area.

4.2. Installation Processes

4.2.1. Standard installation

For the standard installation method, a jackup vessel is used. As the Boreas will be used in the Ecowende case, it is also chosen as the jackup vessel for the Star of the South case to ensure fair comparison. After the monopiles are installed, the Boreas will be outfitted with equipment to install the turbine superstructures. Once this outfitting is complete, the OWT installation process will begin. During this process, a loading-transport-installation cycle will be executed a number of times. How many times it will be executed depends on the capacity of the Boreas. There are 52 turbines to be installed at the Ecowende windfarm (TenneT, 2025). The Boreas is an Atlas C-Class vessel made by Knud E. Hansen. Vessels of this class are able to transport six 15MW turbines at a time (Knud E. Hansen, n.d.). Therefore it will take the Boreas 52/6 = 8.67, so nine trips to install all turbines. Each cycle consists of loading, transport, installation and returning to port. The loading will be done with no pre-assembly of the wind turbines other than the rotor and the nacelle. The towers are loaded onto the Boreas first, followed by the nacelles and lastly the blades. At the port, the blades are placed into a bladerack prior to loading. The bladerack is then loaded onto the ship in one lift. When the Boreas is fully loaded, it sails to the Ecowende installation site. When it has arrived, it will start positioning itself on the right coordinates and start its jackup manoeuvre. Once the vessel is completely lifted out of the water, installation can begin. The installation of turbine parts follows the same order as the loading. First the tower is lifted from the Boreas onto the monopile foundation, after which

it is secured into place with bolts by personnel on the platform. Then, the nacelle is lifted onto the tower, which is also secured with bolts. The last step consists of lifting the blades onto the rotor one by one. When a blade is lifted to the rotor, it is secured, after which the rotor is rotated 120 degrees and a brake is applied to keep the rotor in the correct orientation. When the third blade is installed, the installation activities of the Boreas are complete. The turbine still has to be connected to the cables leading to the transformer and commissioning needs to be completed, but the Boreas is not needed for this. It sails to the next installation site, where the positioning and installation process is repeated. When all its turbines are installed, it sails back to the port. Here it is refuelled, restocked, and the crew is rotated. This can all be done while loading for the next trip is in progress. This marks the beginning of a new installation cycle. This cycle is repeated until all turbines are installed. The Ecowende installation process follows the process shown in Figure 4.3.

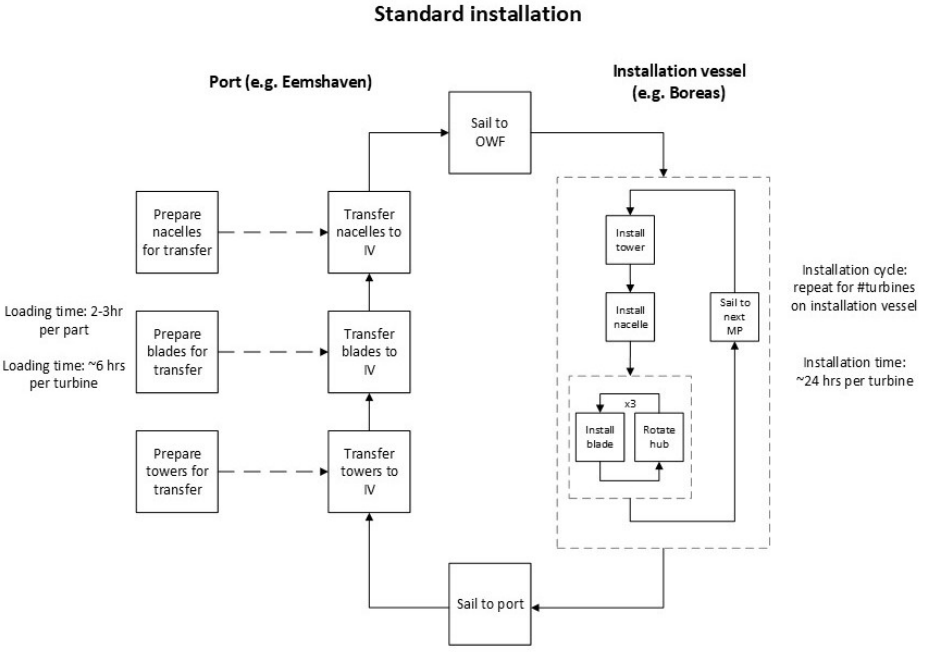

Figure 4.3: The standard installation process using a jackup vessel.

4.2.2. Slipjoint installation

When using the Slipjoint method with full pre-assembly, the installation process changes. The assembly of the OWTs is now done at the port. Port cranes assemble the tower, nacelle and blades on Slipjoint fastening points, see Figure 4.4a. An HLV is needed to lift the complete turbine onto itself. When the HLV is in the port, loading begins by pushing the OWTs off their fastening points, after which the HLV crane lifts the OWTs onto the HLC deck one by one, see Figure 4.4b. The OWTs are placed onto Slipjoint seafastening points on the HLV deck, settling through their own weight, see Figure 4.4c. This makes them secured for transport. The HLV then sails out to the OWF, see Figure 4.4d, where the OWTs are pushed off their seafastenings and installed in a single lift. No fastening of bolts is required for any step of the installation. The installation process is repeated until all OWTs in the batch are installed, after which the HLV returns to port. The assembly of the OWTs in the port runs parallel to the installation of the other OWTs. When all OWTs are installed, the process is finished. The process is shown schematically in Figure 4.5

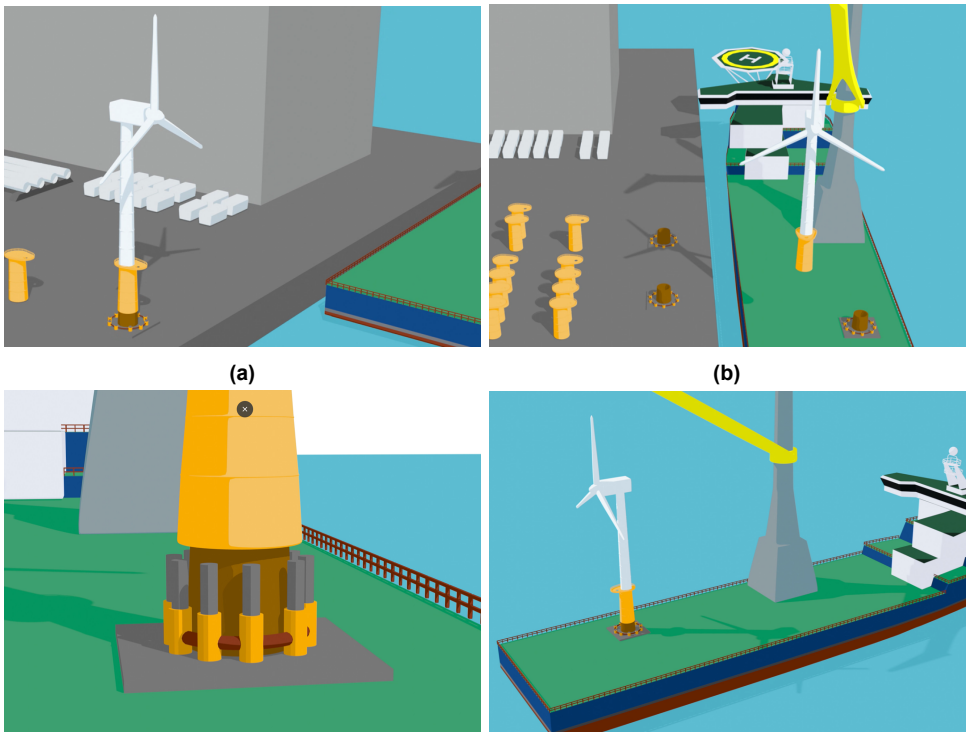

Figure 4.4: Full pre-assembly Slipjoint loading and transportation process. source: (DOT, 2025)

In this chapter, the characteristics of the two case studies on which the model will be run are laid out. The installation processes for the standard and Slipjoint installations were shown. In the next chapter, the installation processes will be applied on the case studies using the model shown in Chapter 3, and the results of these simulation will be shown.

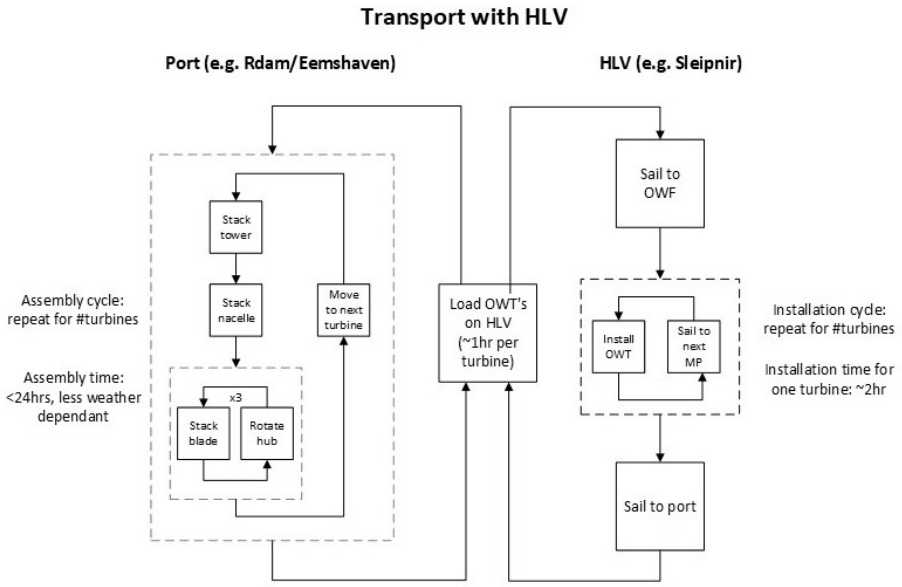

Figure 4.5: The installation process when using the full pre-assembly strategy.

5 Results

In this chapter, the numerical results of different simulation runs are shown and discussed. The model presented in Chapter 3 is executed on both casestudies from Chapter 4 using both installation methods.

5.1. Single Control Run

The ensure the model works correctlye, the model is run on a single run, with given start date. The results of the simulation can be inspected through different plotting methods. A single run of the simulation is executed for the Ecowende case with the Standard installation method, with starting date 01-07-1995. The results are inspected below.

In Figure 5.1 an example of a stepped Gantt chart is shown. From this chart, the progression of the installation can be tracked per loading, transport and installation cycle. It can be seen that some cycles take longer than others, due to weather influences.

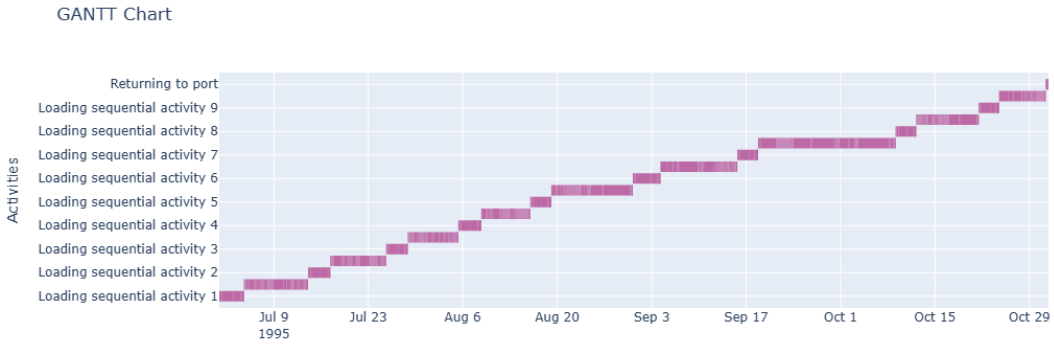

Figure 5.1: Stepped Gantt chart of control run.

Figure 5.2 shows a step chart of the jackup01 and port_site objects, for the three cargo types (towers, nacelles and blades). The port_site is incrementally depleted of its cargo, when it is loaded onto the jackup in phases. The jackup is incrementally loaded with cargo, and offloads the cargo step by step by installing OWTs at their installation site and sailing to the next. The Cargo type Blade has three times as many units as the towers and nacelles. The loading times are, however, much shorter than the loading times of the towers and nacelles, due to the blades being loaded onto the jackup with a single lift in a bladerack.

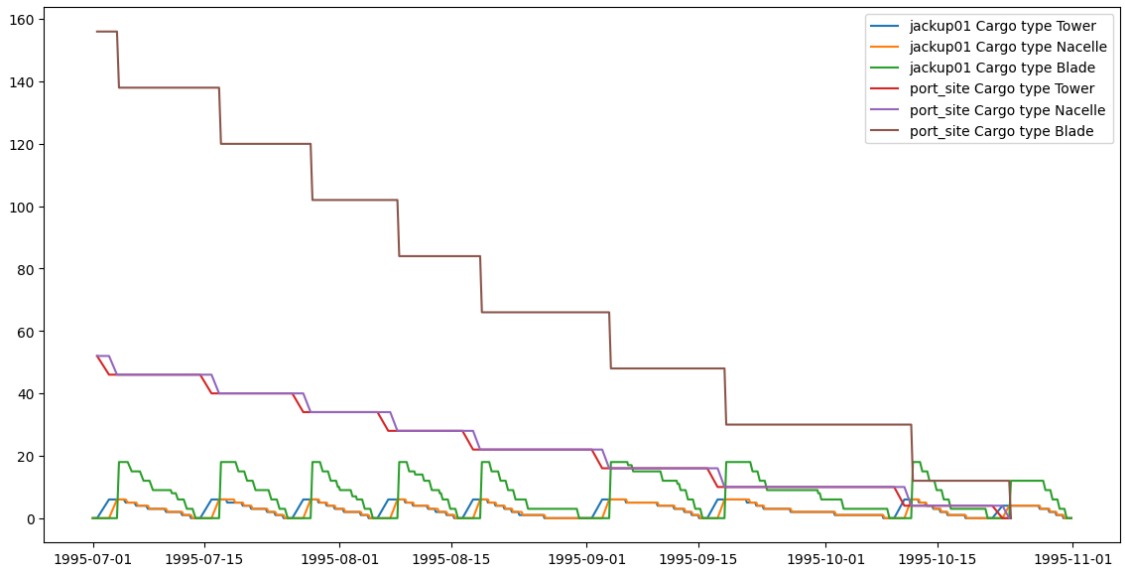

Figure 5.2: Step Chart of control run.

It is also possible to plot the weather conditions during the simulation run. Figure 5.3 shows the wave height, wind speed and linear Gantt chart of the simulation run. The weather limit parameters are also shown in the weather graphs. It can be seen that, when the weather values for wave height or wind speed exceed the set weather limits, the simulation pauses the activities and goes into a waiting state. This is evident from the gaps in the Gantt chart coinciding with the areas where the weather values exceed their limits. These areas also coincide with the longer steps in Figure 5.1 and Figure 5.2.

By inspecting single control runs in this way, it can be confirmed that the model works as intended: the loading, transport and installation cycles are correct, and weather influences work correctly. Single runs were executed and inspected for all combinations of the Ecowende and Tasmania cases and the Standard and Slipjoint installation methods. After verifying these all performed correctly, the multi-year runs could be started.

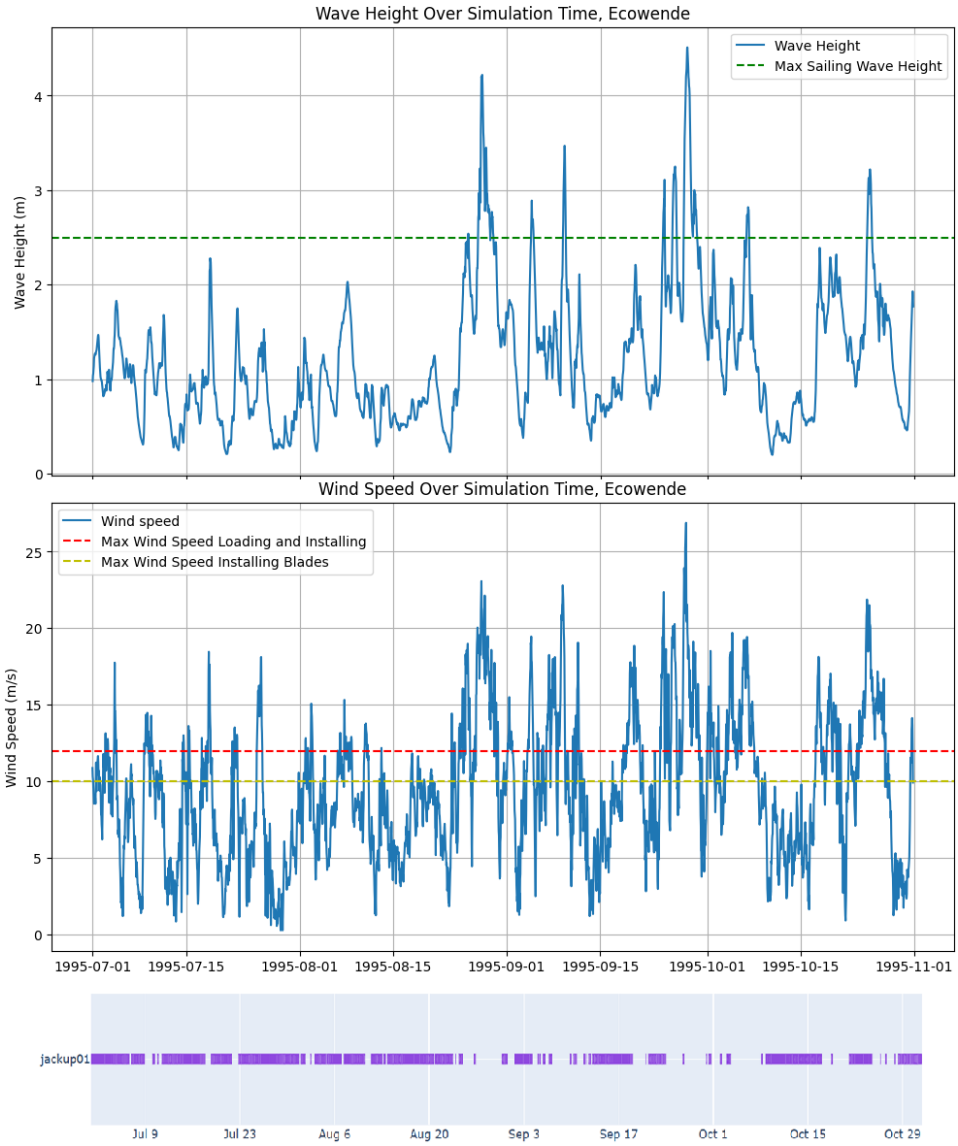

Figure 5.3: Wave height, wind speed and linear Gantt chart with weather limits.

5.2. Comparing Standard and Slipjoint Installation Performance

In this section, the results of simulations of OWFs using the standard installation method and the Slipjoint method are compared. The Slipjoint method is split into two cases: one where the capacity of the HLV is assumed to be 2 OWTs, and one where the capacity is 4 OWTs. This is done because the actual capacity of the HLV to transport completely assembled OWTs is not known. Therefore, it is treated as a variable, and the values 2 and 4 for this variable are evaluated, see also Section 3.7.2. These methods are called 'Slipjoint Capacity 2' and 'Slipjoint Capacity 4', they are also shown in Table 5.1. For each case, the simulation is run over 24 years, starting in 1995, with 24 datapoints (start dates) per year to ensure high fidelity of results. Boxplots of the installation time and costs are shown and discussed.

Name	Installation method	Vessel capacity
Standard	Standard	6 (known)
Slipjoint Capacity 2	Slipjoint	2 (variable instance)
Slipjoint Capacity 4	Slipjoint	4 (variable instance)

Table 5.1: The three evaluated methods in this study.

5.2.1. Installation duration and cost

Ecowende

In Figure 5.4, boxplots of the durations of the Ecowende installation campaigns are shown. It can be seen that the median installation time for the standard method is significantly higher than for the Slipjoint Capacity 2 and Slipjoint Capacity 4 methods. This shows that the Slipjoint method is, over all simulations, faster on average. Both the Inter Quartal Range (IQR) and total range are also higher for the standard method, showing a higher variability in installation time. This shows the standard method is more susceptible to weather influences, as it more often experiences delays, resulting in more severe outliers. The top 'whiskers' on the boxplots are significantly longer than the bottom whiskers, showing that there are more sever outliers towards longer-than-average durations. This could be caused by the stormy nature of the North Sea in the winter. The Slipjoint Capacity 4 has a lower median duration than both other methods, with additionally a smaller variability. The Slipjoint Capacity 2 achieves a 44,2% reduction in mean installation time over the standard method. For the Slipjoint Capacity 4 method, the median installation time is reduced by 58,5% compared to the standard method.

When looking at installation costs, the picture changes. The difference between the standard and Slipjoint methods are reduced significantly. The median cost for the Slipjoint methods is lower than the standard method, but the spread of costs is larger than the standard method. This is due to the higher day rates of the HLV used in the Slipjoint method. Nevertheless, a reduction in median cost of the Slipjoint Capacity 2 method over the standard method of 8,4% is achieved. For the Slipjoint Capacity 4 method, this reduction is increased to 30,8%, suggesting good financial feasibility of the Slipjoint method, provided a HLV capacity can be reached.

To analyse the distribution of the results, S-curves can be used. They are useful for visualising the variability and distribution of the installation duration and costs. By plotting the cumulative probability of results, the S-curves provide an insight into the likelihood of completing a task within a given duration or cost. The S-curve for the Ecowende case is shown in Figure 5.6 The p80 marks are shown, giving a clear performance metric for the installation methods. The p80 durations are 181, 105 and 83 days for the standard, Slipjoint Capacity 2 and Slipjoint Capacity 4 methods, respectively. The p80 costs are 92, 87 and 69 million USD. The steeper angle of the Slipjoint cumulative distributions also show the decreased variability of the method. The

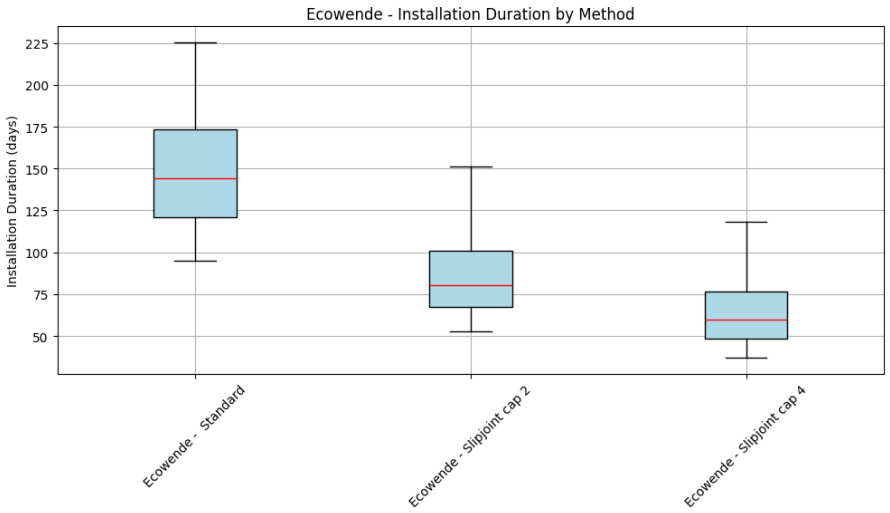

Figure 5.4: Ecowende durations boxplots.

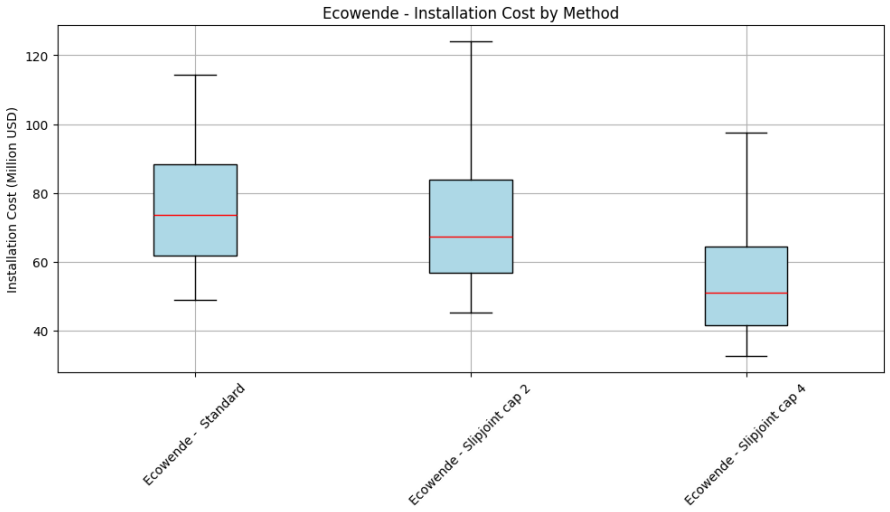

Figure 5.5: Ecowende cost boxplots.

cost performance is however quite similar for the capacity 2 method, but the capacity 4 method significantly outperforms the standard method.

Tasmania

When looking at the durations for the different method in the Tasmania case study in Figure 5.7, it becomes clear that the installation durations are much higher than the Ecowende durations in Figure 5.4. This is for the most part due to the size of the OWF: 150 turbines for Tasmania and 52 for Ecowende. However, the installation time per turbine is higher for the Ecowende case: 2,453 days per turbine for Tasmania (standard installation method), compared to 2,773 days per turbine for Ecowende (standard installation method). This is despite the fact that the Tasmanian OWF is situated further away from the base port, which increases transport time. The lower installation time per turbine is likely caused by the more stable weather conditions in Tasmania; the installation time per turbine in Ecowende is affected by its high variability. These stable conditions in Tasmania can be seen in the durations per start date in Figure 5.13, where the installation durations vary very little throughout the year compared to the Ecowende durations shown in Figure 5.11, where the installation durations vary significantly throughout

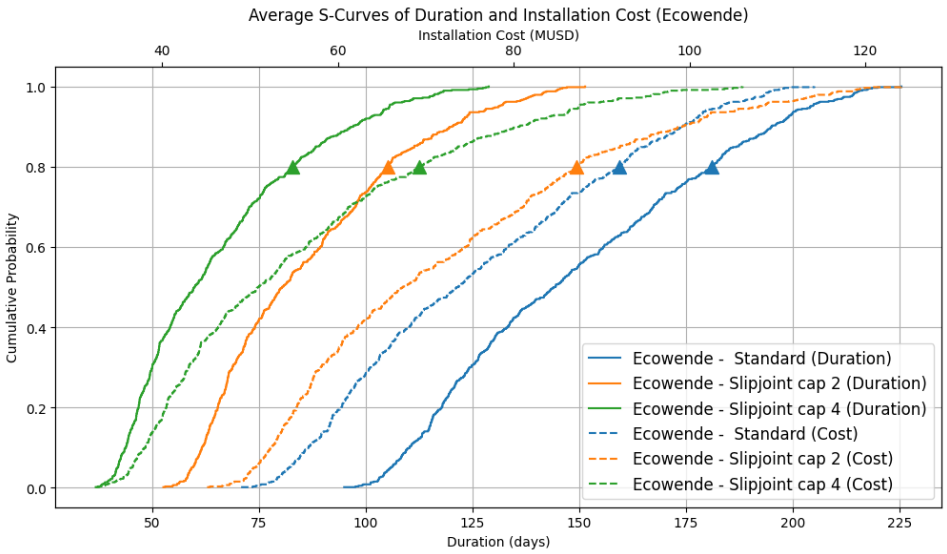

Figure 5.6: S curves for the installation duration and costs cumulative probabilities for the Ecowende case.

the year.

In Figure 5.7 it can be seen that the median installation time for the Slipjoint Capacity 2 method is again lower than the standard method, but with a lower variability. The reduction in median installation time is 35,8%. The Slipjoint Capacity 4 method has a lower median installation time here as well, achieving a 53,8% reduction in median installation time. The variability is similar to the Slipjoint Capacity 2 method. It can be seen that the 'whiskers' of the boxplots are of equal length, showing the stable weather conditions in the Bass Strait.

In the Tasmanian case study, the picture again changes when looking at the costs. Here, the faster installation of the Slipjoint Capacity 2 method is not enough to compensate for the higher costs. The median cost for the Slipjoint Capacity 2 method is 5,0% higher than the standard method. The variability is also higher than the standard method. The Slipjoint Capacity 4 method, however, achieves a 23,1% decrease in median installation cost when compared to the standard method.

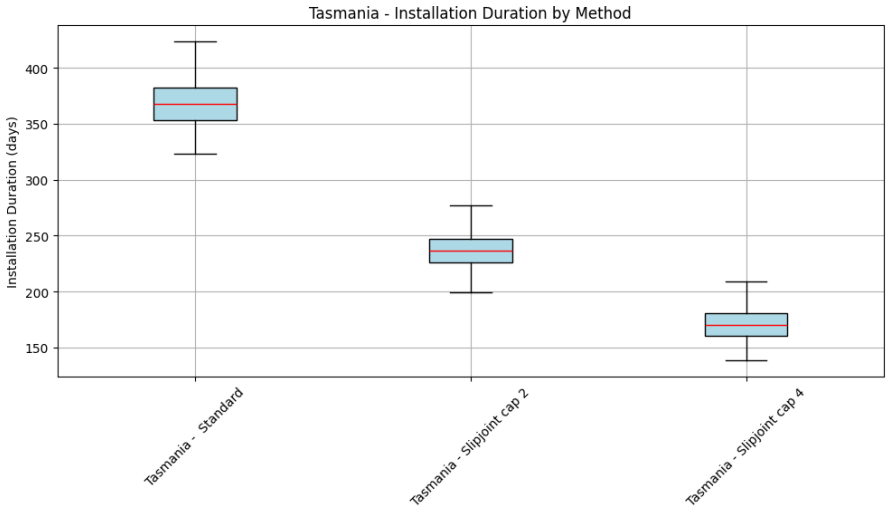

Figure 5.7: Tasmania duration boxplots.

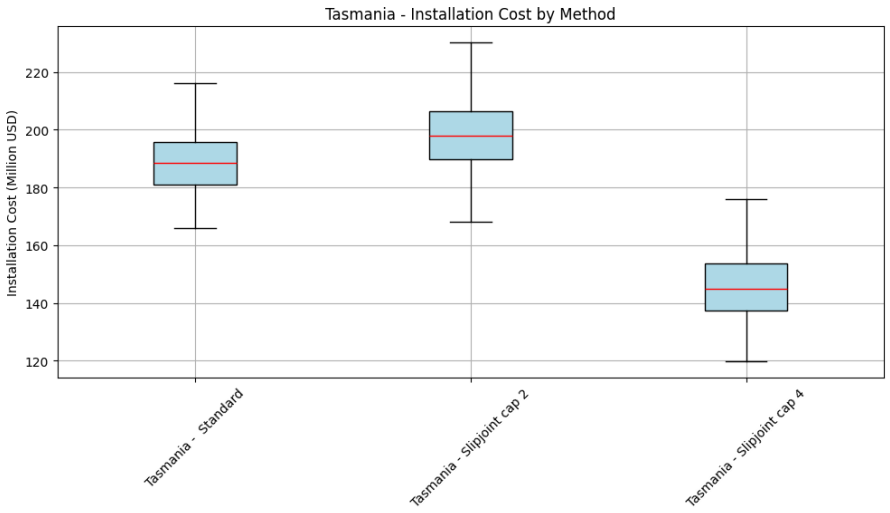

Figure 5.8: Tasmania cost boxplots.

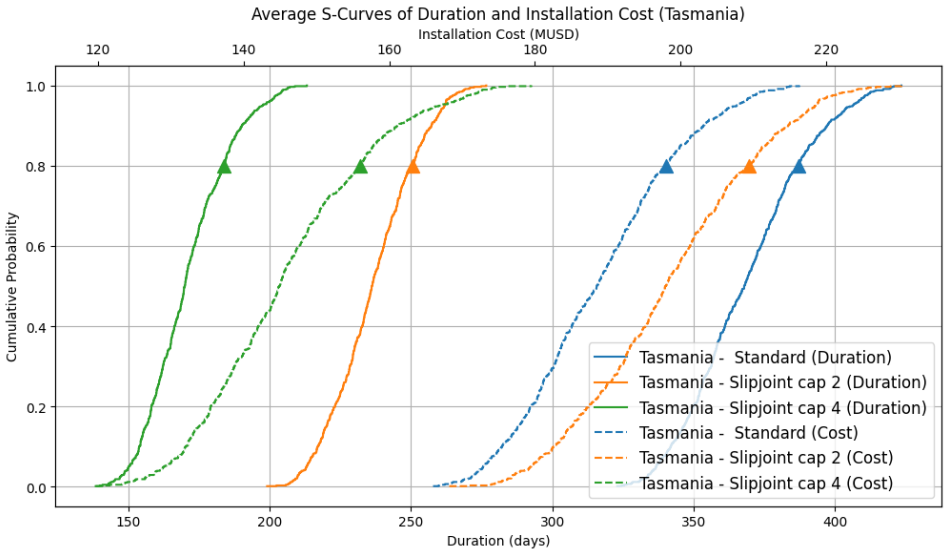

Figure 5.9: S curves for the installation duration and costs cumulative probabilities for the Tasmania case.

Figure 5.9 show the S-curve graph of the cumulative probability distributions for the installation durations and costs for the Star of the South, or Tasmania, case. The p80 durations are 387, 250 and 183 days for the standard, Slipjoint Capacity 2 and Slipjoint Capacity 4 methods, respectively. The p80 costs are 198, 209 and 156 million USD. The decreased cost performance of the Slipjoint Capacity 2 method is clear. The slope is similar across the three methods. However, the Slipjoint Capacity 4 method again shows a significant increase in cost performance over the traditional method.

5.3. Installation Performance as a Function of Start Date

While the median and variability of duration and costs do give some insight into the performance of an installation method, it does not take into account when installation campaigns started. It therefore does not give insight into possible performance differences between installation methods at different points throughout the year. In this section, the installation durations and costs as a function of start date are displayed and discussed for both case studies.

Ecowende

In Figure 5.10 the durations of the installation methods at different start dates throughout the year are given. The average, minimal and maximum durations are given. A slightly modified version of this plot is given in Figure 5.11. Here, the average durations are shown with a $\pm$ 1 standard deviation band, giving a smoother plot with better readability. Other graphs made with the min/max bands will be shown in the appendix. From both figures it again becomes clear how the Slipjoint methods have a shorter average installation time for both capacities. The narrower bands also clearly indicate a smaller variability in installation times per start date. It can be seen that the standard method is more sensitive to seasonal influences: the durations start to increase in length earlier in the year than the Slipjoint methods, and the increase in installation time is more severe. In other words, the weather workability of the Slipjoint method is better than that of the standard method. This is true for most of the year, however near the end of the year, around October to December, the variability of the Slipjoint methods increases to similar values to the standard method. The installation cost can also be plotted as a function

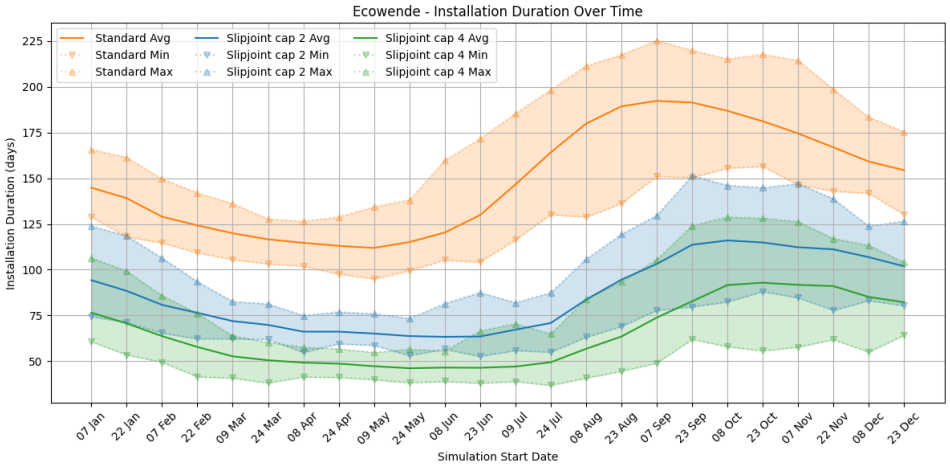

Figure 5.10: Ecowende durations for different start dates with min/max bands.

of the start date. Figure C.1 and Figure 5.12 show the installation costs of the three methods as a function of the start date of the simulated installation campaign. This shows a more nuanced cost performance of the Slipjoint Capacity 2 method. Between the months of October and February, its costs are higher than the standard method. Here, the installation time savings aren't substantial enough to compensate for the increased mobilisation cost and dayrates of the HLV. However, beginning in March, the installation costs start to become increasingly less than the standard method. Interestingly, the optimal season for the Slipjoint Capacity 2 method is shifted to a later time in the year than the standard method. The standard method is optimal around the end of April to the beginning of May, whereas the Slipjoint method is optimal around June. Furthermore, the Slipjoint method stays near the optimum longer than the traditional method, increasing the starting window in which the installation cost will be near-optimal. This is shown with the near-optimal ranges. Within these ranges, the installation costs lie within a 10% increase in costs over the minimum average cost. It can be seen that this window is

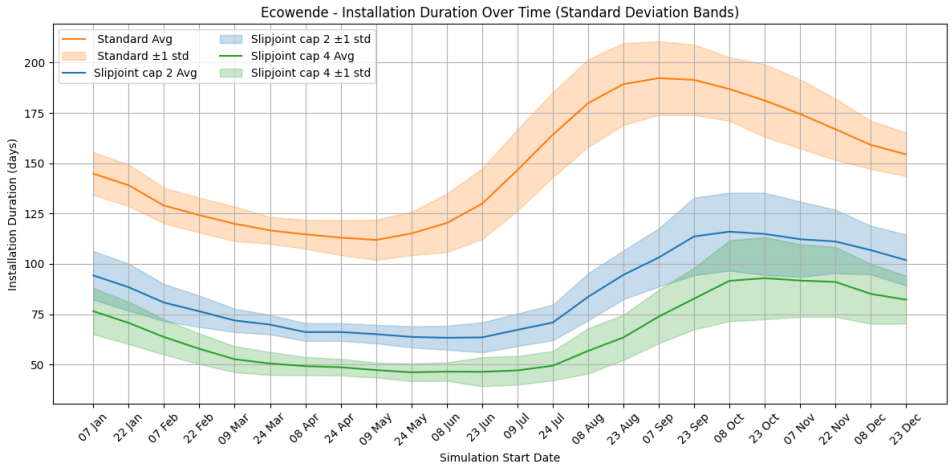

Figure 5.11: Ecowende durations for different start dates with standard deviation bands.

three months long for the standard method, three and a half months long for Slipjoint Capacity 2 and four months for the Slipjoint Capacity 4 method. It also clearly shows the shifting of the optimal starting season towards later in the year. The Slipjoint Capacity 4 method shows a near constant improvement in cost performance over the standard method, and its optimal starting date range is also shifted to later in the year when compared to the standard method.

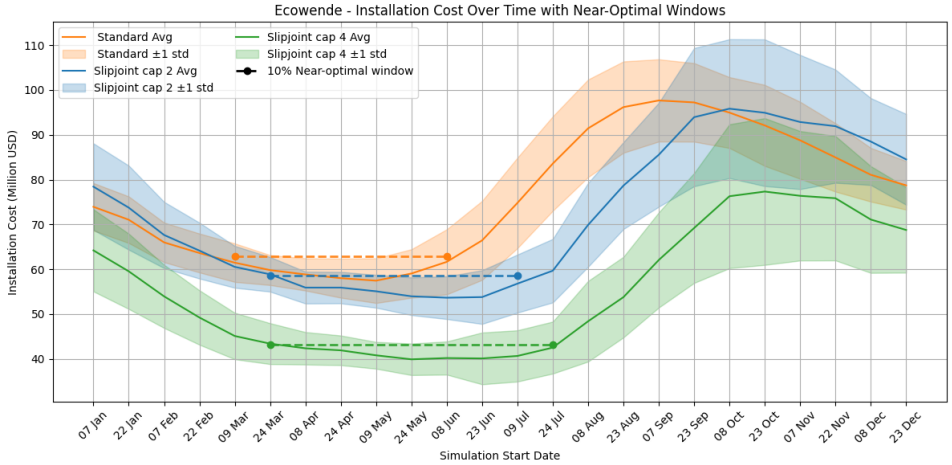

Figure 5.12: Ecowende costs for different start dates with standard deviation bands and near-optimal ranges.

Tasmania

The durations as a function of the start date for the Tasmania casestudy are given in Figure 5.13. A version with min/max bands is available in Appendix C. When comparing these to Figure 5.11, it can be seen that the installation durations are much more constant throughout the year, for all methods. This is a result of the weather conditions in the Bass Strait being more constant than on the North Sea (OWC, 2024). This is due to the relatively sheltered position of the Strait between mainland Australia and Tasmania. However, the Slipjoint methods show more seasonal influences than the traditional method, as shown by the flatter curve for the traditional method. This could be due to the traditional method being more wind-restricted than wave-restricted due to the many lifting operations. The Slipjoint method is more wave-restricted due to the increased number of transits and reduced lifting operations. The wave conditions in the Bass Strait fluctuate more with the season than the wind conditions (Liu et al., 2022) (Vincent & Dowdy, 2024), causing more severe seasonal effects for the wave-restricted Slipjoint methods. Furthermore, the lowest durations can be found between October and January, compared to March and June for the Ecowende case study. This is due to the offset of seasons between Australia and Europe due to the different latitudes. When comparing the different installation methods, it can be seen that the Slipjoint methods again outperform the standard method, achieving lower average installation times and variabilities. The duration ranges for the standard method are quite high. The width of the min/max band for the durations range from 40 to 80 days, making it hard to predict how long an installation campaign will take beforehand. Interesting to note is the discrepancy between the Slipjoint Capacity 2 and capacity 4 methods in terms of optimal installation season. The Slipjoint Capacity 2 method is optimal between September and October, whereas the Slipjoint Capacity 4 is optimal between November and December.

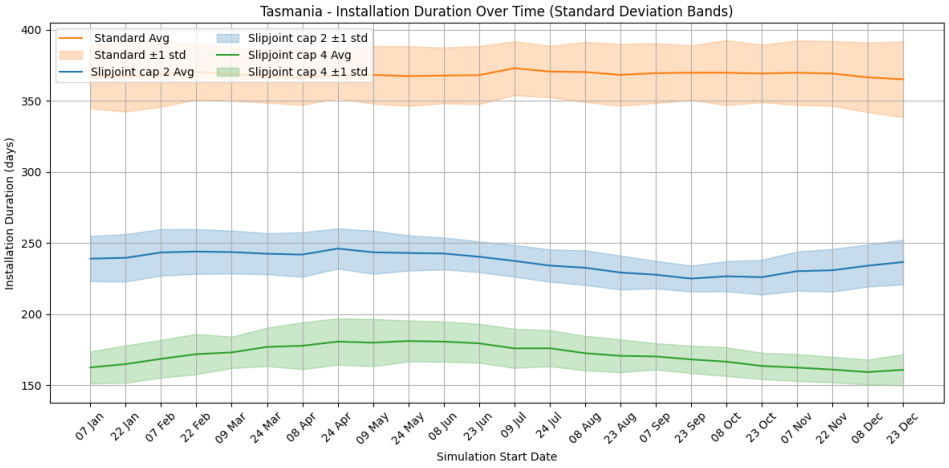

Figure 5.13: Tasmania durations for different start dates with standard deviation bands.

The costs as a function of start date for the Tasmanian case study are given in Figure 5.14. In the Tasmania case study, the costs performance of the Slipjoint Capacity 2 method is again lower than the standard method. However, in the Ecowende case there was a window in which the Slipjoint method outperformed the standard method. In the Tasmania case, the Slipjoint Capacity 2 method consistently has higher installation costs than the standard method, with the exception of late September, where the costs are similar. The Slipjoint Capacity 4 method does outperform the standard method considerably throughout the whole year. Noticeably, both Slipjoint methods display more seasonal effects than the standard installation method, which is very constant in costs throughout the year. Here, the discrepancy in optimal start

date between the two Slipjoint methods is also noticeable.

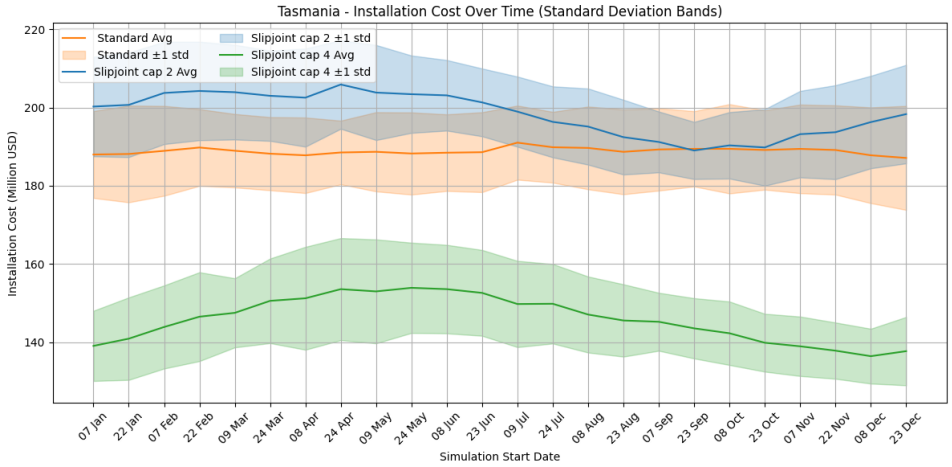

Figure 5.14: Tasmania costs for different start dates with standard deviation bands.

In this chapter, the results of the simulation runs of the case studies were shown. It was found that the Slipjoint methods have shorter installation durations and costs, though the degree in which they outperformed the traditional method depends on the capacity of the Slipjoint method and on the installation timing. In the next chapter, the implications and limitations of the findings will be discussed.

6

Discussion

In this study, the installation performance of the Slipjoint technology for offshore wind turbine (OWT) installation was investigated using Discrete-Event Simulation (DES). Two case studies shown in Chapter 4 were used: one yet to be constructed offshore wind farm (OWF) near the coast of the Netherlands (Ecowende), and one in the Bass Strait between mainland Australia and Tasmania (Star of the South). Simulations of the installation of the OWFs were run for both Slipjoint based installation methods and traditional installation methods. The outcomes of the simulations were then compared in terms of time, cost and weather workability. The results shown in chapter 5 show that the Slipjoint based installation methods consistently lead to shorter installation durations and, depending on vehicle capacity, lower costs compared to traditional installation methods. It also shows a greater resistance to weather influences.

One of the most notable results was the consistent reduction in installation time across all start dates in both cases. This result is likely due to the severely reduced loading and installation times, which more than compensate for the increased transportation time as a result of the higher number of trips due to decreased capacity. For the cost savings, the difference is less stark. The performance gap is decreased due to the increased mobilisation costs and dayrate of the Heavy-Lift Vehicle (HLV) used in the Slipjoint installation methods. While the Slipjoint Capacity 2 method outperforms the traditional method in some cases, the Slipjoint Capacity 4 method outperforms the standard method in both case studies for all start dates, showing a strong dependency of the cost savings on the capacity. Large seasonal differences in installation time and costs were also found in the Ecowende case study, whereas the seasonal differences in the Tasmanian case study were minimal. The savings of the Slipjoint methodology were shown to be more substantial in locations with lower significant wave heights. This is likely due to transportation time being a larger fraction of the total time in the Slipjoint method. The significant wave height is therefore a more critical factor for the Slipjoint method, leading to larger savings of the Slipjoint method in areas with lower wave heights.

These outcomes highlight the potential value of the Slipjoint technology, which could be used to realise substantial cost savings for offshore wind projects. The need for such cost savings in the offshore wind industry is high, as large wind projects are at risk of being cancelled due to the increased costs, as mentioned in Chapter 1. The difference in seasonal influences also highlights the need for careful planning and simulating when realising an OWF. However, the decision-support tool developed in this study also has some limitations due to assumptions made and data availability.

The weather is incorporated into the model in a deterministic way. While this enables reproducibility and ensures an even comparison between the investigated methods, it might not fully encapsulate the unpredictable nature of offshore installation activities due to weather influences. In reality, weather conditions are uncertain and dynamic, possibly causing unforeseen disruptions affecting the installation performance. The assumption that the crew has perfect weather forecasts, no mechanical breakdowns, and full port and vessel availability could cause the model to underestimate installation times. Furthermore, not all operations of the installation of an OWF are modelled. The simulation only models the loading, transport and installation of the wind turbine superstructures. Installation of foundations, cables and transformer stations are not incorporated into the model. These stages of OWF realisation are not completely independent of one another. The exclusion of these possible delays and the other stages of OWF installation is not a consequence of a limitation of the approach, but rather a consequence of the limited time available for this study. Adding these factors into the simulation could present new trade-offs and introduce new areas for optimisation, providing a more representative and holistic approach to OWF installation modelling.

A more real-world problem of the Slipjoint mechanism itself lies in the way offshore wind projects are structured. The monopiles and wind turbines aren't made by the same companies. Steel companies such as Sif manufacture the monopiles, while companies such as Siemens Gamesa manufacture the wind turbines. The Slipjoint connection requires both companies to alter their product and therefore production process, something which they are hesitant to do, as this will increase their production complexity and therefore costs. These companies will have to make agreements on the technical specifications and financial structure of projects using the Slipjoint.

However, the usage of the Slipjoint also offers benefits. Due to the fact that the turbines are built on land, the workers who assemble the turbines don't have to travel offshore, saving costs and improving work-life balance for these workers. Testing of the turbines can also happen on land. If any issues are found, technicians don't have to travel offshore to perform fixes. In general, more of the installation process is moved onshore, reducing costs, risks and travel time.

Despite some limitations, the DES model presented in this study provides an extensive and flexible tool, useful for comparing OWT installation strategies. It enables OWF developers to test different loading, transport and installation strategies at different locations over the world, over long timespans. The model can easily be adapted and expanded to accommodate different vessels, turbines, farms, strategies, and weather conditions. This allows developers to explore and compare the performance of many different variable combinations to find the optimal strategies.

In summary, the Slipjoint installation method shows clear potential for reducing OWF installation cost by reducing offshore time. The effectiveness of these methods is dependent on the timing and location, but more so on the possible capacity of the installation vehicle. The results of this study show the potential of the Slipjoint as a cost-saving measure in offshore wind turbine installation.

7

Conclusion

With growing scale and costs, the offshore wind industry is facing headwinds. There is increasing pressure to develop cost-saving measures to improve the economical feasibility of offshore wind projects and prevent them from being cancelled. The Slipjoint is a novel connector interface which aims to achieve cost savings by reducing offshore time and its associated costs. It is a relatively new technology, which has never been tested at a large scale. It is therefore unknown what the time and cost savings from the use of the Slipjoint are. From this emerges a need for a quantitative simulation model to investigate the potential time and cost savings of the Slipjoint.

The aim of this thesis was to develop and apply a simulation-based Decision-Support Tool (DST) to quantitatively compare the performance of traditional installation methods and the Slipjoint installation method. To fulfil this objective, a quantitative Discrete-Event Simulation (DES) model was developed to simulate offshore wind turbine installation campaigns. The model included realistic process logic, weather influences, and vessel and OWT parameters. The model was applied to two case studies: one Offshore Wind Farm (OWF) near the coast of the Netherlands, Ecowende, and one in the Bass Strait between mainland Australia and Tasmania, the Star of the South. Three installation methods were used in each case: a standard approach using a jack-up vessel, and two Slipjoint approaches using Heavy-Lift Vehicles (HLV). Because the capacity of the HLV to transport completely pre-assembled OWTs is unknown, it is treated as a variable. The case studies were run with two different values for the HLV capacity: 2 and 4. These methods are called the Slipjoint Capacity 2 and Slipjoint Capacity 4 methods.

The results show that, for the Ecowende case, the Slipjoint Capacity 2 installation method achieves a 44,2% reduction in median installation time compared to the standard method, and the Slipjoint Capacity 4 method achieves a 58.5% reduction. The reduction in p80 duration is 42.0% and 54.1%, respectively. For the Tasmanian case, this reduction is 35,8% and 53,8% for the median durations, while the p80 durations showed 35.4% and 52.7% reductions. The results for cost performance show a decrease in median costs for the Slipjoint Capacity 2 method of 8,4%, and 30,8% for the Slipjoint Capacity 4 method, and a decrease in p80 costs of 5.3% and 24.7%. However, in the Tasmanian case, an increase of 5,0% in median installation cost was found for the Slipjoint Capacity 2 method, but the Slipjoint Capacity 4 method achieved a decrease of 23,1%. This also shows in the p80 costs, with a 5.6% increase in costs for the Slipjoint Capacity 2 method, but a 21.2% decrease in costs for the Slipjoint Capacity 4 method.

The results showed a high degree of variability across installation start dates for the Ecowende case, due to seasonal weather influences. This variability was almost absent in the Tasmanian case, highlighting the importance of incorporating weather influences into the model. The Slipjoint had some clear advantages over the standard method that came forth out of the weather variability. Its improved weather workability enabled it to reach lower optimal costs. Furthermore, its near-optimal window, the amount of time per year in which the installation costs lie within 10% of minimal costs, was wider. For the Slipjoint methods, the near-optimal windows were 3.5 and 4 months for the Slipjoint Capacity 2 and 4 methods respectively. This is an improvement compared to the near-optimal window of 3 months for the standard method.

The main research question, formulated in Section 1.4, is as follows:

> *"How can the installation processes of offshore wind farms using the Slipjoint and traditional methods be quantitatively compared to create a decision support tool for offshore wind farm development?"*

Using the findings discussed above, the main research question can be answered. From the literature review it was found that the most suitable modelling method is DES, due to its ability to model cyclic activities using sequencing and logic. Using DES, a simulation tool was developed in which different installation methods can be compared. This simulation tool is customisable to allow modelling of varying pre-assembly, transportation and installation strategies, and to compare their performance. Metrics from the simulation runs, such as durations, weather delays and costs, are used to analyse and plot the performance of the different installation methods. The DST was then applied to two case studies, showcasing how it can be used to aid decision-making in the realisation of OWFs. With the synthesis of the DST, and its application on two case studies, the main research is answered.

The results of the case studies show the benefits of the Slipjoint mechanism to be substantial. The validity of the results do depend on the validity of its inputs, of which some had to be estimated. The model also has several limitations. It assumes perfect weather forecasting, no mechanical failures and complete vessel, port and parts availability. These assumptions simplify the system to make it feasible to develop in the limited time available for the thesis project, but may underestimate project durations and costs. Nevertheless, the DES model developed provides a flexible and useful tool for evaluating installation strategies under realistic weather and logistical constraints. It provides clear performance metrics to assess the performance of different installation strategies. The tool is transparent and reproducible and can be expanded to incorporate other stages of OWF realisation such as foundation, cable or substation installation.

Further research into this topic could look at expanding the model to include the installation of foundations, cables and substations to get a complete understanding of all phases of offshore wind farm installation. Furthermore, different transport and installation strategies, such as a feeder strategy, could be investigated to see if they could lead to decreased installation times and costs. More research could also be done into determining the most suitable HLV for the Slipjoint method. The stability of the vessel while transporting complete OWTs should be calculated, while adhering to size constraints for base ports such as the Eemshaven and Bell Bay. Simulation runs using the DST developed in this study could then be used to verify the economical feasibility of the chosen HLV. Lastly, incorporating the land logistics of turbine parts delivery and pre-assembly could be added into the model. For the Slipjoint methods, it is critical that the pre-assembly of the OWTs at the port is done sufficiently quickly such that the HLV does not have to wait for it to be completed. Incorporating this aspect of the installation process could provide useful insights into the interactions between land and offshore logistics.

References

Noorzeeloket. (2025). Offshore wind energy. https://www.noordzeeloket.nl/en/functions-and-use/offshore-wind-energy/

Johnny Wood. (2023). Wind power costs: Why the industry is facing cost headwinds | World Economic Forum. https://www.weforum.org/stories/2023/11/why-offshore-wind-cost-pressures-rising/

Fuchs, R., Zuckerman, G. R., Duffy, P., Shields, M., Musial, W., Beiter, P., Cooperman, A., & Bredenkamp, S. (2025). The Cost of Offshore Wind Energy in the United States From 2025 to 2050. www.nrel.gov/publications.

Oelker, S., Sander, A., Kreutz, M., Ait-Alla, A., & Freitag, M. (2021). Evaluation of the Impact of Weather-Related Limitations on the Installation of Offshore Wind Turbine Towers. *Energies 2021, Vol. 14, Page 3778*, *14*(13), 3778. https://doi.org/10.3390/EN14133778

OffshoreWIND.biz. (2025). OffshoreWIND.biz. https://www.offshorewind.biz/

DOT. (2025). Slipjoint.tech. https://slipjoint.tech/

Tjaberings, J., Fazi, S., & Ursavas, E. (2022). Evaluating operational strategies for the installation of offshore wind turbine substructures Evaluating operational strategies for the installation of offshore wind turbine substructures. https://doi.org/10.1016/j.rser.2022.112951

Jiang, Z. (2021). Installation of offshore wind turbines: A technical review. *Renewable and Sustainable Energy Reviews*, *139*, 110576. https://doi.org/10.1016/J.RSER.2020.110576

Scholz-Reiter, B., Heger, J., Lütjen, M., & Schweizer, A. (2011). A milp for installation scheduling of offshore wind farms. *International Journal of Mathematical Models and Methods in Applied Sciences*, *5*(2), 371–378.

Barlow, E., Tezcaner Öztürk, D., Revie, M., Boulougouris, E., Day, A. H., & Akartunali, K. (2015). Exploring the impact of innovative developments to the installation process for an offshore wind farm. *Ocean Engineering*, *109*, 623–634. https://doi.org/10.1016/J.OCEANENG.2015.09.047

Smorenberg, M. (n.d.). An investigation of installation strategies to install next-generation offshore wind turbine generator components Feedering vs. Shuttling, an efficient installation process for the future Management of Technology-MSc Thesis.

Heerema. (2022). Heerema installs first wind turbine using novel RNA method. https://www.heerema.com/news/heerema-installs-first-wind-turbine-using-novel-rna-method

DOT. (2019). *DOT6000 FOX-CONFIDENTIAL REPORT TSE HE 2019 Title: Floating Installation of Offshore XXL Wind Turbines Abbreviation: DOT6000 FOX* (tech. rep.).

Segeren, M. (2018). Vibration-induced settlement of a slip-joint connection for offshore wind turbines. https://doi.org/10.4233/uuid:caf8ff62-7b9b-4dc1-b3b9-2087819d2ae1

Kamphuis, T. P. J. (2016). *"Design, testing and verification of the DOT500 slip-joint support structure."* (tech. rep.).

Tempel, J. v. d., & Schipholt, B. L. (2003). The slip-joint connection. https://research.tudelft.nl/en/publications/the-slip-joint-connection

DOT. (2016). *Slip Joint Offshore Research (SJOR) Report* (tech. rep.).

DOT. (2018). *Slip Joint Offshore Qualification (SJOQ) Report* (tech. rep.).

Van Oord. (2020). Van Oord heeft met succes eerste onderwater Slip Joint ter wereld geïnstalleerd. https://www.vanoord.com/nl/updates/van-oord-heeft-met-succes-eerste-onderwater-slip-joint-ter-wereld-geinstalleerd/

Paterson, J., D'Amico, F., Thies, P., Kurt, R., & Harrison, G. (2018). Offshore wind installation vessels – A comparative assessment for UK offshore rounds 1 and 2. *Ocean Engineering*, *148*. https://doi.org/10.1016/j.oceaneng.2017.08.008

Irawan, C. A., Jones, D., & Ouelhadj, D. (2017). Bi-objective optimisation model for installation scheduling in offshore wind farms. *Computers and Operations Research*, *78*, 393–407. https://doi.org/10.1016/j.cor.2015.09.010

Amorosi, L., Fischetti, M., Paradiso, R., & Roberti, R. (2024). Optimization models for the installation planning of offshore wind farms. *European Journal of Operational Research*, *315*(3), 1182–1196. https://doi.org/10.1016/j.ejor.2024.01.011

Barlow, E., Ozturk, D. T., Day, S., Boulougouris, E., Revie, M., & Akartunali, K. (2014). *An Assessment of Vessel Characteristics for the Installation of Offshore Wind Farms* (tech. rep.).

Devoy McAuliffe, F., Judge, F. M., & Murphy, J. (2024). Modelling the installation of next generation floating offshore wind farms. *Applied Energy*, *374*, 124001. https://doi.org/10.1016/J.APENERGY.2024.124001

Vis, I. F., & Ursavas, E. (2016). Assessment approaches to logistics for offshore wind energy installation. *Sustainable Energy Technologies and Assessments*, *14*. https://doi.org/10.1016/J.SETA.2016.02.001

Ait Alla, A., Oelker, S., Lewandowski, M., Freitag, M., & Thoben, K.-D. (2017). A Study of new Installation Concepts of Offshore Wind Farms by Means of Simulation Model.

Oelker, S., Ait-Alla, A., Lütjen, M., Lewandowski, M., Freitag, M., & Thoben, K.-D. (2018, June). A Simulation Study of Feeder-Based Installation Concepts for Offshore Wind Farms. https://dx.doi.org/

Muhabie, Y. T., Rigo, P., Cepeda, M., de Almeida D'Agosto, M., & Caprace, J. D. (2018). A discrete-event simulation approach to evaluate the effect of stochastic parameters on offshore wind farms assembly strategies. *Ocean Engineering*, *149*, 279–290. https://doi.org/10.1016/J.OCEANENG.2017.12.018

O'Sullivan, J., Arjona, J. F., & Aghili, M. (2011). Comparison of Installation Scenarios for Offshore Wind Farms Using Operations Simulator with Markov Wind & Wave Weather Model. *Offshore Technology Conference, Proceedings*, *4*, 3265–3269. https://doi.org/10.4043/22176-MS

OpenCLSim. (2023). Open source Complex Logistics Simulation. https://delightful-cliff-0e49c3503.1.azurestaticapps.net/Intro_draft.html

McDonald, A., & Schrattenholzer, L. (2001). Learning rates for energy technologies. *Energy Policy*, *29*(4), 255–261. https://doi.org/10.1016/S0301-4215(00)00122-1

Wright, T. P. (2012). Factors Affecting the Cost of Airplanes. *https://doi.org/10.2514/8.155*, *3*(4), 122–128. https://doi.org/10.2514/8.155

DHI. (2025). MetOcean Data Portal. https://www.dhigroup.com/technologies/metocean-data-portal

BARRA-R2 Dataset Details. (2025). https://www.metocean-on-demand.com/metadata/waterdata-dataset-Bass_Strait_SW_BARRA

SW_DWF23 Dataset Details. (n.d.). https://www.metocean-on-demand.com/metadata/waterdata-dataset-DWF23_SW_WRF

ERA5 Dataset Details. (n.d.). https://www.metocean-on-demand.com/metadata/waterdata-dataset-Global_WAM_ERA5

TenneT. (2025). Ecowende: toekomst wind op zee. www.ecowende.nl

Knud E. Hansen. (n.d.). Atlas C-Class Wind Turbine Installation Vessel. https://www.knudehansen.com/reference/atlas-c-class/

Van Oord. (2021). Offshore installation vessel Boreas Equipment Leaflet. www.vanoord.com

Kaiser, M. J., & Snyder, B. (2010). Offshore Wind Energy Installation and Decommissioning Cost Estimation in the U.S. Outer Continental Shelf. http://www.mms.gov/tarprojects/.

Melissa Keane, Fahid Ifthekhar, Emily Graham, Anthony Tridgell, & Tristan Kelly. (2023). Getting offshore wind off the ground – procurement risk for jack-up vessels. https://www.allens.com.au/insights-news/insights/2023/09/Getting-offshore-wind-off-the-ground/

Toelatingsbeleid Eemshaven. (n.d.).

Heerema Marine Contractors. (2020). Sleipnir HMC equipment leaflet.

Rippel, D., Jathe, N., L'tjen, M., & Freitag, M. (2019). Evaluation of Loading Bay Restrictions for the Installation of Offshore Wind Farms Using a Combination of Mixed-Integer Linear Programming and Model Predictive Control. *Applied Sciences 2019, Vol. 9, Page 5030*, *9*(23), 5030. https://doi.org/10.3390/APP9235030

Muhabie, Y. T., Caprace, J.-D., Petcu, C., & Rigo, P. (2015). *Improving the Installation of Offshore Wind Farms by the use of Discrete Event Simulation* (tech. rep.).

Karney, C. F. (2013). Algorithms for geodesics. *Journal of Geodesy*, *87*(1), 43–55. https://doi.org/10.1007/S00190-012-0578-Z/METRICS

COSMO-REA6 Dataset details. (2025). https://www.metocean-on-demand.com/metadata/waterdata-dataset-Europe_CREA6_V2

Vestas. (2024). *Life Cycle Assessment of electricity production from an offshore V236-15 MW wind plant* (tech. rep.).

van Bussel, G., & Bierbooms, W. (2004). *Offshore Wind farm Design module 4: Offshore Wind Climate Course Offshore wind farm design OE 5662 Module 4 Offshore Wind Climate Background document* (tech. rep.). TU Delft.

Hsu, S. A., Meindl, E. A., & Gilhousen, D. B. (1994). Determining the Power-Law Wind-Profile Exponent under Near-Neutral Stability Conditions at Sea. *Journal of Applied Meteorology and Climatology*, *33*(6), 757–765. https://doi.org/10.1175/1520-0450(1994)033<0757:DTPLWP>2.0.CO;2

Det Norske Veritas. (2010). *RECOMMENDED PRACTICE ENVIRONMENTAL CONDITIONS AND ENVIRONMENTAL LOADS* (tech. rep.). http://www.dnv.com

LAUTEC. (2015). WindGIS – GIS Web Viewer. https://lautec.com/software/windgis/#

Ministeries van Economische Zaken en Klimaat, Zaken en Koninkrijkrelaties Infrastructuur en Waterstaat en Landbouw, B., & en Voedselkwaliteit, N. (2016). *Bijlagen 1 - 8 MER Kavel VI HKW* (tech. rep.).

RVO. (2025). Windenergiegebied Hollandse Kust (west). https://windopzee.nl/onderwerpen/waar-staan-komen-windparken/windenergiegebied-hollandse-kust-west/

Star of the South. (2020). Project Overview. https://www.staroftheSouth.com.au/project-overview

OWC. (2024). Navigating the Waters of Bass Strait for Offshore Wind Construction. https://owcltd.com/media/blog/navigating-the-turbulent-waters-of-bass-strait-for-offshore-wind-construction/?utm_source=chatgpt.com

Liu, J., Meucci, A., Liu, Q., Babanin, A. V., Ierodiaconou, D., & Young, I. R. (2022). The wave climate of Bass Strait and South-East Australia. *Ocean Modelling*, *172*, 101980. https://doi.org/10.1016/J.OCEMOD.2022.101980

Vincent, C. L., & Dowdy, A. J. (2024). Multi-scale variability of southeastern Australian wind resources. *Atmospheric Chemistry and Physics*, *24*(18), 10209–10223. https://doi.org/10.5194/ACP-24-10209-2024

A

Extra tables

Departure time at port	21-4 23:00					
Arrival time at port	8-5 16:00					
Installation time (days)	16,71					
Arrival time at OWF	22-4 18:00					
Leaving time at OWF	7-5 20:00					
Installation time (days)	15,08					
	OWT 1	OWT 2	OWT 3	OWT 4	OWT 5	OWT 6
Arrival time at OWT (approx)	22-4 18:00	24-4 18:00	26-4 13:00	28-4 19:30	1-5 15:00	5-5 18:00
Departure time at OWT (approx)	24-4 17:00	26-4 12:00	28-4 19:00	1-5 13:00	5-5 15:00	7-5 20:00
Installation time (days)	1,96	1,75	2,25	2,73	4,00	2,08
Sailing speed back to port (empty)	10,6	knots				
Sailing speed out to sea (full)	10	knots				

Table A.1: Wind Peak installation times analysis, performed with Lautec WindGIS

B

Ecowende and Star of the South OWT Coordinates

	Latitude	Longitude		Latitude	Longitude
OWT 1	52,64400	3,81906	OWT 27	52,73767	3,84222
OWT 2	52,65304	3,75149	OWT 28	52,73907	3,82274
OWT 3	52,65613	3,81479	OWT 29	52,74791	3,86563
OWT 4	52,65754	3,79535	OWT 30	52,74931	3,84615
OWT 5	52,67034	3,74837	OWT 31	52,75072	3,82665
OWT 6	52,66638	3,83816	OWT 32	52,75956	3,86957
OWT 7	52,66779	3,81871	OWT 33	52,76096	3,85008
OWT 8	52,66934	3,77773	OWT 34	52,76236	3,83057
OWT 9	52,68338	3,73281	OWT 35	52,77121	3,87350
OWT 10	52,67973	3,78399	OWT 36	52,77261	3,85400
OWT 11	52,68077	3,76447	OWT 37	52,79267	3,88031
OWT 12	52,69643	3,71724	OWT 38	52,78804	3,86222
OWT 13	52,68831	3,84588	OWT 39	52,78342	3,84411
OWT 14	52,68935	3,82636	OWT 40	52,77879	3,82601
OWT 15	52,69040	3,80683	OWT 41	52,69996	3,84928
OWT 16	52,69144	3,78732	OWT 42	52,70101	3,82975
OWT 17	52,69248	3,76780	OWT 43	52,70204	3,81023
OWT 18	52,69352	3,74827	OWT 44	52,70309	3,79070
OWT 19	52,71297	3,85384	OWT 45	52,70413	3,77117
OWT 20	52,71438	3,83437	OWT 46	52,70517	3,75163
OWT 21	52,71577	3,81490	OWT 47	52,80653	3,86509
OWT 22	52,71717	3,79543	OWT 48	52,72744	3,80053
OWT 23	52,72462	3,85777	OWT 49	52,73771	3,80562
OWT 24	52,72602	3,83829	OWT 50	52,74798	3,81072
OWT 25	52,72743	3,81882	OWT 51	52,75825	3,81582
OWT 26	52,73626	3,86170	OWT 52	52,76852	3,82091

Table B.1: Ecowende OWT coordinates

	Latitude	Longitude		Latitude	Longitude		Latitude	Longitude
OWT 1	146,87864	-38,96531	OWT 51	147,03045	-38,77649	OWT 101	147,00712	-38,72417
OWT 2	146,90053	-38,94824	OWT 52	147,00856	-38,79355	OWT 102	147,02901	-38,70711
OWT 3	146,92243	-38,93118	OWT 53	146,98666	-38,81061	OWT 103	147,05090	-38,69005
OWT 4	146,94432	-38,91412	OWT 54	146,96477	-38,82768	OWT 104	147,07279	-38,67298
OWT 5	146,96621	-38,89705	OWT 55	146,94288	-38,84474	OWT 105	147,09469	-38,65592
OWT 6	146,98810	-38,87999	OWT 56	146,92099	-38,86180	OWT 106	147,07961	-38,64417
OWT 7	147,01000	-38,86293	OWT 57	146,89909	-38,87887	OWT 107	147,05772	-38,66123
OWT 8	147,03189	-38,84586	OWT 58	146,87720	-38,89593	OWT 108	147,03583	-38,67830
OWT 9	147,05378	-38,82880	OWT 59	146,85531	-38,91299	OWT 109	147,01393	-38,69536
OWT 10	147,07567	-38,81174	OWT 60	146,83342	-38,93006	OWT 110	146,99204	-38,71242
OWT 11	147,09757	-38,79467	OWT 61	146,81834	-38,91831	OWT 111	146,97015	-38,72949
OWT 12	147,11946	-38,77761	OWT 62	146,84023	-38,90124	OWT 112	146,94826	-38,74655
OWT 13	147,14135	-38,76055	OWT 63	146,86213	-38,88418	OWT 113	146,92636	-38,76361
OWT 14	147,16325	-38,74348	OWT 64	146,88402	-38,86712	OWT 114	146,90447	-38,78068
OWT 15	147,18514	-38,72642	OWT 65	146,90591	-38,85005	OWT 115	146,88258	-38,79774
OWT 16	147,17006	-38,71467	OWT 66	146,92780	-38,83299	OWT 116	146,86069	-38,81480
OWT 17	147,14817	-38,73173	OWT 67	146,94970	-38,81593	OWT 117	146,83879	-38,83187
OWT 18	147,12628	-38,74880	OWT 68	146,97159	-38,79886	OWT 118	146,81690	-38,84893
OWT 19	147,10438	-38,76586	OWT 69	146,99348	-38,78180	OWT 119	146,79501	-38,86600
OWT 20	147,08249	-38,78292	OWT 70	147,01537	-38,76474	OWT 120	146,77312	-38,88306
OWT 21	147,06060	-38,79999	OWT 71	147,03727	-38,74767	OWT 121	146,75804	-38,87131
OWT 22	147,03871	-38,81705	OWT 72	147,05916	-38,73061	OWT 122	146,77993	-38,85425
OWT 23	147,01681	-38,83411	OWT 73	147,08105	-38,71355	OWT 123	146,80183	-38,83718
OWT 24	146,99492	-38,85118	OWT 74	147,10294	-38,69648	OWT 124	146,82372	-38,82012
OWT 25	146,97303	-38,86824	OWT 75	147,12484	-38,67942	OWT 125	146,84561	-38,80306
OWT 26	146,95114	-38,88530	OWT 76	147,10976	-38,66767	OWT 126	146,86750	-38,78599
OWT 27	146,92924	-38,90237	OWT 77	147,08787	-38,68473	OWT 127	146,88940	-38,76893
OWT 28	146,90735	-38,91943	OWT 78	147,06598	-38,70180	OWT 128	146,91129	-38,75186
OWT 29	146,88546	-38,93649	OWT 79	147,04408	-38,71886	OWT 129	146,93318	-38,73480
OWT 30	146,86357	-38,95356	OWT 80	147,02219	-38,73592	OWT 130	146,95507	-38,71774
OWT 31	146,84849	-38,94181	OWT 81	147,00030	-38,75299	OWT 131	146,97697	-38,70067
OWT 32	146,87038	-38,92474	OWT 82	146,97841	-38,77005	OWT 132	146,99886	-38,68361
OWT 33	146,89228	-38,90768	OWT 83	146,95651	-38,78711	OWT 133	147,02075	-38,66655
OWT 34	146,91417	-38,89062	OWT 84	146,93462	-38,80418	OWT 134	147,04264	-38,64948
OWT 35	146,93606	-38,87355	OWT 85	146,91273	-38,82124	OWT 135	147,06454	-38,63242
OWT 36	146,95795	-38,85649	OWT 86	146,89084	-38,83830	OWT 136	147,04946	-38,62067
OWT 37	146,97985	-38,83943	OWT 87	146,86894	-38,85537	OWT 137	147,02757	-38,63773
OWT 38	147,00174	-38,82236	OWT 88	146,84705	-38,87243	OWT 138	147,00568	-38,65480
OWT 39	147,02363	-38,80530	OWT 89	146,82516	-38,88949	OWT 139	146,98378	-38,67186
OWT 40	147,04552	-38,78824	OWT 90	146,80327	-38,90656	OWT 140	146,96189	-38,68893
OWT 41	147,06742	-38,77117	OWT 91	146,78819	-38,89481	OWT 141	146,94000	-38,70599
OWT 42	147,08931	-38,75411	OWT 92	146,81008	-38,87774	OWT 142	146,91811	-38,72305
OWT 43	147,11120	-38,73705	OWT 93	146,83198	-38,86068	OWT 143	146,89621	-38,74012
OWT 44	147,13310	-38,71998	OWT 94	146,85387	-38,84362	OWT 144	146,87432	-38,75718
OWT 45	147,15499	-38,70292	OWT 95	146,87576	-38,82655	OWT 145	146,85243	-38,77424
OWT 46	147,13991	-38,69117	OWT 96	146,89765	-38,80949	OWT 146	146,83054	-38,79131
OWT 47	147,11802	-38,70823	OWT 97	146,91955	-38,79243	OWT 147	146,80864	-38,80837
OWT 48	147,09613	-38,72530	OWT 98	146,94144	-38,77536	OWT 148	146,78675	-38,82543
OWT 49	147,07423	-38,74236	OWT 99	146,96333	-38,75830	OWT 149	146,76486	-38,84250
OWT 50	147,05234	-38,75942	OWT 100	146,98522	-38,74124	OWT 150	146,74297	-38,85956

Table B.2: Star of the South coordinates

C

Extra Graphs

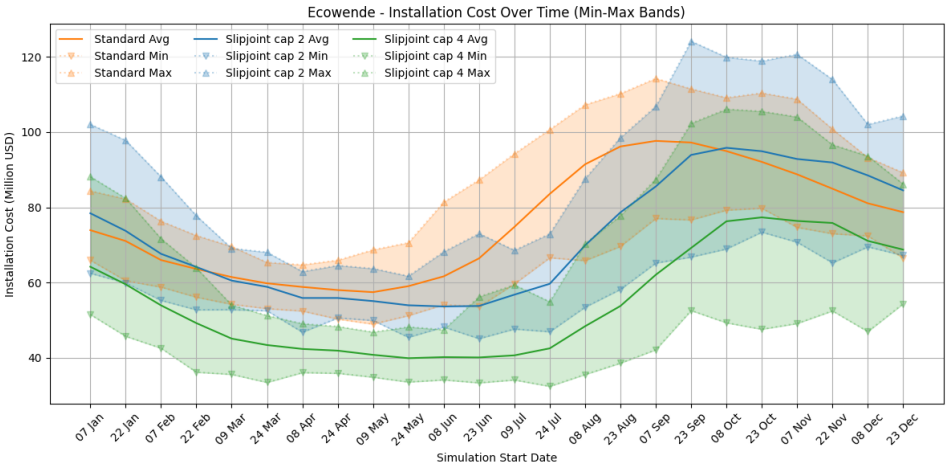

Figure C.1: Ecowende costs for different start dates with min/max bands.

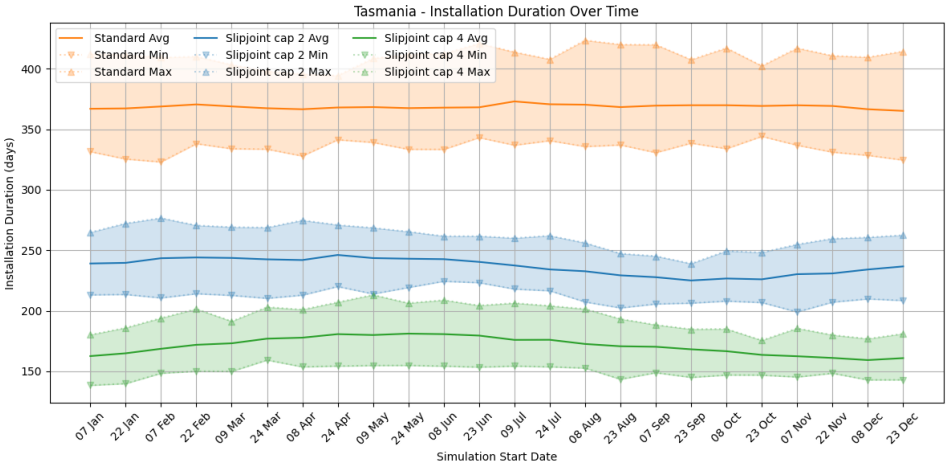

Figure C.2: Tasmania durations for different start dates with min/max bands.

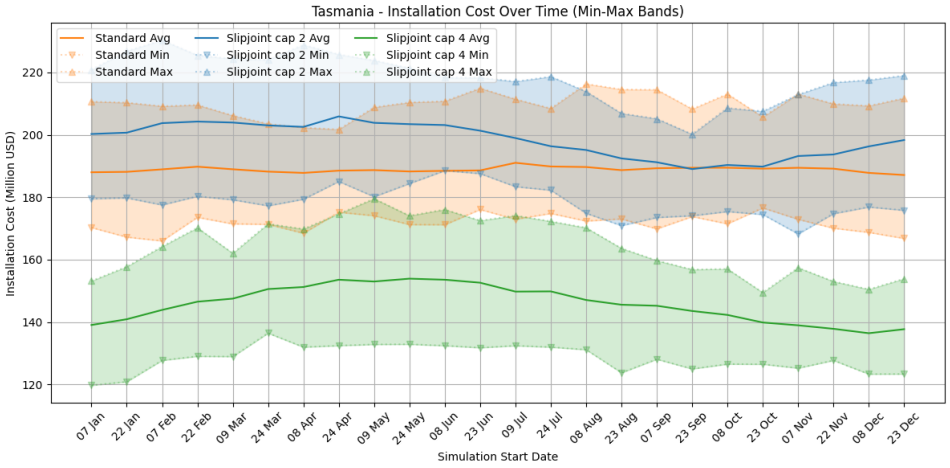

Figure C.3: Tasmania costs for different start dates with min/max bands.

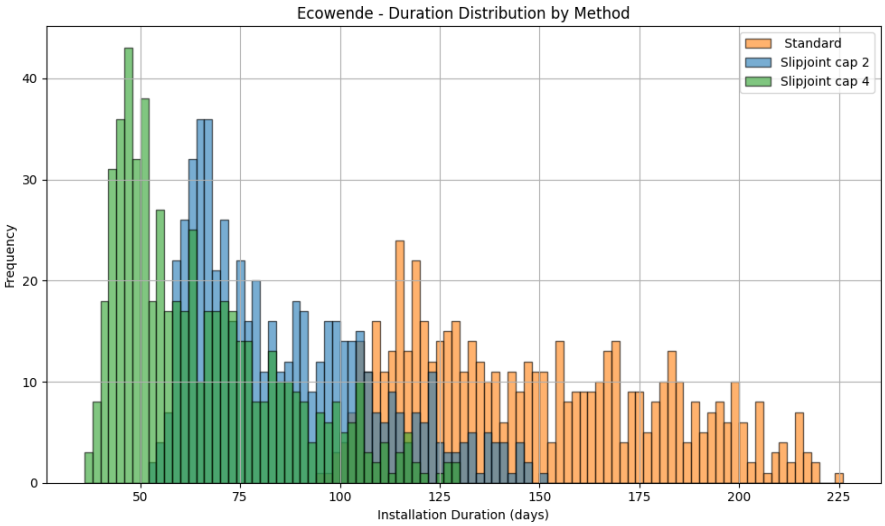

Figure C.4: Ecowende histogram of the installation durations.

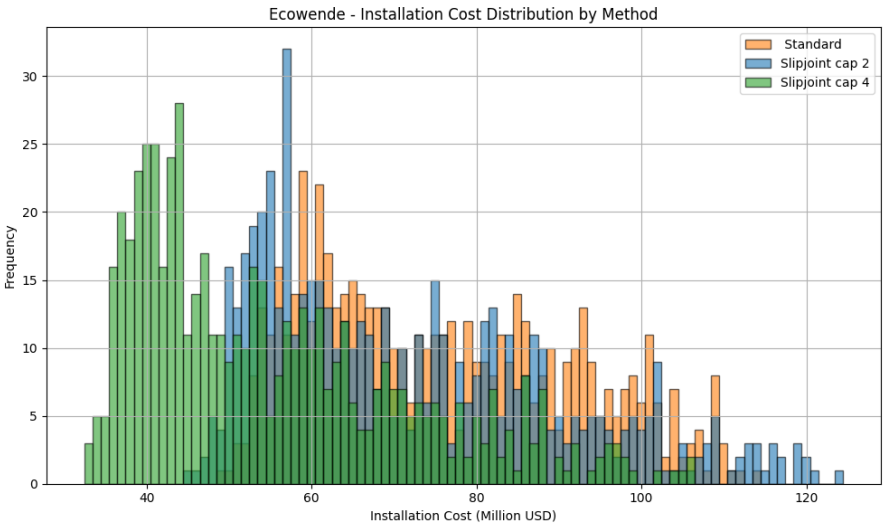

Figure C.5: Ecowende histogram of the installation costs.

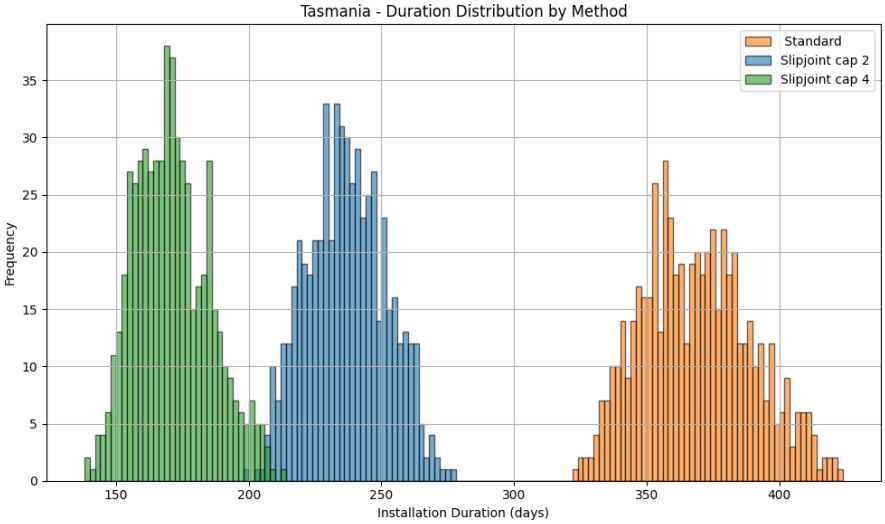

Figure C.6: Tasmania histogram of the installation durations.

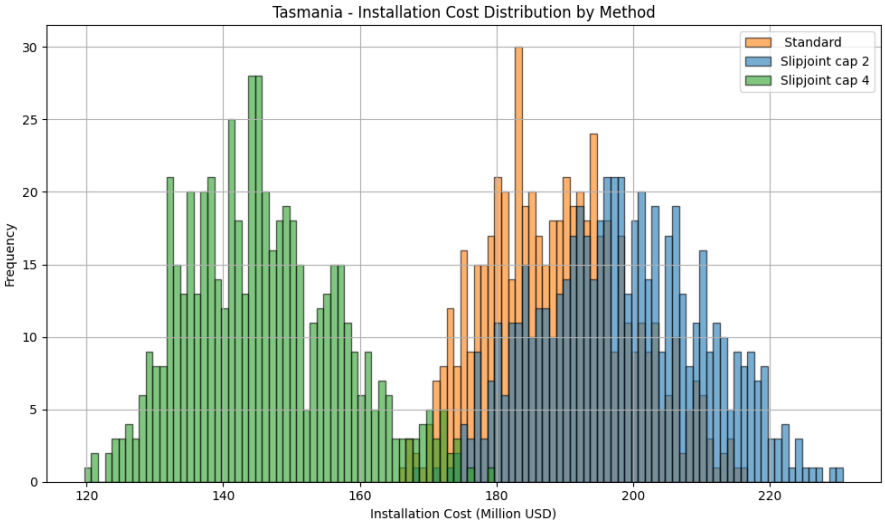

Figure C.7: Tasmania histogram of the installation costs.

D

Scientific Paper

See next page for the scientific paper of this thesis.

Modelling the Economic, Time and Workability Advantages of the Slipjoint through Discrete-Event Simulation

C.Y. Rippen
Faculty of Civil Engineering and Geosciences, Delft University of Technology.

Abstract. In recent years, costs in the offshore wind sector have risen significantly, while at the same time the pressure for realising sustainable energy continues to grow. The installation phase is one of the most expensive and resource-intensive parts of offshore wind projects. Reducing the installation duration could aid in reducing the installation costs, and make offshore wind farms more economically feasible. The Slipjoint is a new connection method developed by Delft Offshore Turbine (DOT) that aims to reduce offshore installation time by removing the need for bolting or grouting. This paper presents a Discrete-Event Simulation (DES) model that compares traditional and Slipjoint-based wind turbine installation methods in terms of time, cost, and weather sensitivity. The model is applied to two case studies: the Ecowende wind farm in the North Sea, and a wind farm off the coast of Tasmania. Results show that the Slipjoint can significantly reduce installation duration and cost, especially when higher capacities can be achieved. The model also gives insight into how weather, vessel characteristics, and campaign timing influence installation performance.

Keywords: Offshore Wind, Wind Turbine Installation, Slipjoint, Discrete-Event Simulation.

1 Introduction

Offshore wind power is expected to grow rapidly over the next decade. In the Netherlands, the amount of electrical power generated by offshore wind farms is expected to grow from 4.7 gigawatt in 2024 to 21.5 gigawatt in 2032 Noorzeeloket (2025). But at the same time, the cost and complexity of offshore wind have also risen quickly. Vattenfall estimates that the cost of building offshore wind farms has gone up by 40% in just a few years, due to factors like inflation, shortage of skilled labour and higher interest rates Johnny Wood (2023). A big part of these costs comes from the installation process. Installing wind turbines at sea is sensitive to weather influences, time-consuming, and requires expensive vessels and skilled personnel. As the most modern turbines continue to grow in size, the installation supply chain is under pressure due to a shortage of suitable equipment and experienced personnel. Reducing the time spent offshore for installation can reduce risk, lower costs, and improve the economical feasibility of offshore wind projects.

The Slipjoint is an alternative connection method between turbine foundation and tower, or tower and nacelle, that reduces the installation time at sea. Instead of bolting or grouting, the connection is made by lowering one conical section onto another, using friction to secure the two turbine parts. While the mechanical design of the Slipjoint has been tested and certified, its logistical benefits have not yet been quantified at scale. This paper presents a simulation model that aims to quantify the benefits of using the Slipjoint in terms of time, costs and weather workability advantages.

The objective of this thesis is to develop and apply a simulation-based Decision-Support Tool (DST) to quantitatively compare the performance of traditional installation methods and the Slipjoint installation method. This leads to the following main research question:

"How can the installation processes of offshore wind farms using the Slipjoint and

traditional methods be quantitatively compared to create a decision support tool for offshore wind farm development?"

In this paper, this questions will be answered, a conclusion will be drawn and recommendations for future work will be made.

2 State of the art

Offshore wind turbine (OWT) installation is a well-studied field, and over the past years, many studies have proposed strategies to improve the efficiency, reduce weather downtime, and optimise the logistics of the installation. However, Slipjoint-based installation is a relatively new concept, and large-scale simulations comparing it to traditional methods have not yet been carried out. In this section, the current state of the art is discussed.

2.1 Offshore Wind Turbine Installation Strategies

Offshore wind installation typically consists of multiple sequential stages: loading components at a base port, transporting them to the installation site, and installing them using wind turbine installation vessels. These activities can all be executed in a number of different ways, each with their own advantages and disadvantages. A common strategy is to transport and install components separately (e.g., towers, nacelles, blades), using jack-up vessels which provide stable working conditions at sea. This is the standard industry method for waters up to 70 meters deep.

An alternative strategy involves partial or full onshore pre-assembly. This reduces the number of offshore lifts and shortens the time spent offshore. Studies such as (Vis and Ursavas, 2016) and (Sarker and Faiz, 2017) show that pre-assembly can significantly shorten installation time and reduce cost, but these benefits depend heavily on vessel capabilities and port infrastructure. A limiting factor for partial or full pre-assembly is the size and weight of pre-assembled turbine parts, which require heavy-lift vessels that are more expensive to operate.

2.2 Modelling Approaches in Offshore Wind Logistics

Different modelling approaches have been used to analyse and optimise offshore wind installation. The two most common approaches are:

- Mixed Integer Linear Programming (MILP) models, which are good for optimizing scheduling and routing decisions, but are often less suited for handling time-dependent and event-driven problems.
- Discrete-Event Simulation (DES) models, which model installation as a sequence of events, with the possibility of stochastic durations. These models are particularly useful for simulating cyclic operations and downtime due to weather windows.

DES is the most suitable method for capturing the installation cycles and weather uncertainty of offshore operations. (Muhabie et al., 2015), (Muhabie et al., 2018), (Oelker et al., 2021), (Barlow et al., 2015), and (Devoy McAuliffe et al., 2024) have all applied DES to model turbine installation, vessel scheduling, and weather delays. Most of the existing DES models focus on conventional turbine installation or using partial pre-assembly. Fully pre-assembled turbine installation in combination with the Slipjoint has never been modelled. This creates a gap in the current literature.

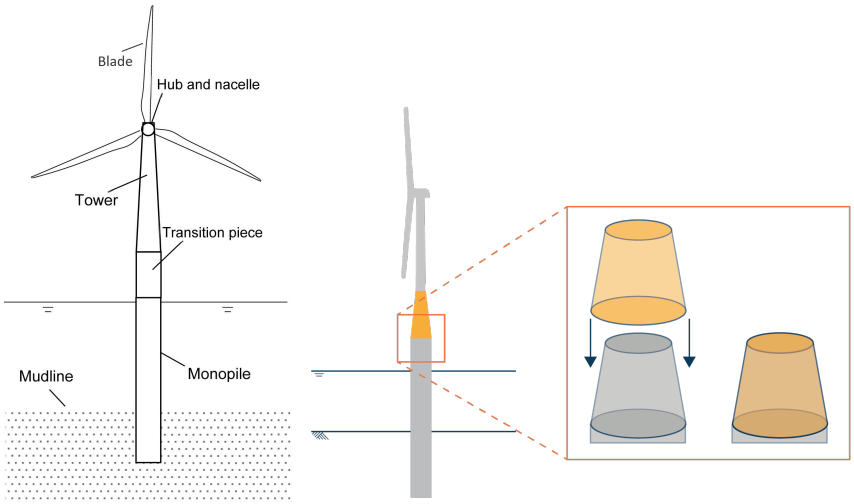

(a) The parts of an OWT. (b) The Slipjoint mechanism (DOT, 2025)

Fig 1: The parts of an OWT, and where the Slipjoint fits in.

2.3 The Slipjoint Connection

The Slipjoint is a friction-based conical connection that replaces traditional bolted or grouted connections between tower sections. It was developed by Delft Offshore Turbine (DOT) and has been successfully tested onshore and offshore (e.g., DOT500 pilot, FOX6000). It consists of two conical sections which slide into one another and are secured due to their geometry and friction. This eliminates the need for offshore bolting or grouting, both of which are time-consuming and weather-sensitive. Figure 1b shows a schematic view of the mechanical principle behind the Slipjoint.

Although the Slipjoint has proven to work mechanically, and small-scale tests have confirmed its feasibility, there has been little research into its logistical or operational impact on a full wind farm installation. No known studies model how the Slipjoint affects the total duration, cost, or weather sensitivity of an offshore installation campaign. Given the potential to reduce offshore time and costs, it is worth investigating.

2.4 Research Gap

While there is a strong body of literature on offshore wind installation strategies and DES modelling, no research has yet been done into the impact of the Slipjoint on offshore logistics. The benefits of full pre-assembly have sometimes been studied, but always without considering Slipjoint technology. The Slipjoint itself has mostly been analysed from a mechanical or structural perspective. Its real-world impact on installation logistics, cost, and installation time has not been quantified. This creates a clear knowledge gap. This study aims to fill that gap by building a DES model that compares traditional and Slipjoint-based installation strategies under realistic weather conditions. The goal is to provide a quantitative assessment of the Slipjoints potential advantages in terms of time, costs and weather workability.

3 Methodology

3.1 Model Structure

A diagram of the simulation model structure is given in Figure 2. The objects in the simulation (vessels, parts, sites) are used in activities. Loading, transport, positioning (including jackup/down or (de)submerging), installation and relocation activities are sequenced and cycled through. Conditional logic controls ensure the new cycle begins at the right activity. Using the shear-corrected weather data (see 3.5) and the operational weather limits, the model generates workable weather windows. These are timeframes in which the weather states do not exceed the operational limits of the vessel or activity being simulated, and allow the activities to take place. The length of the weather window depends on the weather data and on the weather operational limits set by the user. When the simulation has been completed, the model will output the results.

The model is simulated using OpenCLSim. OpenCLSim is a Simpy-based Python package designed for cyclic, rule-driven activities (OpenCLSim, 2023). It was developed by the Ports and Waterways department of the Civil Engineering facility at the TU Delft, along with Van Oord, Deltares and Witteveen+Bos, to model maritime logistics problems. It features a weather plugin, enabling weather-dependant simulation.

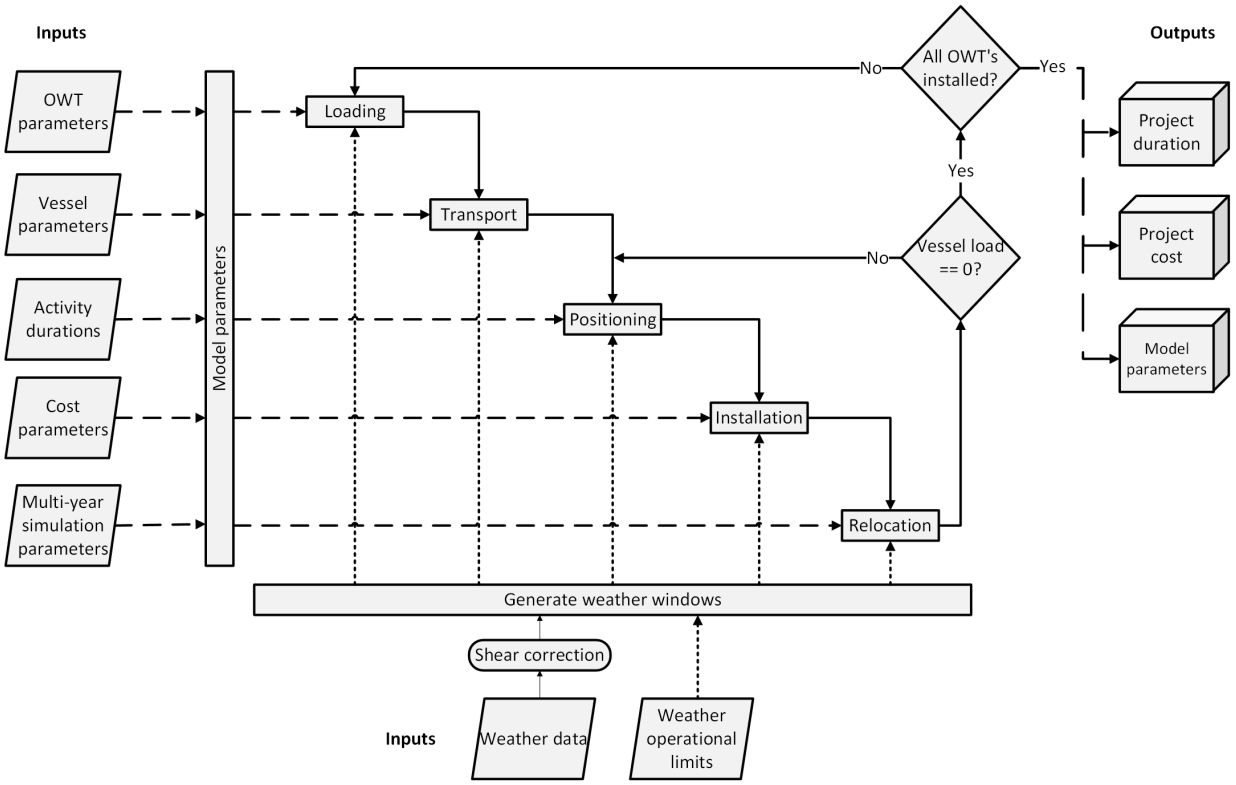

Fig 2: An overview of the DES model structure, inspired by (Tjaberings et al., 2022).

3.2 Modelling Assumptions

To make sure the DES model remains manageable in size and complexity, a set of assumptions have to be made. It is important that the model remains representative of the real-world situation when these assumptions are applied. An overview of the assumptions is given below.

1. **Foundations already in place**
   It is assumed that the monopile foundations for the turbines are all available for installation when the installation of the superstructures begins.
2. **Availability of crew and vessels**
   It is assumed that the crew and vessels are available for the entire duration of the simulation.
3. **No Equipment Failures**
   It is assumed that all equipment, such as vessels and cranes, do not have any failures which hinder their operations. It is also assumed any necessary maintenance which is carried out does not hinder the installation campaign.
4. **Weather Forecast**
   It is assumed that the crew always has accurate weather forecasts at their disposal for the duration of the weather windows, ensuring that no activity will be started which lasts longer than the available weather window.
5. **Limiting weather state**
   For the loading and installation activities, it is assumed that the wind speed will be the weather factor which is the most limiting, as lifting operations will be carried out and the vessel will be stationary. During transport, the significant wave height is assumed to be the limiting weather factor, as the waves will affect the load.

3.3 Learning effects

During an installation campaign, it can be observed that the time it takes to complete certain activities gradually decreases (McDonald and Schrattenholzer, 2001). This is explained by learning effects: as crews gain experience with the tasks they are carrying out and learn the most efficient ways of working, they are able to increase their working speed. This effect is incorporated into the model with the following formula:

$$T_n = T_1 \cdot n^{\frac{\log(1-r)}{\log(2)}} \tag{1}$$

Where:

- T_n is the installation time for the n^{th} batch,
- T_1 is the base installation time,
- n is the batch number,
- r is the learning rate.

In this formula, a learning rate of 10% means that after each doubling of installation cycles, the installation time is 90% of the original installation time. In other words, the installation time is reduced by 10% for every doubling of the number of installation batches. In this study, a learning rate of 10% is chosen for installation activities, as these are activities where there is room for improvement through learning. This value is in line with learning rates for European wind projects (McDonald and Schrattenholzer, 2001). For loading activities, a learning rate of 5% is chosen,

as this is a type of activity where improving efficiency is still possible, but the activities are more routine and therefore the potential improvements are slightly less than installation activities.

3.4 Model Inputs

The Discrete-Event Simulation uses a set of user-defined input parameters to run the model. These include OWT properties, installation vessel parameters, durations of loading and installing activities, maximum weather states, mobilisation costs and day rates, and parameters defining the multi-year simulation. Furthermore, the model takes two Metocean datasets as inputs: one dataset of the wind speed and one for the wave height weather parameters. These datasets are loaded into the model, where they are filtered and processed so the model is able to work with them.

3.5 Wind Shear Correction

The wind speed values of the weather datasets are expressed at a height of 10 metres. However, the loading and installation activities of offshore wind turbines are carried out at much greater heights. When loading and installing towers or complete turbines, the lifting point is located at the hub height. For the Vestas V236 OWT's, the hub height is around 150 metres, as indicated in a life-cycle assessment report by Vestas (Vestas, 2024). To ensure that the model remains accurate in its simulation, this discrepancy between measurement height and lifting height must be corrected. To correct the measurements at 10 metres to the hub height of 150 metres, a wind shear correction is applied, using a power law (van Bussel and Bierbooms, 2004).

The formula uses a wind shear correction factor α. A value of $\alpha = 0.115$ is used (Det Norske Veritas, 2010; Hsu et al., 1994). Using $Z_h = 150$, $U(Z_m) = 10$, and rewriting the power law formula, the wind speed values in the dataset at 10 metres are multiplied by:

$$U(150) = U(10)\left(\frac{150}{10}\right)^{0.115} = 1.365 * U(10) \tag{2}$$

3.6 Model Validation

To verify that the model is accurate, a validation is needed. This is usually done by running a simulation of the model on a certain case for which actual results are available, and comparing the output of the model to the real measurements. As the Ecowende and Star of the South wind farms have both not yet begun with construction, a different source must be found for validation. The Voltaire installation vessel is similar to the Boreas, and already in use. It can therefore be used to validate the model. Data regarding the installation and cycle times is not publicly available. However, the vessel can be tracked using public Automatic Information System (AIS) data. Using the Lautec WindGIS online application (LAUTEC, 2015), the time spent at port and the time spent offshore can be tracked.

To perform the validation, the model is set to install 20 turbines at the Dogger Bank A wind farm from the port of Able Seaton, the same number it has currently installed. The simulation was run over 24 years, and the results are shown in Table 1.

It can be seen that the actual offshore and port times are highly variable, causing some discrepancies between the model and reality. The model tends to give more consistent offshore and port

	Port Stay			Offshore Time		
	Real	Model	Difference	Real	Model	Difference
Batch 1	3,66	3,47	-5%	14,91	15,14	2%
Batch 2	3,23	3,15	-2%	15,53	13,45	-13%
Batch 3	10,83	3,16	-71%	12,91	11,98	-7%
Batch 4	6,71	3,04	-55%	12,45	10,18	-18%

Table 1: Voltaire validation

times, which reduce throughout the progress of the project due to the weather becoming more favourable. It is hard to say what causes the variability in the actual offshore and port times, as the only available information about the vessels is their location, not what their current activities are. Nevertheless, the model is able to accurately model the port and offshore times to within a few percent of the actual offshore and port times, when there are seemingly no other factors delaying these times. The model underestimating installation time is consistent with the assumptions made in the model, namely to exclude mechanical breakdowns, maintenance and crew availability which could cause delays. In other words, the model is accurate in estimating lower bounds for the installation times. Furthermore, it should be noted that this validation is performed while the project is only just underway. The Voltaire has installed just 7% of its total turbines. Re-evaluating the validation of the model when the wind farm is finished would likely yield results closer to reality, as the installation times per turbine reduce.

4 Case Studies

To quantify the possible benefits of the use of a Slipjoint, two case studies are used. The model is applied to the installation campaign of two yet to be built OWF's. The first is Ecowende, an OWF off the west coast of the Netherlands. The second is the Star of the South OWF, off the south east coast of Australia, near Tasmania.

4.1 Ecowende

The first case study is performed on the Karel VI installation site, also known as Ecowende. The Ecowende installation site lies around 50 kilometres off of the west coast of the Netherlands. The base port for the installation of the turbines, however, is the Eemshaven in Groningen, in the north. The sailing distance from the Eemshaven to Ecowende is around 230 kilometres. The installation site has an area of just 90 km^2, and will house 52 turbines.

4.2 Star of the South

For the second case study, an OWF near the south east coast of Australia is chosen. This wind park was chosen because it is different to Ecowende in several aspects, making it possible to analyse in which circumstances the Slipjoint can offer the most benefits. The OWF which will be used in the case study is the Star of the South wind farm, shown in Figure 3b. This site is one of several development sites in the Bass Strait, the body of water between mainland Australia and Tasmania. The license site sits just 15 kilometres off the coast of mainland Australia, and has an area of 586 km^2. It is planned to house 150 turbines, however, as this project is at an earlier stage of development, these numbers are preliminary.

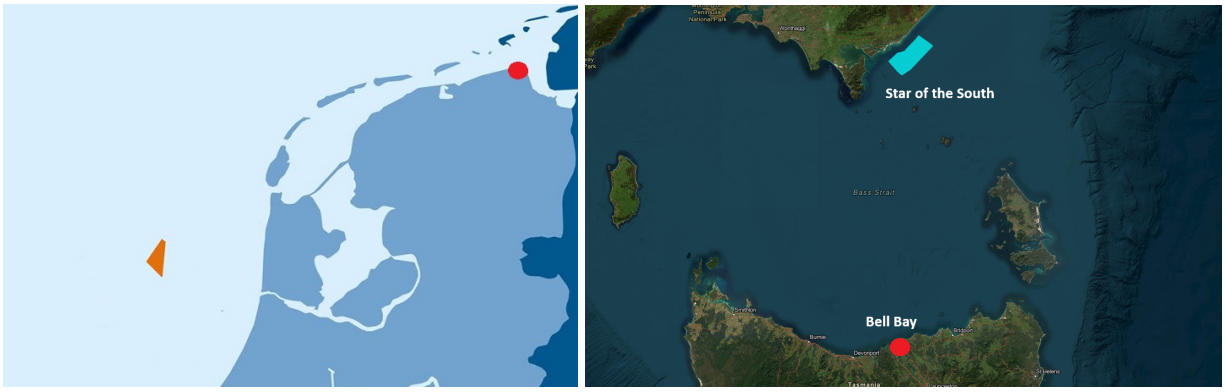

(a) The location of the Ecowende wind farm. (b) The location of the Star of the South wind farm.

Fig 3: The locations of the case OWFs.

An overview of the most important differences between Ecowende and Star of the South is given in Table 2. The base port for the case study will be Bell Bay. This port is located on the north end of Tasmania, at a sailing distance of around 260 kilometres from the site, and is currently expanding its staging areas in preparation for the installation of the foundations and superstructures for the different wind farms in the Bass Strait.

		Ecowende	Star of the South
Area	[km^2]	90	586
# Turbines	[-]	52	150
Turbine power	[MW]	15	15
Total capacity	[GW]	0.76	2.2
Foundation type	[-]	Monopile	Monopile
Distance from base port	[km]	230-245	260-280

Table 2: Overview of the main characteristics of the two case study wind farms

5 Results

To evaluate the performance of the standard and Slipjoint installation methods, they are compared in terms of time, costs and weather workability. The performance of the different methods depends on the start date of the installation project. The installation durations and costs as a function of start date are displayed and discussed for both case studies. The Slipjoint method is split into two cases: one where the capacity of the HLV is assumed to be 2 OWTs, and one where the capacity is 4 OWTs. This is done because the actual capacity of the HLV to transport completely assembled OWTs is not known. Therefore, it is treated as a variable, and the values 2 and 4 for this variable are evaluated. These methods are called 'Slipjoint Capacity 2' and 'Slipjoint Capacity 4', and they will be compared to the 'Standard' method. For each case, the simulation is run over 24 years, starting in 1995, with 24 datapoints (start dates) per year to ensure high fidelity of results.

5.1 Ecowende

In Figure 4 the durations of the installation methods at different start dates throughout the year are given. The average durations are shown with a $\pm$ 1 standard deviation band, giving a smooth plot

with good readability. From the figure it becomes clear how the Slipjoint methods have a shorter average installation time than the standard method, for both the capacity 2 and 4 methods. The narrower error bands also clearly indicate a smaller variability in installation times per start date. It can be seen that the standard method is more sensitive to seasonal influences: the durations start to increase in length earlier in the year than the Slipjoint methods, and the increase in installation time is more severe. In other words, the weather workability of the Slipjoint method is better than that of the standard method. The installation cost can also be plotted as a function of the

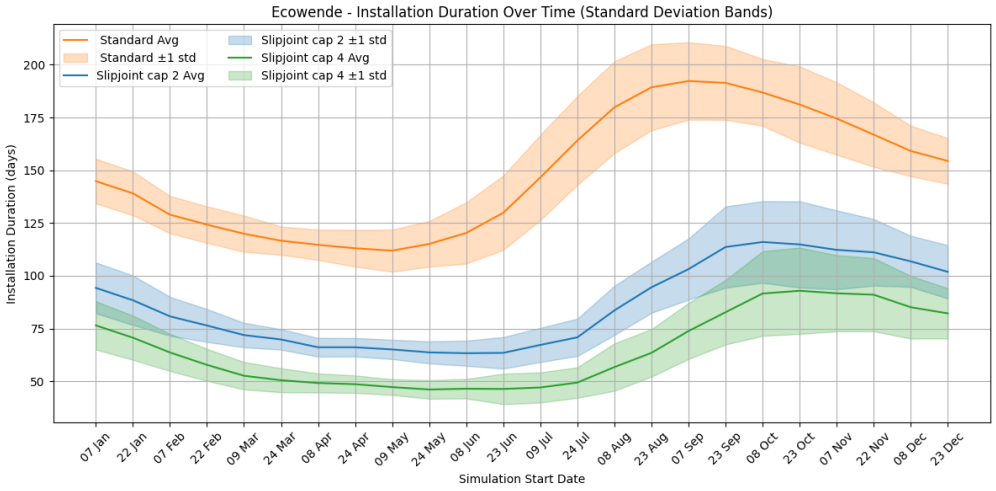

Fig 4: Ecowende durations for different start dates with standard deviation bands.

start date. Figure 5 shows the installation costs of the three methods as a function of the start date of the simulated installation campaign. This shows a more nuanced cost performance of the Slipjoint capacity 2 method. Between the months of October and February, its costs are higher than the standard method. Here, the installation time savings aren't substantial enough to compensate for the increased mobilisation cost and dayrates of the HLV. However, beginning in March, the installation costs start to become increasingly less than the standard method. The Slipjoint method stays near its optimum longer than the traditional method, increasing the starting window in which the installation cost will be near-optimal. This is shown with the near-optimal ranges. Within these ranges, the installation costs lie within a 10% increase in costs over the minimum average cost. It can be seen that this window is three months long for the standard method, three and a half months long for Slipjoint capacity 2 and four months for the Slipjoint capacity 4 method. The Slipjoint capacity 4 method shows a near constant improvement in cost performance over the standard method, and its optimal starting date range is also shifted to later in the year when compared to the standard method.

5.2 Tasmania

The durations as a function of the start date for the Tasmania casestudy are given in Figure 6. When comparing these to Figure 4, it can be seen that the installation durations are much more constant throughout the year, for all methods. This is a result of the weather conditions in the Bass Strait being more constant than on the North Sea OWC (2024). The Slipjoint methods show more seasonal influences than the traditional method, as shown by the flatter curve for the traditional method. This could be due to the traditional method being more wind-restricted than wave-restricted due

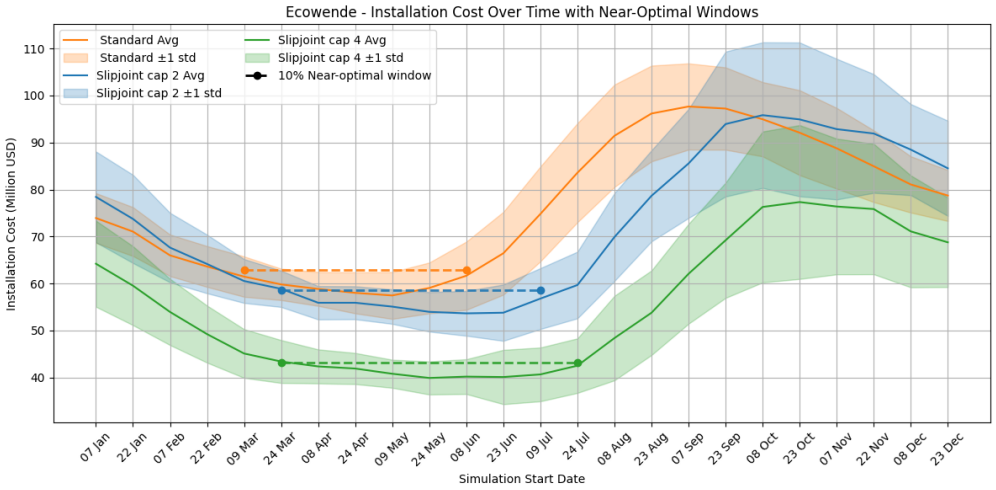

Fig 5: Ecowende costs for different start dates with standard deviation bands and near-optimal ranges.

to the many lifting operations. The Slipjoint method is more wave-restricted due to the increased number of transits and reduced lifting operations. The wave conditions in the Bass Strait fluctuate more with the season than the wind conditions Liu et al. (2022) Vincent and Dowdy (2024), causing more severe seasonal effects for the wave-restricted Slipjoint methods. When comparing the different installation methods, it can be seen that the Slipjoint methods again outperform the standard method, achieving lower average installation times and variabilities. The duration ranges for the standard method are quite high. The width of the error band for the durations is around 50 days, making it hard to predict how long an installation campaign will take beforehand.

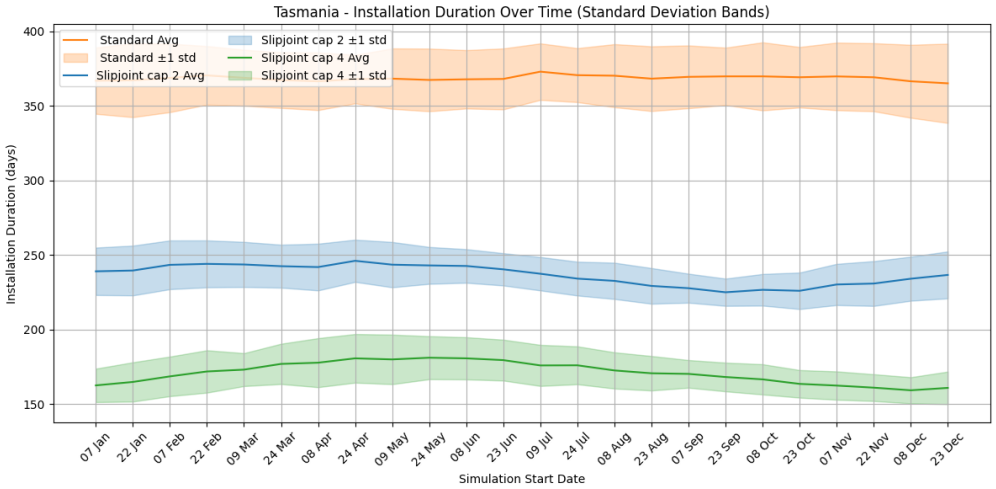

Fig 6: Tasmania durations for different start dates with standard deviation bands.

The costs as a function of start date for the Tasmanian case study is given in Figure 7. In the Tasmania case study, the costs performance of the Slipjoint capacity 2 method is again lower than the standard method. However, in the Ecowende case there was a window in which the Slipjoint method outperformed the standard method. In the Tasmania case, the Slipjoint capacity 2 method consistently has higher installation costs than the standard method, with the exception

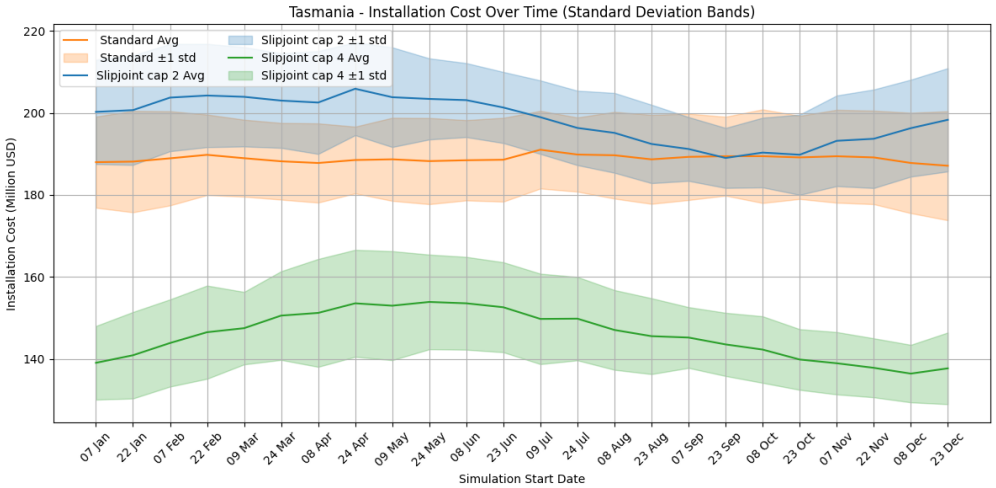

Fig 7: Tasmania costs for different start dates with standard deviation bands.

of late September, where the costs are similar. The Slipjoint capacity 4 method does outperform the standard method considerably throughout the whole year. Noticeably, both Slipjoint methods display more seasonal effects than the standard installation method, which is very constant in costs throughout the year. Here, the discrepancy in optimal start date between the two Slipjoint methods is also noticeable.

6 Discussion

In this study, the installation performance of the Slipjoint technology for offshore wind turbine (OWT) installation was investigated using Discrete-Event Simulation (DES). Two case studies shown in section 4 were used: one yet to be constructed offshore wind farm (OWF) near the coast of the Netherlands (Ecowende), and one in the Bass Strait between mainland Australia and Tasmania (Star of the South). Simulations of the installation of the OWF's were run for both Slipjoint based installation methods and traditional installation methods. The outcomes of the simulations were then compared in terms of time, cost and weather workability. The results shown in section 5 show that the Slipjoint based installation methods consistently lead to shorter installation durations and, depending on vehicle capacity, lower costs compared to traditional installation methods. It also shows a greater resistance to weather influences.

These outcomes highlight the potential value of the Slipjoint technology, which could be used to realise substantial cost savings for offshore wind projects. The need for such cost savings in the offshore wind industry is high, as large wind projects are at risk of being cancelled due to the increased costs, as mentioned in section 1. However, the decision-support tool developed in this study also has some limitations due to assumptions made and data availability.

The assumption that the crew has perfect weather forecasts, no mechanical breakdowns, and full port and vessel availability could cause the model to underestimate installation times. Furthermore, the installation stages of foundations, cables and transformer stations are not incorporated into the model. The exclusion of these possible delays and the other stages of OWF installation is not a consequence of a limitation of the approach, but rather a consequence of the limited time available for this study. Adding these factors into the simulation could present new trade-offs and

introduce new areas for optimisation, providing a more representative and holistic approach to OWF installation modelling.

Despite these limitations, the DES model presented in this study provides an extensive and flexible tool, useful for comparing OWT installation strategies. It enables OWF developers to test different loading, transport and installation strategies at different locations over the world, over long timespans. The model can easily be adapted and expanded to the needs of the user. This allows developers to explore and compare the performance of many different variable combinations to find the optimal strategies.

In summary, the Slipjoint installation method shows clear potential for reducing OWF installation cost by reducing offshore time. The effectiveness of these methods is dependent on the timing and location, but more so on the possible capacity of the installation vehicle. The results of this study show the potential of the Slipjoint as a cost-saving measure in offshore wind turbine installation.

7 Conclusion

With growing scale and costs, the offshore wind industry is facing headwinds. There is increasing pressure to develop cost-saving measures to improve the economical feasibility of offshore wind projects and prevent them from being cancelled. The Slipjoint is a novel connector interface which aims to achieve cost savings by reducing offshore time and its associated costs. It is a relatively new technology, which has never been tested at a large scale. It is therefore unknown what the time and cost savings from the use of the Slipjoint are. From this emerges a need for a quantitative simulation model to investigate the potential time and cost savings of the Slipjoint.

The aim of this thesis was to develop and apply a simulation-based Decision-Support Tool (DST) to quantitatively compare the performance of traditional installation methods and the Slipjoint installation method. To fulfil this objective, a quantitative Discrete-Event Simulation (DES) model was developed to simulate offshore wind turbine installation campaigns. The model included realistic process logic, weather influences, and vessel and OWT parameters. The model was applied to two case studies. Three installation methods were used in each case: a standard approach using a jack-up vessel, and two Slipjoint approaches with two different values for the HLV capacity.

The results showed a high degree of variability across installation start dates for the Ecowende case, due to seasonal weather influences. This variability was almost absent in the Tasmanian case, highlighting the importance of incorporating weather influences into the model. The Slipjoint had some clear advantages over the standard method that came forth out of the weather variability. Its improved weather workability enabled it to reach lower optimal costs. The Slipjoint Capacity 4 method achieved a 30.8% decrease in median costs when compared to the standard method in the Ecowende case, and a 23.1% decrease in the Tasmania case. Furthermore, its near-optimal window, the amount of time per year in which the installation costs lie within 10% of minimal costs, was wider. For the Slipjoint methods, the near-optimal windows were 3.5 and 4 months for the Slipjoint Capacity 2 and 4 methods respectively. This is an improvement compared to the near-optimal window of 3 months for the standard method. This means that Slipjoint-based methods have a wider window in which they can start and still be near-optimal in terms of costs.

The main research question, formulated in section 1, is as follows:

"How can the installation processes of offshore wind farms using the Slipjoint and traditional methods be quantitatively compared to create a decision support tool for offshore wind farm development?"

Using the findings discussed above, the main research question can be answered. From the literature review it was found that the most suitable modelling method is DES, due to its ability to model cyclic activities using sequencing and logic. Using DES, a simulation tool was developed in which different installation methods can be compared. This simulation tool is customisable to allow modelling of varying pre-assembly, transportation and installation strategies, and to compare their performance. Metrics from the simulation runs, such as durations, weather delays and costs, are used to analyse and plot the performance of the different installation methods. The DST was then applied to two case studies, showcasing how it can be used to aid decision-making in the realisation of OWFs. With the synthesis of the DST, and its application on two case studies, the main research is answered.

The results of the case studies show the benefits of the Slipjoint mechanism to be substantial. The validity of the results do depend on the validity of its inputs, of which some had to be estimated. These assumptions made in the model simplify the system to make it feasible to develop in the limited time available for the thesis project, but may cause it to underestimate project durations and costs. Nevertheless, the DES model developed provides a flexible and useful tool for evaluating installation strategies under realistic weather and logistical constraints. The tool is transparent and reproducible and can be expanded to incorporate other stages of OWF realisation such as foundation, cable or substation installation.

Further research into this topic could look at expanding the model to include the installation of foundations, cables and substations to get a complete understanding of all phases of offshore wind farm installation. Furthermore, different transport and installation strategies, such as a feeder strategy, could be investigated to see if they could lead to decreased installation times and costs. More research could also be done into determining a more suitable HLV for the Slipjoint method, as the chosen HLV (the Sleipnir) is too large to fit into many base ports. The stability of the vessel while transporting complete OWTs should be taken into account. Lastly, incorporating the land logistics of turbine parts delivery and pre-assembly could be added into the model. For the Slipjoint methods, it is critical that the pre-assembly of the OWTs at the port is done sufficiently quickly such that the HLV does not have to wait for it to be completed. Incorporating this aspect of the installation process could provide useful insights into the interactions between land and offshore logistics.

References

Barlow, E., Tezcaner Öztürk, D., Revie, M., Boulougouris, E., Day, A. H., and Akartunali, K. (2015). Exploring the impact of innovative developments to the installation process for an offshore wind farm. *Ocean Engineering*, 109:623–634.

Det Norske Veritas (2010). RECOMMENDED PRACTICE ENVIRONMENTAL CONDITIONS AND ENVIRONMENTAL LOADS. Technical report.

Devoy McAuliffe, F., Judge, F. M., and Murphy, J. (2024). Modelling the installation of next generation floating offshore wind farms. *Applied Energy*, 374:124001.

DOT (2025). Slipjoint.tech.

Hsu, S. A., Meindl, E. A., and Gilhousen, D. B. (1994). Determining the Power-Law Wind-Profile Exponent under Near-Neutral Stability Conditions at Sea. *Journal of Applied Meteorology and Climatology*, 33(6):757–765.

Johnny Wood (2023). Wind power costs: Why the industry is facing cost headwinds — World Economic Forum.

LAUTEC (2015). WindGIS – GIS Web Viewer.

Liu, J., Meucci, A., Liu, Q., Babanin, A. V., Ierodiaconou, D., and Young, I. R. (2022). The wave climate of Bass Strait and South-East Australia. *Ocean Modelling*, 172:101980.

McDonald, A. and Schrattenholzer, L. (2001). Learning rates for energy technologies. *Energy Policy*, 29(4):255–261.

Muhabie, Y. T., Caprace, J.-D., Petcu, C., and Rigo, P. (2015). Improving the Installation of Offshore Wind Farms by the use of Discrete Event Simulation. Technical report.

Muhabie, Y. T., Rigo, P., Cepeda, M., de Almeida D'Agosto, M., and Caprace, J. D. (2018). A discrete-event simulation approach to evaluate the effect of stochastic parameters on offshore wind farms assembly strategies. *Ocean Engineering*, 149:279–290.

Noorzeeloket (2025). Offshore wind energy.

Oelker, S., Sander, A., Kreutz, M., Ait-Alla, A., and Freitag, M. (2021). Evaluation of the Impact of Weather-Related Limitations on the Installation of Offshore Wind Turbine Towers. *Energies 2021, Vol. 14, Page 3778*, 14(13):3778.

OpenCLSim (2023). Open source Complex Logistics Simulation.

OWC (2024). Navigating the Waters of Bass Strait for Offshore Wind Construction.

Sarker, B. R. and Faiz, T. I. (2017). Minimizing transportation and installation costs for turbines in offshore wind farms. *Renewable Energy*, 101:667–679.

Tjaberings, J., Fazi, S., and Ursavas, E. (2022). Evaluating operational strategies for the installation of offshore wind turbine substructures Evaluating operational strategies for the installation of offshore wind turbine substructures.

van Bussel, G. and Bierbooms, W. (2004). Offshore Wind farm Design module 4: Offshore Wind Climate Course Offshore wind farm design OE 5662 Module 4 Offshore Wind Climate Background document. Technical report, TU Delft.

Vestas (2024). Life Cycle Assessment of electricity production from an offshore V236-15 MW wind plant. Technical report.

Vincent, C. L. and Dowdy, A. J. (2024). Multi-scale variability of southeastern Australian wind resources. *Atmospheric Chemistry and Physics*, 24(18):10209–10223.

Vis, I. F. and Ursavas, E. (2016). Assessment approaches to logistics for offshore wind energy installation. *Sustainable Energy Technologies and Assessments*, 14.